

1 **The dimorphic diaspore model *Aethionema arabicum* (Brassicaceae): Distinct
2 molecular and morphological control of responses to parental and germination
3 temperatures**

4

5 Jake O. Chandler¹, Per K.I. Wilhelmsson², Noe Fernandez-Pozo^{2,3}, Kai Graeber¹, Waheed
6 Arshad¹, Marta Pérez¹, Tina Steinbrecher¹, Kristian K. Ullrich^{2,†}, Thu-Phuong Nguyen⁴,
7 Zsuzsanna Mérai⁵, Klaus Mummenhoff⁶, Günter Theißen⁷, Miroslav Strnad⁸, Ortrun Mittelsten
8 Scheid⁵, M. Eric Schranz⁴, Ivan Petřík⁸, Danuše Tarkowská⁸, Ondřej Novák⁸, Stefan A.
9 Rensing^{2,9,*}, Gerhard Leubner-Metzger^{1,8,*}

10

11 ¹ Department of Biological Sciences, Royal Holloway University of London, Egham, Surrey,
12 TW20 0EX, United Kingdom, Web: 'The Seed Biology Place' - www.seedbiology.eu

13 ² Plant Cell Biology, Faculty of Biology, University of Marburg, 35043 Marburg, Germany

14 ³ Institute for Mediterranean and Subtropical Horticulture "La Mayora" (IHSM-CSIC-UMA),
15 29010 Málaga, Spain

16 ⁴ Biosystematics Group, Wageningen University, 6700 PB Wageningen, The Netherlands

17 ⁵ Gregor Mendel Institute of Molecular Plant Biology, Austrian Academy of Sciences, Vienna
18 Biocenter (VBC), 1030 Vienna, Austria

19 ⁶ Department of Biology, Botany, University of Osnabrück, 49076 Osnabrück, Germany

20 ⁷ Matthias Schleiden Institute / Genetics, Friedrich Schiller University Jena, 07743 Jena,
21 Germany

22 ⁸ Laboratory of Growth Regulators, Faculty of Science, Palacký University and Institute of
23 Experimental Botany, Czech Academy of Sciences, 78371 Olomouc, Czech Republic

24 ⁹ Centre for Biological Signalling Studies (BI OSS), University of Freiburg, 79104 Freiburg,
25 Germany

26

27 * Authors for correspondence: Gerhard.Leubner@rhul.ac.uk (G.L.-M.) and
28 stefan.rensing@cup.uni-freiburg.de (S.A.R.)

29

30 † Current address: Max Planck Institute for Evolutionary Biology, Department of Evolutionary
31 Biology, 24306 Plön, Germany

32

33 The authors responsible for distribution of materials integral to the findings presented in this
34 article in accordance with the policy described in the Instructions for Authors
35 (<https://academic.oup.com/plcell/pages/General-Instructions>) are: Gerhard Leubner-Metzger
36 (Gerhard.Leubner@rhul.ac.uk) and stefan.rensing@cup.uni-freiburg.de (S.A.R.).
37

38 Journal: **The Plant Cell**

39 Section: **Large-Scale Biology**

40

41 Short title: **Dimorphic Germination Control**

42

43 Manuscript number: TPC2023-LSB-00654R1

44 Revised manuscript received: 12/12/2023.

45 Accepted: 2023.

46

47 © The Author(s) 2023. Published by Oxford University Press on behalf of American Society of
48 Plant Biologists.

49 This is an Open Access article distributed under the terms of the Creative Commons
50 Attribution-NonCommercial-NoDerivs licence (<https://creativecommons.org/licenses/by-nc-nd/4.0/>), which permits non-commercial reproduction and distribution of the work, in any
51 medium, provided the original work is not altered or transformed in any way, and that the work
52 is properly cited. For commercial re-use, please contact journals.permissions@oup.com

53

54 **ORCIDs:**

55 ORCID Jake O Chandler: 0000-0003-0955-9241

56 ORCID Per KI Wilhelmsson: 0000-0002-8578-3387

57 ORCID Noe Fernandez-Pozo: 0000-0002-6489-5566

58 ORCID Kai Graeber: 0000-0003-2948-0856

59 ORCID Waheed Arshad: 0000-0002-9413-2279

60 ORCID Marta Pérez: 0000-0002-6802-205X

61 ORCID Thu-Phuong Nguyen: 0000-0003-3492-1062

62 ORCID Zsuzsanna Mérai: 0000-0002-2048-1628

63 ORCID Tina Steinbrecher: 0000-0003-3282-6029

64 ORCID Kristian K. Ullrich: 0000-0003-4308-9626

65 ORCID Ivan Petřík: 0000-0001-5320-7599

66 ORCID Danuše Tarkowská: 0000-0003-1478-1904

67 ORCID Klaus Mummenhoff: 0000-0002-8449-1593

68 ORCID Günter Theißen: 0000-0003-4854-8692

69 ORCID Miroslav Strnad: 0000-0002-2806-794X

70 ORCID Ortrun Mittelsten Scheid: 0000-0002-7757-4809

71 ORCID M Eric Schranz: 0000-0001-6777-6565

72 ORCID Ondřej Novák: 0000-0003-3452-0154

73 ORCID Stefan A Rensing: 0000-0002-0225-873X

74 ORCID Gerhard Leubner-Metzger: 0000-0002-6045-8713

77 **Abstract**

78

79 Plants in habitats with unpredictable conditions are often characterized by diversifying their
80 bet-hedging strategies that ensure fitness over a wider range of variable environmental
81 factors. A striking example is the diaspore (seed and fruit) heteromorphism that evolved to
82 maximize species survival in *Aethionema arabicum* (Brassicaceae) in which external and
83 endogenous triggers allow the production of two distinct diaspores on the same plant. Using
84 this dimorphic diaspore model, we identified contrasting molecular, biophysical, and
85 ecophysiological mechanisms in the germination responses to different temperatures of the
86 mucilaginous seeds (M^+ seed morphs), the dispersed indehiscent fruits (IND fruit morphs),
87 and the bare non-mucilaginous M^- seeds obtained by pericarp (fruit coat) removal from IND
88 fruits. Large-scale comparative transcriptome and hormone analyses of M^+ seeds, IND fruits,
89 and M^- seeds provided comprehensive datasets for their distinct thermal responses. Morph-
90 specific differences in co-expressed gene modules in seeds, as well as seed and pericarp
91 hormone contents identified a role of the IND pericarp in imposing coat dormancy by
92 generating hypoxia affecting ABA sensitivity. This involved expression of morph-specific
93 transcription factors, hypoxia response and cell wall-remodeling genes, as well as altered
94 abscisic acid (ABA) metabolism, transport, and signaling. Parental temperature affected ABA
95 contents and ABA-related gene expression and altered IND pericarp biomechanical
96 properties. Elucidating the molecular framework underlying the diaspore heteromorphism can
97 provide insight into developmental responses to globally changing temperatures.

98

99

100

101

102 **IN A NUTSHELL**

103

104 **Background:** Heteromorphic diaspores (fruits and seeds) are an adaptive bet-hedging
105 strategy to ensure survival in spatiotemporally variable environments. The stone cress
106 *Aethionema arabicum*, an annual plant native to semi-arid habitats in Anatolia (Turkey), one
107 of the world's hotspots of biodiversity. It is a close relative of *Arabidopsis*, rapeseed, cabbage
108 and other *Brassica* crops, but in contrast to these *Ae. arabicum* disperses two distinct

109 diaspores from the same plant. These dimorphic diaspores are the mucilaginous seeds
110 (dispersed by pod shatter) and indehiscent fruits (dispersed by abscission). The wing-like
111 pericarp (fruit coat) of the single-seeded indehiscent fruit allows wind dispersal over large
112 distances. The amounts and ratios of the dimorphic diaspores are variable and depend on the
113 environmental conditions. The dimorphic diaspores differ in morphology, dormancy and
114 germination properties and thereby make *Ae. arabicum* an excellent model for the
115 comparative investigation of the underpinning molecular mechanisms.

116

117 **Question:** We asked how temperature during fruit and seed formation and during seed
118 germination affect dormancy release and germination speed, and how the morphology,
119 hormonal regulation, and the expression of genes differ between the dimorphic diaspores.

120

121 **Findings:** Large-scale comparative transcriptome and hormone analyses of the mucilaginous
122 seeds and the indehiscent fruits, as well as the seeds artificially extracted from indehiscent
123 fruits by pericarp (fruit coat) removal, provided comprehensive datasets for their distinct
124 thermal responses. Material obtained from plants grown at different temperatures during
125 reproduction was imbibed at different temperatures for germination. This altered the abscisic
126 acid (ABA) metabolism and the pericarp biomechanical properties. Diaspore-specific
127 differences in response to distinct imbibition temperatures identified distinct gene expression
128 patterns in seeds, distinct seed and pericarp hormone contents, and a role of the pericarp in
129 generating hypoxia inside the fruit and imposing coat dormancy. This revealed distinct
130 combinations of specific transcription factors, hypoxia responses and cell wall-remodeling
131 genes, as well as altered signaling pathway genes.

132

133 **Next steps:** Our large-scale comparative transcriptome datasets are easily and publicly
134 accessible via the *Aethionema arabicum* web portal (https://plantcode.cup.uni-freiburg.de/aetar_db/index.php). We plan to expand this by future work on seedlings derived
135 from the dimorphic diaspores, by comparing different *Ae. arabicum* genotypes, and by
136 studying responses to specific stresses. Understanding the molecular basis of this fascinating
137 example of developmental diversity and plasticity and its regulation by temperature is
138 expected to add insight how plants respond to changing environmental conditions.

139

141 **Introduction**

142

143 Fruits and seeds as propagation and dispersal units (diaspores) have evolved an outstanding
144 diversity and specialization of morphological, physiological, and biomechanical features
145 during angiosperm evolution. Coordination of diaspore maturation as well as of diaspore
146 germination timing with environmental conditions is essential for the critical phase of
147 establishing the next generation of plants (Finch-Savage and Leubner-Metzger, 2006;
148 Donohue et al., 2010). This is especially critical in annual species that must establish
149 germination and plant growth in a given season or persist as diaspores in the seedbank for
150 germination in a later season (Finch-Savage and Footitt, 2017). Seed dormancy, i.e., innate
151 block(s) to the completion of germination of an intact viable diaspore under favorable
152 conditions, is the key regulatory mechanism involved in this timing. Temperature during plant
153 reproduction (parental growth temperature) and temperature sensing by the dispersed
154 diaspore provide input determining dormancy depth, germination timing, and adaptation to
155 climatic change (Walck et al., 2011; Fernandez-Pascual et al., 2019; Batlla et al., 2022;
156 Iwasaki et al., 2022; Zhang et al., 2022).

157

158 Most species with dry fruits, including *Arabidopsis thaliana* (Brassicaceae), produce seed
159 diaspores released by dehiscence, spontaneous opening at preformed structures from mature
160 fruits (Mühlhausen et al., 2013). Other species have dry indehiscent fruits where one or more
161 seeds remain encased by the pericarp (fruit coat). These indehiscent fruits are dispersed by
162 abscission, exemplified by several Brassicaceae species (Lu et al., 2015b; Sperber et al.,
163 2017; Mohammed et al., 2019). The pericarp of these indehiscent fruit diaspores may confer
164 coat-imposed dormancy and delayed germination of the enclosed seeds. While most plants
165 have evolved single types of diaspores that are optimized to the respective habitat, other
166 plants employ a bet-hedging strategy by producing different types of diaspores on the same
167 individual plant.

168

169 In these cases of diaspore heteromorphism, seeds and fruits differ in morphology, dormancy
170 and germination properties, ecophysiology, and/or tolerance to biotic and abiotic stresses
171 (Imbert, 2002; Baskin et al., 2014; Gianella et al., 2021). This diversity maximizes the
172 persistence of a species in environments with variable and unpredictable conditions. Diaspore

173 heteromorphism evolved independently in 26 angiosperm families and is common in the
174 Asteraceae, Amaranthaceae, and Brassicaceae. Examples of seed dimorphism include the
175 black and brown seed morphs of *Chenopodium album* and *Suaeda salsa* (Amaranthaceae),
176 which differ in dormancy and responses to salinity (Baskin et al., 2014; Liu et al., 2018;
177 Loades et al., 2023). The *Cakile* clade (Brassicaceae) produces fully indehiscent or
178 segmented, partially indehiscent fruits (Hall et al., 2006). The dimorphic desert annual
179 *Diptychocarpus strictus* (Brassicaceae) disperses short-lived winged, mucilaginous seeds and
180 long-lived indehiscent siliques each containing about 11 seeds (Lu et al., 2015a). While the
181 ecophysiology of these three dimorphic species is well described, the underpinning molecular
182 mechanisms remain largely unknown.

183

184 As a model system to investigate the principles of diaspore dimorphism, we have chosen
185 *Aethionema arabicum*, a small, diploid, annual, herbaceous species in the sister lineage of
186 the core Brassicaceae, in which seed and fruit dimorphism was associated with a switch to an
187 annual life history (Mohammadin et al., 2017). Genome and transcriptome information is
188 available (Haudry et al., 2013; Nguyen et al., 2019; Wilhelmsson et al., 2019; Arshad et al.,
189 2021; Fernandez-Pozo et al., 2021). *Aethionema arabicum* is adapted to arid and semiarid
190 environments. Its life-history strategy appears to be a blend of bet-hedging and plasticity
191 (Bhattacharya et al., 2019), and it exhibits true seed and fruit dimorphism with no intermediate
192 morphs (Lensser et al., 2016). Two distinct fruit types are produced on the same fruiting
193 inflorescence (infructescence): dehiscent (DEH) fruits with four to six mucilaginous (M^+)
194 seeds, and indehiscent (IND) fruits each containing a single non-mucilaginous (M^-) seed.
195 Upon maturity, DEH fruits shatter, releasing the M^+ seeds, while the dry IND fruits are
196 dispersed in their entirety by abscission. Dimorphic fruits and seeds differ in their
197 transcriptomes throughout their development and in the mature dry state upon dispersal, and
198 the dimorphic diaspores (M^+ seeds and IND fruits) differ in their water uptake patterns and
199 germination timing (Lensser et al., 2018; Arshad et al., 2019; Merai et al., 2019; Wilhelmsson
200 et al., 2019; Nichols et al., 2020; Arshad et al., 2021). Together, these features qualify *Ae.*
201 *arabicum* as a suitable model to investigate the molecular and genetic base of diaspore
202 dimorphism.

203

204 Temperature is a main ambient factor affecting reproduction, dormancy and germination of
205 plants (Walck et al., 2011; Fernandez-Pascual et al., 2019; Batlla et al., 2022; Iwasaki et al.,
206 2022; Zhang et al., 2022) and temperature during reproductive growth is known to affect the
207 ratio of IND/DEH fruit production of *Ae. arabicum* (Lenser et al., 2016). In our large-scale
208 biology study, we provide a comprehensive comparative analysis of gene expression levels,
209 hormonal status, biophysical and morphological properties underpinning the distinct *Ae.*
210 *arabicum* dimorphic diaspore responses to ambient temperatures. By comparing M⁺ seeds
211 dispersed from the fruits by dehiscence, indehiscent fruits containing M⁻ seeds dispersed by
212 abscission, and bare M⁻ seeds obtained from IND fruits by manually removing the pericarp,
213 we show that growth temperature during reproduction of the parent plant and a wide range of
214 imbibition temperatures either promote or delay germination. We demonstrate how the
215 pericarp of the IND fruit morph imposes coat dormancy.

216

217

218 Results

219

220 *Aethionema arabicum* reproductive plasticity and morph-specific responses to 221 parental and imbibition temperatures

222

223 As described in the introduction, *Ae. arabicum* disperses two morphologically distinct
224 diaspores (morphs), namely M⁺ seeds and IND fruits, that are produced at the same
225 inflorescence (Figure 1A). The larger dehiscent fruits (DEH) release several M⁺ seeds upon
226 maturation by dehiscence, whereas the smaller indehiscent fruits (IND) each containing a
227 single M⁻ seed are dispersed by abscission (Figure 1A). Previous work (Lenser et al., 2016)
228 showed that a 5°C increase in the ambient temperature during reproduction reduced the
229 overall number of fruits and shifted the ratio between the two fruit types towards the DEH
230 type. This parental temperature effect was confirmed here in a large-scale experiment with
231 ca. 2000 plants at two parental temperature regimes during reproduction (20°C and 25°C;
232 Figure 1B, Supplemental Figure S1A and Table S1). In earlier work (Lenser et al., 2016) we
233 used 14°C as imbibition temperature to compare the germination and water uptake kinetics of
234 the dimorphic diaspores from the 20°C parental temperature (PT) regime (20M⁺ seeds and
235 20IND fruits). This demonstrated that the germination of seeds enclosed in the 20IND fruits

236 was much delayed compared to 20M⁺ seeds and bare 20M⁻ seeds obtained from the artificial
237 separation of 20IND fruits by pericarp removal (Figure 1A). In the IND fruit, the pericarp
238 makes up 74.4% of the morph's mass but at maturity does not contain living cells (Arshad et
239 al., 2019; Arshad et al., 2020; Arshad et al., 2021). The maximal germination percentage
240 (G_{max}) of the 20IND fruits was also much reduced compared to 20M⁺ and 20M⁻ seeds imbibed
241 at 14°C (Lenser et al., 2016), indicating that the pericarp may impose coat dormancy.

242

243 Here, we used the material generated in the large-scale experiment (Figure 1B) with two
244 distinct parental temperatures, but otherwise identical growth conditions to address several
245 aspects of the mechanisms underlying the diaspore dimorphism, especially the pericarp-
246 imposed dormancy in a wide range of imbibition temperatures (Figure 1C). To investigate this
247 pericarp effect more closer, we compared the germination-permissive temperature windows
248 of freshly harvested mature M⁺ seeds with IND fruits as well as with bare M⁻ seeds (M⁻
249 obtained from IND by pericarp removal), obtained from plants grown at either 20°C (20M⁺,
250 20IND, 20M⁻) or 25°C (25M⁺, 25IND, 25M⁻) during reproduction. Seeds and fruits were
251 imbibed at a range of temperatures between 5°C and 30°C, and their G_{max} as well as their
252 germination rates ($GR_{50\%} = 1/T_{50\%}$, a measure for the speed of germination with $T_{50\%}$ being
253 the time required to reach 50% G_{max}) were quantified (Figure 1C). IND fruits from plants
254 matured at 20°C had a slower germination speed (lower germination rate, $GR_{50\%}$), a lower
255 G_{max} at germination-permissive temperatures, and a narrower temperature range allowing
256 near optimal germination, compared to M⁺ seeds from the same parents. For example, the
257 20IND fruits reached their highest G_{max} (ca. 50%) at 9°C but imbibed at even 2.5°C higher or
258 lower, only reached 25% germination. On the other hand, the corresponding 20M⁺ seeds
259 reached a G_{max} of above 85% from 5°C to 17.5°C. Pericarp removal demonstrated that 20M⁻
260 seeds had a similar optimum germination window as the 20M⁺ seeds, confirming the role of
261 the IND pericarp in blocking germination (coat dormancy) at otherwise permissive
262 temperatures for M⁺ and M⁻ seed germination.

263

264 M⁺ and M⁻ seeds from plants grown at the 20°C or 25°C parental temperature regimes had
265 similar germination kinetics, although 25M⁺ and 25M⁻ seeds generally had a higher $GR_{50\%}$,
266 and 25M⁺ seeds germinated slightly better at supra-optimal (warmer) temperatures
267 (Figure 1C). Interestingly, the 25M⁺ seeds germinated much faster ($t_{50\%}$ 29 h) than 20M⁺

268 seeds when imbibed at 17°C ($T_{50\%}$ 54 h). Most different were 25IND fruits, which had a much
269 higher G_{max} at germination-permissive temperatures than 20IND fruits (Figure 1C). 25IND
270 fruits reached 87% to 98% germination at temperatures between 7°C and 12°C. Nonetheless,
271 removal of the pericarp (IND vs M⁻) increased G_{max} and $GR_{50\%}$, especially at supra-optimal
272 temperatures, for example, from 77% to 98% at 14°C and from 36% to 100% at 17°C. The
273 pericarp therefore narrowed the permissive germination window by ca. 5°C at supra-optimal
274 imbibition temperatures irrespective of the parental temperature. Thus, pericarp-imposed
275 dormancy was still evident, although less extreme in 25IND fruits compared to 20IND fruits. At
276 germination-permissive imbibition temperatures, the 25IND and 20IND pericarps therefore
277 differed in their coat dormancy-imposing capabilities.

278

279 **Large-scale RNAseq and hormone quantification to identify morph-specific**
280 **germination and dormancy mechanisms in *Ae. arabicum***

281

282 The contrasting pericarp-imposed dormancy and germination kinetics of M⁺, IND, and M⁻
283 showed that the two morphs integrate the signal of ambient imbibition temperature differently
284 and suggest that one component is the ambient temperature during the reproduction of the
285 parental plant (Figure 1). We hypothesized that the different germination responses to
286 imbibition temperatures are mediated, at least in part, by transcriptional and hormonal
287 changes during imbibition. We therefore collected M⁺, M⁻ and IND samples from plants grown
288 at 20°C and 25°C parental temperature, respectively, during imbibition at four representative
289 temperatures (9°C, 14°C, 20°C, and 24°C). In the sampling scheme (Supplemental
290 Figure S1B), we considered physical (dry seed, 24 h imbibition) and physiological ($T_{1\%}$) times
291 representing the progression of germination. 9°C is the most germination-permissive (G_{max})
292 temperature for all morphs, still with a strong pericarp effect for 20IND (Figure 1C,
293 Supplemental Figure S1C). At 14°C, M⁺ and M⁻ seed germination is permitted, while
294 particularly 20IND fruit germination is inhibited more than at 9°C. This temperature was,
295 therefore, chosen to examine the effect of the pericarp further. Imbibition at 20°C represents
296 conditions when germination of all morphs is relatively inhibited, although a parental effect is
297 evident, as 25M⁺ seeds germinate more readily than 20M⁺ seeds. At 24°C, germination of all
298 diaspores is completely inhibited.

299

300 In the RNAseq analyses, counts of transcripts for 23594 genes of *Ae. arabicum* genome
301 version 2.5 (Haudry et al., 2013) were obtained for each sample (Supplemental Data Set 1).
302 To make the transcript abundance data easily and publicly accessible, we generated a gene
303 expression atlas which is implemented in the *Ae. arabicum* genome database (DB)
304 (Fernandez-Pozo et al., 2021) at https://plantcode.cup.uni-freiburg.de/aetar_db/index.php.
305 This tool is based on EasyGDB, a system to develop genomics portals and gene expression
306 atlases, which facilitates the maintenance and integration of new data and tools in future
307 (Fernandez-Pozo and Bombarely, 2022). The *Ae. arabicum* gene expression atlas is very
308 interactive and user-friendly, with tools to compare several genes simultaneously and multiple
309 visualization methods to explore gene expression. It includes the transcriptome results of this
310 work (135 datasets), of *Ae. arabicum* RNAseq work published earlier (Merai et al., 2019;
311 Wilhelmsson et al., 2019; Arshad et al., 2021), and allows adding future transcriptome
312 datasets. It also links to the newest version 3.1 of the *Ae. arabicum* genome annotation and
313 sequence DB (Fernandez-Pozo et al., 2021) and allows linking to any improved future
314 genome version. Further details and examples for the *Ae. arabicum* gene expression atlas, its
315 analysis and visualization tools are presented in Supplemental Figure S2.

316
317 Principal component analysis (PCA) based on Log (normalized counts) from 22200 of 23594
318 genes after removing those with zero counts was used to observe general trends in the
319 transcriptomes across the collected samples (Figure 2, Supplemental Figure S3). Prior to
320 imbibition, there were differences in the dry seed transcriptomes, and although these samples
321 cluster together in negative PC1 and PC2 coordinates (bottom left, Area A, Figure 2), a
322 modest number of differentially expressed genes (DEGs) were identified between the
323 samples (Supplemental Data Set 1). For example, there are 322 DEGs between the dry 20M⁺
324 seed and dry 25M⁺ seed transcriptomes, and 580 DEGs between dry 25M⁺ and dry 25M⁻
325 seed transcriptomes (Area A, Figure 2). Therefore, parental temperature and the pericarp
326 (IND vs DEH fruit development) therefore affected the dry seed transcriptomes. A broad trend
327 observed was that following increasing imbibition time: samples from seeds sown under
328 generally germination-permissive conditions traveled positively along PC1 (to Areas C and D,
329 Figure 2). Samples from seeds sown under germination-inhibiting conditions stay relatively
330 closer to dry seeds, further supporting that PC1 represents 'progress towards completing
331 germination' (Areas B, E and F, Figure 2). Reinforcing this, gene expression at an early

332 imbibition timepoint of the 20M⁺ seeds is closer to the 'dry seed' state (Area B, Figure 2). The
333 association between PC1 and final germination percentage is also evident in Supplemental
334 Figure S3, which provides an extended PCA analysis.

335

336 PC2 appears to generally separate IND and M⁺ from bare M⁻ seed, suggesting that PC2
337 relates to the 'pericarp removal' effect on transcriptome changes. However, 20M⁻ imbibed for
338 24 h at 9°C are amongst M⁺ samples on the PC2 axis (Area E, Figure 2). In particular, IND
339 fruits under non-germination permissive conditions, form a relatively tight cluster in the
340 negative PC1 and positive PC2 coordinates (Area F, Figure 2). Interestingly, during the
341 imbibition time course for 20M⁻ and 25M⁻, the 24 h time point is farther along the PC1 axis
342 positively than the later time points (100 h for 25M⁻, 75 h for 20M⁻), indicating the
343 transcriptomes in the later time points resemble that of the dry-seed transcriptome more so
344 than the earlier imbibition time points (Area B, Figure 2). Supporting this, more DEGs were
345 found between the 24 h time points of 20M⁻ (4402) and dry 20M⁻ seed compared to the 75 h
346 time point and dry 20M⁻ seed (3822), although there were fewer DEGs between the 24 h time
347 points of 25M⁻ (3400) and dry 25M⁻ seed compared to the 100 h time point and dry 25M⁻ seed
348 (3913) (Supplemental Data Set 1). Indeed, there is more variation than explained by only PC1
349 and PC2. While PC1 accounts for 25% and PC2 account for 14% of the variance (Figure 2),
350 PC3 accounts for 11% of the variance and may have some relation to imbibition temperature
351 (Supplemental Figure S3).

352

353 Despite 9°C imbibition permitting ca. 50% final germination, all imbibed 20IND fruit
354 transcriptomes (24, 75, 125 h) clustered within Area F (Figure 2). Whereas 25IND fruits
355 imbibed at 9°C for 24 h were also in Area F, 25IND fruit transcriptomes imbibed at 9°C for
356 75 h were in Area D together with the 'germinating' transcriptomes of M⁺ seed imbibed at 9°C
357 and 14°C. Further, pericarp removal resulted in transcriptomes of M⁻ seed located in Area C
358 at 75 h, indicating a strong effect of the pericarp on the 20IND fruit transcriptomes (Figure 2).
359 Thus, it is evident that M⁺ and M⁻ differ in gene expression already in the dry state, and M⁺, M⁻
360 , and IND differ more so following imbibition. Further, the transcriptomes are strongly
361 influenced by imbibition temperature and pericarp removal. As a whole, the transcriptomes
362 appear to reflect the status in terms of progress towards germination or dormancy, and the
363 presence or absence of the pericarp in the case of seeds from IND fruits.

364

365 **Co-expressed gene modules in dry and imbibed seed transcriptomes associated with**
366 **morph-specific germination responses**

367

368 To further compare gene expression patterns between M⁺, M⁻, and IND at different imbibition
369 temperatures associated with the regulation of germination progression, we grouped genes
370 by their temperature-, time-, and morph-dependent expression patterns using weighted gene
371 correlation network analysis (WGCNA) (Zhang and Horvath, 2005). This separated 11260
372 expressed genes into 11 modules each containing co-expressed genes (Figure 3A,
373 Supplemental Figure S4, gene lists in Supplemental Data Set 2): black (523 genes); blue
374 (1439); brown (1373); green (649); grey (2214); magenta (341); pink (365); purple (259); red
375 (560); turquoise (2213); and yellow (1324). Figure 3A shows how neighboring genes in the
376 PCA are clustered together and documents expression of genes in the modules during
377 imbibition at 9°C.

378

379 Correlation between genes in the modules and associated PCs, temperatures, traits (morph,
380 GR_{50%}, G_{max}), and quantified seed hormone contents facilitated investigation of potential roles
381 of gene modules in morph-specific germination responses (Figure 4). Sample traits were
382 clustered by their correlation patterns with module gene expression (using absolute values
383 allowed positive and negative correlations to cluster together). Expression of purple and
384 turquoise module genes was strongly positively correlated with GR_{50%} and G_{max}. In contrast,
385 expression of genes in the yellow, green, and red modules was strongly negatively correlated
386 with GR_{50%} and G_{max}. This suggested that expression of genes in the turquoise and purple
387 modules supports a germination-promoting program. In contrast, expression of genes in the
388 green, yellow, and red modules drives germination prevention or dormancy. Sample PC1
389 coordinates showed a similar trend reflecting the previously mentioned association between
390 PC1 and germination. Seed ABA content, which showed the inverse pattern consistent with
391 its negative association with germination, was highly positively correlated with yellow and
392 green module gene expression and negatively correlated with blue, purple, and turquoise
393 module gene expression. Brown and black module gene expression was highly positively
394 correlated, and the pink module strongly negatively correlated with pericarp presence and
395 PC2. Expression of yellow, green, and red module genes was also positively correlated with

396 imbibition temperature and PC3 (reflecting the association previously mentioned), and purple
397 and turquoise negatively correlated with imbibition temperature. This is consistent with the
398 association between high temperatures and delayed germination. However, the overall
399 correlation trends differed from those with G_{max} and $GR_{50\%}$ demonstrated by tree distance.
400 This can be explained by differences, such as in magenta module gene expression, which
401 was strongly negatively correlated with temperature, but not strongly correlated with
402 germination traits. Parental temperature *per se* was not strongly correlated to any module
403 eigengene.

404

405 We further investigated differences in module gene expression between specific sample pairs
406 on a per module basis. Expression of genes in the black module was for example elevated in
407 IND fruits and M^+ seeds compared to M^- seeds, indicating it is associated with pericarp
408 presence, but not germination kinetics *per se*, as expression in IND fruits and M^+ seed is
409 similar despite their contrasting germination kinetics. Expression within the brown module was
410 elevated in IND fruits compared to both M^+ and M^- at all imbibition temperatures, indicating a
411 morph-specific and pericarp-dependent expression pattern associated with a delay in
412 germination. Expression within the red module was strongly negatively correlated with
413 germination, increased during imbibition under non-permissive germination conditions and
414 tended to be more highly expressed in IND than M^- (for example during imbibition at 20°C).
415 Expression within the green module was strongly correlated with conditions non-permissive
416 for germination: higher in germination-delayed IND than in M^+ and M^- germinating at 9°C and
417 14°C. Expression was high in all parental temperature \times morphs at 20°C, perhaps except for
418 25 M^+ , which did indeed germinate better relative to the other parental temperature \times morphs
419 at 20°C. Expression within the green module was higher in 20IND than 25IND at 9°C and
420 14°C correlating with strength of the pericarp-dependent delay of germination at these
421 temperatures.

422

423 Genes within the yellow module were highly expressed in dry seeds compared to imbibed
424 seeds and also strongly negatively correlated with germination (Figures 3A and 4). Gene
425 expression decrease in the yellow module over time was delayed under conditions preventing
426 germination and by the presence of the IND pericarp, more in 20IND than 25IND. Yellow
427 module gene expression may be maintained or increased during prolonged inhibition of

428 germination. For example, yellow module gene expression increased in M⁻ seeds, and
429 perhaps in 20M⁺, imbibed at 20°C. Inverse to this pattern is the turquoise module where
430 expression was strongly correlated with germination and repressed by the presence of the
431 pericarp, especially in IND fruits from plants grown at 20°C. Expression within the pink
432 module was strongly correlated with pericarp removal: highly expressed in M⁻ seed compared
433 to IND fruit and M⁺ seed. Compared to other modules, genes in the grey module were more
434 stably expressed across all treatments, but expression correlated positively with germination
435 and negatively with imbibition and imbibition temperature. Genes in the magenta module were
436 expressed more highly at lower than higher imbibition temperatures, and their expression was
437 generally higher in IND than in M⁺ or M⁻ (apart from seeds/fruits from plants grown at 20°C
438 and imbibed at 9°C). This module appears to be mostly associated with imbibition
439 temperature.

440

441 Expression within the blue module was not generally strongly contrasting dependent on
442 morph or pericarp removal, increased following imbibition, and was generally elevated during
443 imbibition at lower temperatures. Expression within the purple module was strongly positively
444 correlated with germination and negatively with imbibition temperature. Its expression was
445 somewhat opposite of the green module, with high expression associated with germination
446 permissive temperatures for M⁺, M⁻, and IND, and higher in 25IND than 20IND at 9°C and
447 14°C, also indicating negative association with pericarp-dependent delay of germination.

448

449 To gain further insight into which biological processes are associated with the promotion or
450 delay of germination by morph, pericarp, imbibition temperature, or parental growth
451 temperature, we performed Gene Ontology (GO) term enrichment analysis of the co-
452 expressed gene modules (Supplemental Data Set 2). This revealed links between expression
453 trends and module gene functions. For example, the GO terms 'seed dormancy process' was
454 the most enriched in the green module, with 'response to abscisic acid' also the 24th most
455 enriched GO term. Other terms enriched in the green and yellow modules were also
456 suggestive of dormancy, for example, 'lipid storage' and 'chlorophyll catabolic process'.
457 Conversely, 'translation' was the most enriched GO term in the turquoise module, with a
458 number of cell-wall remodeling-related GO terms (e.g. 'cell wall pectin metabolic process',
459 'plant-type cell wall organization') and terms suggestive of increased metabolism, promotion

460 of growth and transition to seedling highlighted in the turquoise and purple modules in which
461 expression of the included genes was positively correlated with germination (e.g. 'isopentenyl
462 diphosphate biosynthetic process', 'methylerythritol 4-phosphate pathway', 'response to
463 cytokinin', 'multidimensional cell growth', 'photosystem II assembly', 'gluconeogenesis' and
464 'glycolytic process'). Consistent with module gene functional enrichment and module gene
465 expression correlation with ABA content (Figure 4), genes related to abscisic acid (ABA)
466 biosynthesis are, for example, in the yellow, green, and brown module, for ABA degradation
467 in the blue and grey module, and ABA receptor genes in the turquoise and purple module.
468 ABA and cell-wall remodeling processes are discussed in more detail below.

469
470 In summary, out of these 11 gene modules (Figure 3), four are mainly associated with
471 germination delay (brown, red, green, yellow); four are associated with germination
472 stimulation (purple, turquoise, pink, grey); two are associated with imbibition temperature
473 (grey, magenta); one associated mainly with imbibition (blue), four are associated with
474 pericarp presence (black, brown, red, yellow), and one is associated with pericarp removal
475 (pink).

476
477 **The role of the pericarp in altering abscisic acid metabolism and in morph-specific
478 hormonal mechanisms to control dormancy and germination responses to temperature**
479

480 While obviously many parameters contribute to the control of germination via modified gene
481 expression patterns, the final "decision" depends to a large extend on the level and balance of
482 several plant hormones in *A. thaliana* (Finch-Savage and Leubner-Metzger, 2006; Nambara
483 et al., 2010; Linkies and Leubner-Metzger, 2012) and *Ae. arabicum* (Merai et al., 2019; Merai
484 et al., 2023). We therefore quantified plant hormone metabolites using the same sampling
485 scheme as for the RNAseq analysis (Supplemental Figure S1). In the IND fruit, the pericarp
486 makes up 74.4% of the morph's mass but at maturity does not contain living cells (Arshad et
487 al., 2019; Arshad et al., 2020; Arshad et al., 2021). Transcript abundance patterns for mature
488 dry and imbibed IND fruits therefore represent gene expression changes solely in the M⁻ seed
489 (Lensser et al., 2016; Wilhelmsson et al., 2019; Arshad et al., 2021). The dead IND pericarp
490 however contains hormone metabolites (Lensser et al., 2018) and we therefore quantified the
491 hormone metabolites separately for the two fruit compartments (M⁻ seed and IND pericarp).

492 The pericarp-imposed dormancy of 20IND fruits at 9°C and 14°C imbibition temperature was
493 associated with abscisic acid (ABA) accumulation in 20M⁻ seeds during the imbibition of intact
494 20IND fruits (that is ABA content inside M⁻ seeds which were separated from the pericarp
495 after imbibition at the times indicated) (Figure 5). In contrast, the ABA contents of 20M⁺ seeds
496 and of bare 20M⁻ seeds (that is ABA content in imbibed M⁻ seeds which were separated from
497 the pericarp *prior* to imbibition, i.e. in the dry state) steadily decreased upon imbibition at
498 permissive temperatures.

499

500 In agreement with the high ABA content in seeds, transcript abundance for *AearNCED6* (9-
501 *cis*-epoxycarotenoid dioxygenase), a key gene in ABA biosynthesis, increased in the seeds of
502 imbibed 20IND fruits, and decreased in 20M⁺ and bare 20M⁻ seeds upon imbibition at 9°C and
503 14°C (Figure 5). A similar expression pattern was evident for other ABA biosynthesis genes
504 (Supplemental Figure S5). Consistent with a role of parental temperature, the pericarp-
505 imposed dormancy was reduced in 25IND as compared to 20IND fruits, and the ABA contents
506 declined in the seeds of imbibed 25IND fruits, as well as in 25M⁺ and bare 25M⁻ seeds upon
507 imbibition at 9°C and 14°C (Figure 5). Despite this decline, the ABA content in seeds of
508 imbibed 25IND fruits remained higher compared to 25M⁺ and 25M⁻ seeds. The observed
509 increase of transcript abundance for *AearNCED6* and other ABA biosynthesis genes at 9°C
510 and 14°C imbibition temperature was somewhat reduced in 25IND compared to 20IND fruits
511 (Figure 5, Supplemental Figure S5). At the non-permissive imbibition temperatures 20°C and
512 24°C for 20IND and 25IND germination, transcripts for *AearNCED6* and other ABA
513 biosynthesis genes accumulated most strongly in seeds of imbibed IND fruits, also somewhat
514 in bare M⁻ seeds, but not in M⁺ seeds. At 20°C imbibition temperature, the ABA content also
515 increased in seeds of imbibed IND fruits and in bare M⁻ seeds, but not in M⁺ seeds. Taken
516 together, these findings suggest that ABA accumulation due to *de novo* ABA biosynthesis by
517 *AearNCED6* and other ABA biosynthesis genes explains, at least in part, the distinct
518 responses of the morphs to parental and imbibition temperatures, revealing that germination
519 inhibition by elevated ABA levels is a key mechanism of the pericarp-imposed dormancy in
520 20IND fruits.

521

522 In further support of the importance of ABA in the control of the pericarp-imposed dormancy,
523 the enhanced degradation of ABA in the M⁺ seed morph upon imbibition was associated with

524 increased transcript abundances for *AearCYP707A3* and other ABA 8'-hydroxylases, while
525 their expression remained low in the corresponding IND fruit morph (Figure 5, Supplemental
526 Figure S5). Therefore, the expression patterns of *AearCYP707A3* (highest in M⁺ seeds,
527 lowest in IND fruits, intermediate in M⁻ seeds) were, in most cases, inverse to the *AearNCED6*
528 expression patterns. Further to this, the expression patterns for gibberellin biosynthesis (GA3-
529 oxidases) and inactivation (GA2-oxidases) genes were inverse to the ABA biosynthesis
530 (NCED) and inactivation (CYP707A) genes (Supplemental Figure S5D). In addition to ABA
531 metabolism, the presence of the pericarp also enhanced the transcript accumulation for the
532 plasma membrane ABA uptake transporter gene *AearABCG40* (an ABC transporter of the G
533 subfamily) and the *AearDOG1* (*Delay of germination 1*) dormancy gene in a morph-specific
534 and temperature-dependent manner (Figure 5).

535
536 Hormone metabolite contents per pericarp of ABA, its 8'-hydroxylase pathway breakdown
537 compounds phaseic acid (PA) and dihydrophaseic acid (DPA), as well as for jasmonic acid
538 (JA), its bioactive isoleucine conjugate (JA-Ile) and for salicylic acid (SA), were in general 10
539 to 20 fold higher in the dry state declined rapidly in the pericarp upon imbibition at any
540 temperature (Figure 6A; Supplemental Figure S6). In contrast to these hormone metabolites,
541 the contents per pericarp of *cis*-(+)-12-oxophytodienoic acid (OPDA), which is an oxylipin
542 signaling molecule and JA biosynthesis precursor (Linkies and Leubner-Metzger, 2012; Dave
543 et al., 2016), did not decline during imbibition and its contents in the pericarp remained much
544 higher compared to the encased M⁻ seed (Supplemental Figure S6B,C). When the ABA, PA,
545 DPA, JA, JA-Ile, SA, and OPDA contents of diaspore compartment (seed *versus* pericarp)
546 were compared, they were, in general, >20 times (dry state) and >5 times (imbibed state)
547 higher in the pericarp compared to the M⁻ seed extracted from the IND fruit (Figure 6A;
548 Supplemental Figure S6). An exception from this was ABA in 20IND fruits where the contents
549 per compartment (pericarp *versus* encased M⁻ seed) during late imbibition at 9°C and 14°C
550 were roughly equal, but in 25IND fruits ABA was higher in the pericarp compared to the
551 encased M⁻ seed also during imbibition (Figure 6A; Supplemental Figure S6C). Although SA
552 declined rapidly in the pericarp during imbibition, its contents remained much higher in the
553 pericarp also during late imbibition as compared to the encased M⁻ seed. Further to this
554 comparison (pericarp *versus* encased M⁻ seed), the hormone metabolite contents of imbibed
555 bare M⁻ seeds and imbibed M⁺ seeds were always lower compared to IND fruits (Figures 6A;

556 Supplemental Figure S6). The contents of the auxin indole-3-acetic acid (IAA) were low in M⁺
557 and M⁻ seeds. IAA was below limit of detection in pericarp tissue, but significant amounts of
558 the major IAA degradation product 2-oxoindole-3-acetic acid (oxIAA) were detected
559 (Supplemental Figure S6), suggesting that IAA degradation occurred during the late stages of
560 pericarp development.

561

562 Leachates of inhibitors from pericarp tissue, including ABA, OPDA, and phenolic compounds,
563 may inhibit germination and thereby contribute to coat dormancy (Ignatz et al., 2019;
564 Mohammed et al., 2019; Grafi, 2020). In agreement with this, pericarp extracts (PE) and ABA
565 both delayed the germination of bare M⁻ seeds (Supplemental Figure S7A). PE application
566 explained the delayed 20IND fruit germination only partially, but the delay could be fully
567 mimicked by exposure to 5 μ M ABA (Supplemental Figure S6A). Treatment of M⁻ seeds with
568 PE delayed their germination, concordant to the delay of 25IND fruit germination at 9°C
569 imbibition (Supplemental Figure S7C). In contrast to PE and ABA, treatment of seeds with
570 SA, OPDA, JA, or JA-Ile did not appreciably affect seed germination (Supplemental Figure
571 S6D), and PE from 20IND and 25IND pericarps did not differ in their inhibitory effects
572 (Supplemental Figure S7C-D). To investigate if PE and ABA treatment of bare M⁻ seeds can
573 mimic the pericarp effect on gene expression as observed in imbibed IND fruits, we
574 conducted RT-qPCR of representative genes for each WGCNA module. In several cases, the
575 ABA treatment indeed mimicked the PE effect (Supplemental Figure S7B), but neither PE nor
576 ABA could fully mimic the effect of the intact pericarp. We, therefore, conclude that leaching
577 of ABA or other inhibitors from the pericarp is not the major component by which the pericarp
578 exerts its effects on gene expression and germination responses.

579

580 Pericarp properties are known to affect embryo ABA sensitivity, oxygen availability, and the
581 biomechanics of germination (Benech-Arnold et al., 2006; Hoang et al., 2013; Steinbrecher
582 and Leubner-Metzger, 2017). Biomechanical analysis revealed that the tissue resistance at
583 the micropylar pericarp (where the radicle emerges during germination of fruit-enclosed
584 seeds) was slightly higher in 20IND as compared to 25IND pericarps (Figure 6B and
585 Supplemental Figure S8). Tissue resistance at the non-micropylar pericarp was higher and
586 did not differ between 20IND and 25IND. Parental temperature is also known to affect
587 dormancy via the seed coat pro-anthocyanidin content. Multispectral imaging (MSI) can

588 visualize this and unknown differences in the biochemical composition of seed coats that
589 affect reflectance spectra (Penfield and MacGregor, 2017). Figure 6C shows that MSI
590 detected unknown differences in the biochemical composition between 20IND and 25IND
591 fruits. The distinct parental temperatures therefore affected pericarp development leading to
592 distinct biochemical compositions upon maturity. These differences in 20IND and 25IND
593 pericarp biomechanics and biochemistry may also be associated with altered pericarp oxygen
594 permeability.

595

596 **Evidence for pericarp-mediated hypoxia, morph-specific transcription factor
597 expression, and ABA signaling in the control of *Ae. arabicum* dormancy and
598 germination**

599

600 To identify transcription factor (TF) genes and corresponding target *cis*-regulatory elements
601 (TF binding motifs/sites), we conducted enrichment analyses for each WGCNA module
602 described above. Enriched motifs from the ArabidopsisDAPv1 database (O'Malley et al.,
603 2016) for each module are compiled in Supplemental Data Set 3. The chord diagram
604 (Figure 7A) shows identified *Ae. arabicum* TF genes in each WGCNA module and their
605 connection to corresponding target *cis*-regulatory motifs. For example, for ABA-related bZIP
606 TFs (Nambara et al., 2010) such as ABA Insensitive 5 (ABI5, green module), ABA-responsive
607 element (ABRE)-binding proteins or ABRE-binding factors (ABFs) such as AREB3 (yellow
608 module), G-box binding factors (GBFs) such as GBF3 (red module), motifs were enriched in
609 the green module (Figure 7A, Supplemental Data Set 3). Another example are hypoxia-
610 related TFs of the ethylene response factor (ERF) group VII that are known to induce gene
611 expression upon hypoxia by binding to motifs such as the ERF73 *cis*-regulatory element and
612 the hypoxia-responsive promoter element (HRPE) of hypoxia-responsive genes (Gasch et al.,
613 2016). In *A. thaliana* the ERF group VII has five members: ERF73/HRE1 (HYPOXIA
614 RESPONSIVE ERF1), ERF71/HRE2, RAP2.2 (RELATED TO APETALA2.2), RAP2.3, and
615 RAP2.12. A comparison of several Brassicaceae genomes, including *A. thaliana* and *Ae.
616 arabicum*, revealed a high number of conserved noncoding sequences (Haudry et al, 2013).
617 The ABRE and HRPE motifs and the TFs binding to these *cis*-regulatory elements, are
618 enriched in promoters of hypoxia-responsive and ABA-responsive genes and widely
619 conserved among multiple species (Gasch et al. 2016; Gomez-Porras et al., 2007; O'Malley

620 et al. 2016). Their roles in inducing their hypoxia-responsive target genes have been well
621 investigated for the fermentation enzymes alcohol dehydrogenase (ADH) and pyruvate
622 dehydrogenase (PDC) (Kürsteiner et al., 2003; Yang et al., 2011; Papdi et al., 2015; Gasch et
623 al., 2016; Seok et al., 2022). In *Ae. arabicum* ERF73 and HRPE motifs were enriched in the
624 grey, yellow, and brown modules, and putative target genes *AearADH1a* and *AearPDC2* are
625 gene members of these modules (Figure 7A, Supplemental Data Set 3). In contrast to *A. thaliana*
626 which has *AtERF71* and *AtERF73* as two highly related group VII ERF genes, there
627 is only one homolog in *Ae. arabicum*, member of the grey module, which we named
628 *AearERF71/73* (*AearHRE1/2*) as its sequence is equally homologous to either of the two *A. thaliana*
629 genes. Also, in contrast to *A. thaliana*, which has only one ADH gene (*AtADH1*),
630 there are two ADH genes in *Ae. arabicum*, namely *AearADH1a* (brown module) and
631 *AearADH1b* (green module) (Figure 7A).

632

633 Figure 7B shows that *AearERF71/73* and *AearADH1a* transcripts accumulated in *Ae. arabicum* IND fruits upon imbibition, while their transcript abundances in M⁻ and M⁺ seeds
634 remained low. *AearPDC2* had a similar expression pattern in that the transcript abundances
635 were highest in IND fruits (Supplemental Figure S9). In contrast to *AearADH1a* and
636 *AearPDC2*, the expression of *AearADH1b* (the second *Ae. arabicum* ADH gene) and
637 *AearPDC1* remained comparatively low, and *AearLDH* (lactate dehydrogenase) was less
638 consistently elevated in imbibed IND fruits compared to M⁻ and M⁺ seeds (Figure 7B;
639 Supplemental Figure S9). Taken together, this suggested that hypoxia conferred to IND fruits
640 by the pericarp may lead to the induction of the ethanolic fermentation pathway with
641 *AearADH1a* and *AearPDC2* as hypoxia-responsive target genes (Figure 7C), as it is known
642 for the hypoxia-response of the *AtADH1* and *AtPDC1* genes (Kürsteiner et al., 2003; Yang et
643 al., 2011; Papdi et al., 2015; Gasch et al., 2016; Seok et al., 2022). To investigate the ABA
645 and hypoxia-regulated expression further, we compared the *Ae. arabicum* and *A. thaliana*
646 *ADH*, *PDC*, *ERF71/73*, *LDH*, and *DOG1* genes for *cis*-regulatory binding motifs using FIMO
647 (Figure 7C, D; Supplemental Figures S9, S10; Supplemental Data Set 4). The focus of this
648 analysis was on the widely conserved general HRPE, ABRE, ERF73, and binding motifs for
649 Homeobox (HB) TFs (see Supplemental Figure S10A for best possible matches of *cis*-
650 regulatory binding motifs in *Ae. arabicum* genes). The binding motifs for HB TF were included
651 in this analysis because they are known to control seed-to-seedling phase transition, seed

652 ABA sensitivity, dormancy, longevity and embryo growth in *A. thaliana* (Barrero et al., 2010;
653 Wang et al., 2011; Bueso et al., 2014; Silva et al., 2016; Stamm et al., 2017). The
654 *AearADH1a* and *AearPDC2* 5'-regulatory gene region contain ERF73 and HRPE motifs and
655 are distinct from the *AtADH1*, *AearPDC1* and *AearADH1b* 5'-regulatory gene regions in that
656 they don't contain G-box/ABRE motifs (Figure 7C, Supplemental Figure S9). The
657 *AearERF71/73* 5'-regulatory gene region was also distinct from its *A. thaliana* homologs by
658 the presence of two ERF73 motifs, suggesting that the *AearERF71/73* gene possibly provides
659 a positive feedback regulation on the pericarp/hypoxia-mediated *AearADH1a*, *AearPDC2* and
660 *AearERF71/73* expression (Figure 7C). Further details of this hypothetical working model are
661 described and discussed in Supplemental Figure S9. In contrast to the ethanolic fermentation
662 pathway (PDC-ADH, substrate pyruvate), which is up-regulated in IND fruits (Figure 7,
663 Supplemental Figure S9), the seed-specific 'Perl's pathway,' which controls pyruvate
664 production (Weitbrecht et al., 2011), is down-regulated in IND fruits as compared to bare M⁻
665 seeds (Supplemental Figure S11).

666

667 To test if *AearERF71/73*, *AearADH1a* and *AearPDC2* and other candidate genes are indeed
668 regulated by hypoxia we analyzed their expression in bare M⁻ seeds imbibed under hypoxia
669 conditions (Figure 8). Gasch et al. (2016) identified a list of 49 core hypoxia-responsive genes
670 in *A. thaliana* seedlings which includes *AtERF73*, *AtADH1* and *AtPDC2*. Of these 49 core
671 hypoxia-responsive *A. thaliana* genes, we identified from the transcriptome analysis that
672 expression of 14 of 41 putative *Ae. arabicum* orthologs was elevated in IND fruits, whereas
673 their expression in M⁻ and M⁺ seeds remained low. Examples are presented in Supplemental
674 Figure S12 and include *AearHRA1*, *AearETR2*, *AearNAC102*, *AearJAZ3*, *AearHHO2*, and
675 other *Ae. arabicum* homologs from the core list of *A. thaliana* hypoxia-responsive genes
676 (Christianson et al., 2009; Gasch et al., 2016; Ju et al., 2019). Figure 8A shows that the
677 germination of bare M⁻ seeds is indeed severely delayed under hypoxia (4.5% oxygen) as
678 compared to normoxia (21% oxygen) conditions. This resulted in the hypoxia-mediated
679 induction of the *AearERF71/73*, *AearADH1a*, *AearPDC2*, *AearHRA1*, *AearETR2*, *AearJAZ3*,
680 *AearNAC102*, *AearHHO2*, and other genes (Figure 8A, Supplemental Figure S13A). Hypoxia
681 delayed the germination of bare M⁻ seeds similar to the pericarp in IND fruits, in both cases
682 the T_{1%} was ca. 100 h (Supplemental Figure S13B). M⁻ seed germination was also delayed by

683 5 μ M ABA, and the combined treatment (hypoxia+ABA) had a stronger inhibitory effect on
684 germination (Figure 8A).

685

686 The importance of ABA signaling in the control of *Ae. arabicum* pericarp-imposed dormancy
687 of IND fruits was evident in the expression patterns of ABRE-binding (ABI5, AREBs/ABFs)
688 and G-box-binding (GBFs) bZIP TF genes. Transcripts of *AearAREB3a*, *AearAREB3b*,
689 *AearABI5*, *AearABF1*, *AearABF2*, *AearABF3*, *AearABF4*, *AearGBF1*, *AearGBF2*, *AearGBF3*,
690 and *AearGBF4* were up-regulated in M⁻ seeds inside IND fruits, and in general expressed
691 lowly in isolated M⁻ seeds and in M⁺ seeds (Figure 9; Supplemental Figure S14A). By
692 contrast, *AearGBF5*, *AearRAP2.12*, and the transcript abundances of several HB TF including
693 *AearHB13* were down-regulated in M⁻ seeds inside IND fruits (Figure 9, Supplemental
694 Figure S14B). In *A. thaliana*, these bZIP TFs are also known to control the ABA-related
695 expression, including for the *AtADH1* gene, by binding to G-box and ABRE 5'-regulatory
696 motifs (Lu et al., 1996; Gomez-Porras et al., 2007; Nambara et al., 2010; Yoshida et al., 2010;
697 O'Malley et al., 2016). HB13 and HB20 TFs constitute node-regulators within the co-
698 expression network controlling seed-to-seedling phase transition (Silva et al., 2016) while
699 other HB TFs control seed ABA sensitivity, dormancy, longevity and embryo growth (Barrero
700 et al., 2010; Wang et al., 2011; Bueso et al., 2014; Stamm et al., 2017; Renard et al., 2021).
701 Transcript abundance patterns of ABA signaling components including for the protein
702 phosphatase 2C protein HAB1 (Nambara et al., 2010) also exhibit pericarp-affected
703 expression patterns in the *Ae. arabicum* morphs (Supplemental Figure S14C). Figure 8A
704 shows that in bare M⁻ seeds imbibed under hypoxia, many ABA-related genes and the
705 dormancy gene *AearDOG1* are up-regulated by hypoxia. In contrast to this, hypoxia or the
706 presence of the pericarp caused down-regulation of genes encoding cell wall-remodeling
707 proteins (see next section). Expression of components of the general RNA polymerase II
708 transcription elongation complex, ribosomal proteins, and 20S proteasome subunits differed
709 during *Ae. arabicum* fruit morph development (Wilhelmsson et al., 2019). Related *Ae.*
710 *arabicum* genes, especially of the turquoise, purple, and pink WGCNA modules, exhibited
711 distinct pericarp-affected expression patterns (Supplemental Figure S15), which persisted
712 throughout imbibition.

713

714 **The role of morph-specific and temperature-dependent expression patterns of cell wall-
715 remodeling genes for *Ae. arabicum* germination and dormancy responses**

716

717 Cell wall-remodeling by expansins, and enzymes targeting xyloglucans, pectins, and other
718 cell wall components are required for successful embryo growth and for restraint weakening
719 of covering structures in seed and fruit biology (Graeber et al., 2014; Shigeyama et al., 2016;
720 Steinbrecher and Leubner-Metzger, 2017; Arshad et al., 2021; Steinbrecher and Leubner-
721 Metzger, 2022). The expression ratio of expansin genes between M⁺ seed within IND fruit and
722 bare M⁻ seed at 24 h or T_{1%} remained very low at any imbibition temperature (Figure 10A;
723 Supplemental Figure S16A). Consistent with this, transcripts of all *Ae. arabicum* type
724 expansins (Figure 10C; Supplemental Figure S16C) were only induced in M⁺ and bare M⁻
725 seeds, but not appreciably in imbibed IND fruits. Similar results were obtained for xyloglucan
726 endotransglycosylases/hydrolases (XTHs) for 20IND fruits, whereas considerable induction
727 was observed for 25IND fruits at the permissive imbibition temperatures (9°C and 14°C). In
728 addition to XTHs, xyloglucan remodeling is achieved by a battery of bond-specific
729 transferases and hydrolases (Figure 10B), and in the *Ae. arabicum* transcriptomes, most of
730 them belong to the turquoise WGCNA module with *αXYL1* as an example (Figure 10). Higher
731 transcript expression in bare 20M⁻ seeds as compared to 20IND fruits was observed for
732 *αFUCs*, *βGALs*, *βXYL*, and *GATs* (Supplemental Figure S16D), suggesting that the pericarp-
733 mediated repression and the resultant reduction in xyloglucan remodeling is part of the 20IND
734 dormancy mechanism. The induction in 25IND fruits that eventually germinate further
735 supports the importance of these genes and their products in the germination process.
736 Expression comparison of M⁺ seeds and isolated M⁻ seeds further confirm that the presence
737 of the pericarp is the most important factor for the expression differences between the
738 dimorphic diaspores.

739

740 In contrast to the observed hypoxia-induced expression of many genes, hypoxia inhibited the
741 induction of the expansin, XTH and *αXYL1* cell wall-remodeling gene expression in imbibed
742 bare M⁻ seeds (Figure 8A). Compared to hypoxia, ABA was far less effective and did not
743 appreciably inhibit the induction of the accumulation of *AearEXPA2*, *AearEXPA9*, *AearXTH4*,
744 *AearXTH16a* and *AearαXYL1* transcripts. The pericarp effect on the gene expression patterns
745 (IND fruits versus bare M⁻ seeds) observed in the transcriptome analysis was confirmed in the

746 completely independent RT-qPCR experiment for these cell wall-remodeling genes and for
747 most of the total of 32 genes investigated (Supplemental Figure S13C). While for the
748 representative genes for each WGCNA module pericarp extract did not affect the gene
749 expression of bare M⁻ seeds (Supplemental Figure S13C), hypoxia conditions affected it for
750 about half of the representative genes (Figure 8B). Correlation analysis between the pericarp
751 effect imposed to M⁻ seeds in imbibed IND fruits and the hypoxia and ABA effects on imbibed
752 bare M⁻ seeds was conducted for the 32 genes of the RT-qPCR experiment (Figure 8C). This
753 revealed strong linear relationships (R^2 0.7-0.8) for hypoxia versus pericarp, and
754 hypoxia+ABA versus pericarp, but not for ABA alone versus pericarp. Taken together,
755 hypoxia generated by the pericarp seems to be the most important mechanism of the
756 pericarp-mediated dormancy of IND fruits, it seems to act upstream of ABA and affects the
757 gene expression in M⁻ seed encased by the pericarp to control the observed distinct
758 dormancy and germination responses at the different imbibition temperatures.

759

760

761 **Discussion**

762

763 ***Aethionema arabicum* seed and fruit dimorphism: large-scale molecular data sets**
764 **reveal diaspore bet-hedging strategy mechanisms in variable environments**

765

766 Ambient temperature during seed reproduction (parental temperature) and after dispersal
767 (including imbibition temperature) is a major determinant for fecundity, yield, seed
768 germinability (i.e. nondormancy versus dormancy of different depth), and environmental
769 adaptation. The effect of temperature variability has been well-studied in monomorphic annual
770 plants and mechanisms underpinning the germinability of the dispersed seeds were
771 elucidated (Donohue et al., 2010; Finch-Savage and Footitt, 2017; Fernandez-Pascual et al.,
772 2019; Iwasaki et al., 2022; Zhang et al., 2022). In contrast to monomorphic species, very little
773 is known about the morphological and molecular mechanisms that facilitate survival of
774 heteromorphic annual species. Diaspore heteromorphism is the prime example of bet-
775 hedging in angiosperms and is phenologically the production by an individual plant of two
776 (dimorphism) or more seed/fruit morphs that differ in morphology, germinability, and stress
777 ecophysiology to 'hedge its bets' in variable (unpredictable) environments (Imbert, 2002;
778 Baskin et al., 2014; Gianella et al., 2021).

779

780 An advantage of *Ae. arabicum* as a model system is that it exhibits true seed and fruit
781 dimorphism with no intermediate morphs (Lenser et al., 2016). Our earlier work revealed
782 molecular and morphological mechanisms underlying the dimorphic fruit and seed
783 development (Lenser et al., 2018; Wilhelmsson et al., 2019; Arshad et al., 2021), the distinct
784 dispersal properties of the M⁺ seed and IND fruit morphs (Arshad et al., 2019; Arshad et al.,
785 2020; Nichols et al., 2020), and the adaptation to specific environmental conditions
786 (Mohammadin et al., 2017; Bhattacharya et al., 2019; Merai et al., 2019; Merai et al., 2023).
787 Transcriptome and imaging analyses of the seed coat developmental program of the
788 mucilaginous *Ae. arabicum* M⁺ seed morph revealed that it resembles the 'default' program
789 known from the mucilaginous seeds of *A. thaliana*, *Lepidium sativum*, and other Brassicaceae
790 (Graeber et al., 2014; Scheler et al., 2015; Lenser et al., 2016; Arshad et al., 2021;
791 Steinbrecher and Leubner-Metzger, 2022). In contrast to this, the non-mucilaginous *Ae.*
792 *arabicum* M⁻ seed morph resembles *A. thaliana* seed mucilage mutants and thereby highlights

793 that the dimorphic diaspores enable the comparative analysis of distinct developmental
794 programs without the need for mutants. *Arabidopsis thaliana* accessions differ in depth of
795 their primary seed dormancy, reaching from the deep physiological to shallow dormancy
796 (Cadman et al., 2006; Barrero et al., 2010; Finch-Savage and Footitt, 2017); and *L. sativum*
797 seeds are completely non-dormant (Graeber et al., 2014). During seed imbibition, distinct
798 transcriptional and hormonal regulation either leads to the completion of germination or to
799 dormancy maintenance for which ABA metabolism and signaling, *DOG1* expression,
800 downstream cell wall remodeling and seed coat properties are key components (Finch-
801 Savage and Leubner-Metzger, 2006; Graeber et al., 2014; Footitt et al., 2020; Iwasaki et al.,
802 2022). The transcriptome and hormone data for *Ae. arabicum* M⁺ seeds confirmed these
803 mechanisms and their dependence on the imbibition temperature to either mount a
804 germination or a dormancy program typical for mucilaginous seeds (Cadman et al., 2006;
805 Scheler et al., 2015; Iwasaki et al., 2022). The *Ae. arabicum* dimorphic diaspore comparison
806 of these M⁺ seeds to IND fruits (and the bare M⁻ seeds) revealed how the pericarp of the IND
807 fruit morph imposes the observed coat dormancy.

808

809 **Pericarp-imposed dormancy: comparative analyses of indehiscent fruit and seed 810 morph germinability reveals mechanisms and roles in thermal responses**

811

812 The typical Brassicaceae fruit is dehiscent, opens during fruit maturation (dehiscence, *A.*
813 *thaliana* seed, *Ae. arabicum* M⁺ seed morph), and is considered to represent the ancestral
814 fruit type (Mühlhausen et al., 2013). Nevertheless, monomorphic species that disperse
815 various indehiscent fruit types by abscission evolved many times independently within the
816 Brassicaceae. Different roles of the pericarp in these dry indehiscent Brassicaceae diaspores
817 (siliques and silicles) were identified, including dispersal by wind, persistence in the seed
818 bank, retaining seed viability, delaying water uptake, releasing allelochemicals, and imposing
819 coat dormancy (Mamut et al., 2014; Lu et al., 2015b; Lu et al., 2017b, a; Sperber et al., 2017;
820 Mohammed et al., 2019; Khadka et al., 2020). Many of these monomorphic Brassicaceae
821 species with indehiscent fruits are desert annuals. Their indehiscent diaspores were not
822 investigated for the molecular mechanisms responding to distinct parental and imbibitional
823 temperatures. The *Ae. arabicum* dimorphic diaspore system with its single-seeded IND fruit
824 morph, provides an excellent system for investigating these mechanisms.

825

826 The pericarp of mature *Ae. arabicum* IND fruits is dead tissue that contains high amounts of
827 ABA, OPDA, JA, JA-Ile, and SA, as well as degradation products of ABA and IAA. Leaching
828 of these and other compounds into the fruit's proximal environment could have roles in
829 allelopathic interactions, as described for the dead pericarp of other species (Grafi, 2020;
830 Khadka et al., 2020). Leaching of pericarp inhibitors into the encased seed could also delay
831 fruit germination or confer 'chemical coat dormancy', as it was demonstrated for pericarp-
832 derived ABA in *Lepidium draba* (Mohammed et al., 2019), *Beta vulgaris* (Ignatz et al., 2019),
833 and *Salsola komarovii* (Takeno and Yamaguchi, 1991). Pericarp extracts of *Ae. arabicum* IND
834 fruits as well as ABA delayed M⁻ seed germination, but they could not fully mimic the pericarp-
835 imposed dormancy and effect on gene expression (Figure 5). Acting as a mechanical restraint
836 to water uptake and/or radicle protrusion is another way by which the pericarp may delay
837 germination or confer 'mechanical coat dormancy' (Sperber et al., 2017; Steinbrecher and
838 Leubner-Metzger, 2017). The *Ae. arabicum* IND pericarp is water-permeable (Lenser et al.,
839 2016), and we showed here that it weakens during imbibition. *Aethionema arabicum* pericarp-
840 imposed dormancy was enhanced by the lower parental temperature (20°C, 20IND fruits) as
841 compared to the higher parental temperature (25°C, 25IND fruits). This altered the pericarp
842 biochemically and its mechanical resistance, which was higher in 20IND pericarps (Figure 6),
843 as was the pericarp-imposed dormancy (Figure 1).

844

845 The role of the pericarp and other seed-covering structures in limiting oxygen availability to
846 the embryo (hypoxia) is another mechanism for coat-imposed dormancy (Benech-Arnold et
847 al., 2006; Mendiondo et al., 2010; Dominguez et al., 2019). Comparative transcriptome and
848 hormone analyses (IND, M⁻, M⁺) identified that upregulated expression of hypoxia-responsive
849 genes is a hallmark of imbibed IND fruits (i.e., in M⁻ seeds encased by the dead pericarp) as
850 compared to M⁺ seeds and bare M⁻ seeds (Figure 7). Identified hypoxia-responsive genes
851 include the hypoxia-induced ERF-VII TF *AearERF71/73* and the fermentation genes
852 *AearADH1a* and *AearPDC2*, but not *AearADH1b* and *AearPDC1*. While the *AearADH1a*,
853 *AearPDC2*, and *AtPDC1* gene 5'-regulatory region contain ERF73 and HRPE motifs, they do
854 not contain G-box/ABRE motifs as this is the case for the *AearADH1b*, *AearPDC1*, and
855 *AtADH1* genes. The relative importance of *AtERF71/73*, ABA-related, and other TFs in the
856 hypoxia-induced expression of the *AtADH1* gene in *A. thaliana* is not completely resolved (Lu

857 et al., 1996; Kürsteiner et al., 2003; Gomez-Porras et al., 2007; Yang et al., 2011; Papdi et al.,
858 2015; Gasch et al., 2016; Seok et al., 2022). For *Ae. arabicum*, we speculate that the
859 observed duplication of the ADH genes, the differences in the *cis*-regulatory motifs, the
860 accumulation of *AearADH1a* and *AearPDC2* transcripts in M⁻ seeds inside IND fruits, and
861 pericarp-mediated hypoxia leading to PDC-ADH catalyzed ethanolic fermentation constitute a
862 morph-specific adaptation that contributes to the increased dormancy of IND fruits.

863

864 **Morphological and hormonal regulation: pericarp-ABA interactions as a key**
865 **mechanism for distinct post-dispersal dimorphic diaspore responses to environmental**
866 **cues**

867

868 Earlier work with dormant barley grains and sunflower demonstrated that hypoxia, imposed
869 either artificially or by the maternal seed covering structures (barley glumellae, sunflower
870 pericarp), interfered with ABA metabolism and increased embryo ABA sensitivity (Benech-
871 Arnold et al., 2006; Mendiondo et al., 2010; Andrade et al., 2015; Dominguez et al., 2019). In
872 barley, this included transient ABA accumulation and ABI5 gene expression during dormancy
873 maintenance. In sunflower, the pericarp-imposed dormancy was associated with increased
874 embryo sensitivity to hypoxia and ABA, but with no change in embryo ABA content
875 (Dominguez et al., 2019). As in *Ae. arabicum* pericarp (Figure 6), sunflower pericarp also
876 contained considerable amounts of ABA, SA, OPDA, JA, and JA-Ile (Andrade et al., 2015). In
877 general, their contents declined during imbibition in both species, except ABA, which
878 accumulated transiently in the sunflower pericarp, but declined in the dead pericarp of *Ae.*
879 *arabicum*. The *Ae. arabicum* IND fruit versus M⁻ seed comparison revealed the decisive role
880 of the pericarp and ABA in narrowing the germination-permissive window (Figure 1). Using
881 the three-way transcriptome and hormone comparison (IND, M⁻, M⁺), we could identify
882 mechanisms not existing in monomorphic species. These include a very clear temperature-
883 dependent up-regulation of ABA biosynthesis genes (including *AearNCED6*) and down-
884 regulation of ABA 8'-hydroxylase (including *AearCYP707A3*) in M⁻ seeds within imbibed IND
885 fruit morphs as compared to imbibed bare M⁻ seeds and the M⁺ seed morphs (Figure 5). At
886 the 9°C and 14°C imbibition temperatures, the resultant ABA accumulation in M⁻ seeds inside
887 IND fruits was especially elevated in the more dormant 20IND fruits as compared to the less
888 dormant 25IND fruits.

889

890 In agreement with a pericarp-enhanced ABA sensitivity of M^+ embryos inside IND fruits,
891 pericarp-enhanced expression of numerous ABA-related TFs including *AearAREB3*,
892 *AearABI5*, *AearABF1*, and *AearGBF3* (Figure 8) became evident during imbibition. Further,
893 the presence of the pericarp affected the expression patterns for major ABA signaling genes,
894 including for ABA receptors, PP2Cs, and SnRK2, which control the ABA-related TFs. The
895 control of germinability by ABA signaling is, in part, achieved by regulating the expression of
896 downstream cell wall remodeling genes (e.g. Finch-Savage and Leubner-Metzger, 2006;
897 Barrero et al., 2010; Shigeyama et al., 2016; Steinbrecher and Leubner-Metzger, 2017;
898 Holloway et al., 2021; Steinbrecher and Leubner-Metzger, 2022). Their expression in imbibed
899 *Ae. arabicum* IND fruits, M^+ and M^- seeds also exhibited pericarp- and temperature-
900 dependent patterns (turquoise module in most cases), which is mainly mediated by hypoxia
901 affecting ABA sensitivity and gene expression (Figures 8 and 10).

902

903 The presented new, comprehensive molecular datasets on responses of dispersed dimorphic
904 diaspores to ambient temperature, together with previous work on fruit/seed development
905 (Lenser et al., 2018; Wilhelmsson et al., 2019; Arshad et al., 2021), highlights *Ae. arabicum*
906 as the best experimental model system for heteromorphism so far. It provides a growing
907 potential to understand developmental control and plasticity of fruit and seed dimorphism and
908 it's underpinning molecular, evolutionary, and ecological mechanisms as adaptation to
909 environmental change. The comparative analysis of the M^+ seed morph, the IND fruit morph,
910 and the bare M^- seed revealed morphological, hormonal, and gene regulatory mechanisms of
911 the pericarp-imposed dormancy. The dimorphic diaspores integrate parental and imbibition
912 temperature differently, involving distinct transcriptional changes and ABA-related regulation.
913 The *Ae. arabicum* web portal (https://plantcode.cup.uni-freiburg.de/aetar_db/index.php) with
914 its genome database and gene expression atlas comprises published transcriptome results
915 (this work and Merai et al., 2019; Wilhelmsson et al., 2019; Arshad et al., 2021), is open for
916 dataset additions, makes the data widely accessible, and providing a valuable source for
917 future work on diaspore heteromorphism.

918

919 **Materials and Methods**

920

921 **Plant material, experimental growth conditions, and germination assays**

922 Plants of *Aethionema arabicum* (L.) Andr. ex DC. were grown from accessions TUR ES1020
923 (from Turkey) (Mohammadin et al., 2017; Mohammadin et al., 2018; Merai et al., 2019), in
924 Levington compost with added horticultural grade sand (F2+S), under long-day conditions
925 (16 h light/ 20°C and 8 h dark/ 18°C) in a glasshouse. Upon onset of flowering, plants were
926 transferred to distinct parental temperature regimes (20°C versus 25°C) during reproduction in
927 otherwise identical growth chambers as described (Supplemental Figure S1A). Mature M⁺
928 seeds and IND fruits were harvested (Supplemental Table S1), further dried over silica gel for
929 a week and either used immediately or stored at -20°C in air-tight containers. For germination
930 assays, dry mature seeds (M⁺ or M⁻) or IND fruits were placed in 3 cm Petri dishes containing
931 two layers of filter paper, 3 ml distilled water and 0.1% Plant Preservative Mixture (Plant Cell
932 Technology). Temperature response profiles (Figure 1C) were obtained by incubating plates
933 on a GRD1-LH temperature gradient plate device (Grant Instruments Ltd., Cambridge, UK).
934 Subsequent germination assays were conducted by incubating plates in MLR-350 Versatile
935 Environmental Test Chambers (Sanyo-Panasonic) at the indicated imbibition temperature and
936 100 $\mu\text{mol} \cdot \text{s}^{-1} \cdot \text{m}^{-2}$ continuous white light (Lenser et al., 2016). Germination assays under
937 hypoxia conditions compressed air (UN1002, BOC Ltd., Woking, UK) and oxygen-free
938 nitrogen (BOC UN1066) were mixed to generate a 4.5±0.2% oxygen atmosphere in hypoxia
939 chambers (Stemcell Technologies, Waterbeach, Cambridge, UK) with the plates (14°C,
940 continuous white light). Seed germination, scored as radicle emergence, of 3 biological
941 replicates each with 20 to 25 seeds or fruits were analyzed.

942

943 **Multispectral Imaging (MSI), biomechanical and pericarp extract assays**

944 Multispectral imaging was performed with a VideometerLab (Mark4, Series 11, Videometer
945 A/S, Denmark). Images were transformed using normalized canonical discriminant analysis
946 (nCDA) to compare the two parental temperatures. Biomechanical properties of the fruit coats
947 were measured using a universal material testing machine (ZwickiLine Z0.5, Zwick Roell,
948 Germany). Fruits were imbibed for 1 h before cutting them in half (fruit half covering the
949 micropylar end of the seed and non-micropylar end of the seed) and re-dried overnight.
950 Seeds were removed from the pericarps, and a metal probe with a diameter of 0.3 mm was

951 driven into the sample at a speed of 2 mm/min while recording force and displacement.
952 Tissue resistance was determined to be the maximal force from the force-displacement curve.
953 Pericarp extract (PE) was obtained as aqueous leachate by incubating ca. 0.5 g IND pericarp
954 in 15 ml H₂O on a shaker for 2 hours, followed by cleaning it using a 0.2 µm filter.
955 Germination assays were conducted by comparing PE, H₂O (control), *cis,trans*-S(+) -ABA
956 (ABA; Duchefa Biochemie, Haarlem, The Netherlands), salicylic acid (SA; Alfa Aesar,
957 Lancashire, UK), *cis*-(+)-12-oxophytodienoic acid (OPDA; Cayman Chemical, MI), (-)-
958 jasmonic acid (JA; Cayman Chemical, MI, USA), or its isoleucine conjugate (JA-Ile; Cayman
959 Chemical) at the concentrations indicated.
960

961 **RNA-seq and quantitative reverse transcription-PCR (RT-qPCR)**

962 Sampling of dry or imbibed M⁺ seeds, M⁻ seeds, and IND fruits for molecular analyses was as
963 described in the sampling scheme (Supplemental Figure S1). Biological replicates of samples
964 each corresponding to 20 mg dry weight of seed material, were pulverized in liquid N₂ using
965 mortar and pestle. Extraction of total RNA was performed as described by Graeber et al.
966 (2011). RNA quantity and purity were determined using a NanoDrop™ spectrophotometer
967 (ND-1000, ThermoScientific™, Delaware, USA) and an Agilent 2100 Bioanalyzer with the
968 RNA 6000 Nano Kit (Agilent Technologies, CA, USA) using the 2100 Expert Software to
969 calculate RNA Integrity Number (RIN) values. Four (RT-qPCR) or three (RNAseq) biological
970 replicates of RNA samples were used for downstream applications (Sample naming scheme:
971 Supplemental Table S2). Sequencing was performed at the Vienna BioCenter Core Facilities
972 (VBCF) Next Generation Sequencing Unit, Vienna, Austria (www.vbcf.ac.at). RNA-seq
973 libraries were sequenced in 50 bp single-end mode on Illumina® HiSeq 2000 Analyzers using
974 the manufacturer's standard module generation and sequencing protocols. The overall
975 sequencing and mapping statistics for each library and the read counts are presented in
976 Supplemental Data Set 1. RNA for RT-qPCR was extracted in an independent experiment
977 using the RNAqueous Total RNA Isolation Kit with the addition of the Plant RNA Isolation Aid
978 (Ambion, Thermo Fisher Scientific, Basingstoke, UK), followed by treatment with DNaseI
979 (QIAGEN Ltd., Manchester, UK) and precipitation in 2 M LiCl. Precipitated RNA was washed
980 in 70% ethanol and resuspended in RNase-free water. RT-qPCR was conducted and
981 analyzed as described (Graeber et al., 2011; Untergasser et al., 2012; Arshad et al., 2021)
982 using primer sequences and reference genes listed in Supplemental Table S3.

983

984 **Analyses of transcriptome data**

985 Transcriptome assembly, data trimming, filtering, read mapping and feature counting, and
986 DEG detection were performed as previously described (Wilhelmsson et al., 2019; Arshad et
987 al., 2021). Principal component analysis (PCA) was performed using the built-in R package
988 "prcomp" (www.r-project.org) on $\log(x+1)$ transformed RPKM values for 22200 genes with
989 non-zero values in at least one sample. Sample replicate RPKM values were averaged for
990 45 treatments and WGCNA (Zhang and Horvath, 2005) implementation (Langfelder and
991 Horvath, 2008) in R was performed on $\log_2(x+1)$ transformed RPKM values for 11260 genes
992 whose average expression was >4 RPKM across all samples. The function blockwiseModules
993 was used with default settings, other than to create a signed hybrid network distinguishing
994 between positive and negative Pearson correlations using a soft power threshold of 24,
995 minModuleSize of 50, mergeCutHeight of 0.25, and pamRespectsDendro set to False in
996 single block. Module membership and significance for each gene were calculated (Pearson
997 correlation with module eigengene) (Supplemental Data Set 2). PCA analysis (Wickham,
998 2016) for the 11260 genes was performed as outlined above with transposed data. Module
999 eigengene expression was correlated with sample traits using Pearson correlation. GO term
1000 enrichment in module gene lists was calculated using the R package topGO (Alexa and
1001 Rahnenfuhrer, 2023) using the elim or classic method with Fisher's exact test. Geneious 8.1.9
1002 (<https://www.geneious.com>) was used to visualize motif positions. Gene identifier and
1003 symbols (Supplemental Table S2) are according to earlier publications of the *Ae. arabicum*
1004 genome and transcriptome (Haudry et al., 2013; Merai et al., 2019; Nguyen et al., 2019;
1005 Wilhelmsson et al., 2019; Arshad et al., 2021) and the *Ae. arabicum* web portal
1006 (https://plantcode.cup.uni-freiburg.de/aetar_db/index.php) links this to the current (Fernandez-
1007 Pozo et al., 2021) and future genome DB and gene expression atlas.

1008

1009 **Gene promoter analyses**

1010 Promoter motif enrichment in the start codon -1000 to +100 bp region was analyzed using the
1011 Analysis of Motif Enrichment tool (McLeay and Bailey, 2010) using MEME Suite
1012 (<https://meme-suite.org/>) (Bailey et al., 2015) to identify enrichment of motifs from the
1013 *ArabidopsisDAPv1* database (O'Malley et al., 2016). Input sequences (module gene list) were
1014 compared to control sequences (all promoter sequences) using average odds score, Fisher's

1015 exact test, fractional score threshold of 0.25, E-value cutoff of 10, and 0-order background
1016 model. FIMO (Grant et al., 2011) on MEME Suite was used to scan sequences for chosen
1017 motifs. Chord diagram was drawn using R package "circlize" (Gu et al., 2014).

1018

1019 **Phytohormone quantification**

1020 For quantification of jasmonates (JA, JA-Ile and *cis*-OPDA), auxins (IAA and its catabolite
1021 oxiIAA), abscisates (ABA, PA and DPA) and salicylic acid (SA), internal standards, containing
1022 20 pmol of [²H₄]SA and [²H₅]OPDA, 10 pmol each of [²H₆]ABA, [²H₆]JA and [²H₂]JA-Ile, and 5
1023 pmol each of [²H₃]PA, [²H₃]DPA, [¹³C₆]IAA and [¹³C₆]oxIAA (all from Olchemim Ltd, Czech
1024 Republic), and 1 ml of ice-cold methanol: water (10:90, v/v) were added to 10 mg of freeze-
1025 dried and homogenized samples. Sample mixtures were homogenized using an MM400
1026 vibration mill for 5 min at 27 Hz (Retsch Technology GmbH, Germany), sonicated for 3 min at
1027 4 °C using an ultrasonic bath, and then extracted for 30 min (15 rpm) at 4°C using a rotary
1028 disk shaker. Samples were centrifuged at 20,000 rpm (15 min, 4 °C), the supernatant purified
1029 using pre-equilibrated Oasis HLB cartridges (1 cc, 30 mg, Waters), and evaporated to
1030 dryness under nitrogen (30°C) (Flokova et al., 2014). The evaporated samples were
1031 reconstituted in 40 µl of the mobile phase (15% acetonitrile, v/v) and analyzed by UHPLC-
1032 ESI-MS/MS as described by Šimura et al. (2018). All phytohormones were detected using a
1033 multiple-reaction monitoring mode of the transition of the precursor ion to the appropriate
1034 product ion. Masslynx 4.1 software (Waters, Milford, MA, USA) was used to analyze the data,
1035 and the standard isotope dilution method (Rittenberg and Foster, 1940) was used to quantify
1036 the phytohormone levels. Five independent biological replicates were performed.

1037

1038 **Statistical analysis**

1039 Germination data were evaluated by comparing final germination percentage (G_{max}) and
1040 germination rate (speed). Germination curve fits and T_{50%} were calculated with
1041 GERMINATOR (Joosen et al., 2010). An unpaired t-test was used to compare the mean
1042 values for tissue resistance (biomechanical analysis of pericarp) of the two parental
1043 temperatures. All statistical analyses were performed in GraphPad Prism (v. 8.01, GraphPad
1044 Software Inc., San Diego, California, USA).

1045

1046 **Data availability and accession numbers**

1047 The RNAseq data discussed in this publication have been deposited at the NCBI Sequencing
1048 Read Archive (SRA), BioProjects PRJNA611900 (dry seed) and PRJNA639669 (imbibed
1049 seed), accessible at <https://www.ncbi.nlm.nih.gov/sra>; metadata about the samples are also
1050 available as part of this publication (Supplemental Data Set 1). Further, normalized
1051 transcriptome data from this study and associated previous studies (Merai et al., 2019;
1052 Wilhelmsson et al., 2019; Arshad et al., 2021) can be accessed and visualized at the *Ae.*
1053 *arabicum* web portal (https://plantcode.cup.uni-freiburg.de/aetar_db/index.php). For *Ae.*
1054 *arabicum* gene IDs see Supplemental Figures S15, S16, Supplemental Table 2 or the
1055 Expression Atlas (https://plantcode.cup.uni-freiburg.de/aetar_db/index.php); for RNAseq
1056 single values see the Expression Atlas or Supplemental Data Set 1. All other data presented
1057 or analyzed in this published article are available online through the supplements.
1058
1059

1060 **Supplemental data**

1061 The following materials are available in the online version of this article.

1062 **Supplemental Figure S1.** Large-scale diaspora production experiment and sampling

1063 **Supplemental Figure S2.** *Aethionema arabicum* gene expression atlas

1064 **Supplemental Figure S3.** PCA of transcriptome data (RNA-seq)

1065 **Supplemental Figure S4.** Expression of WGCNA modules

1066 **Supplemental Figure S5.** Temperature responses and ABA metabolism

1067 **Supplemental Figure S6.** Hormone contents in response to temperatures

1068 **Supplemental Figure S7.** Effects of pericarp extract on germination and gene expression

1069 **Supplemental Figure S8.** Pericarp biomechanics

1070 **Supplemental Figure S9.** Transcription factors and promoter motifs of fermentation genes

1071 **Supplemental Figure S10.** Detail comparison of fermentation gene promoters

1072 **Supplemental Figure S11.** Transcript abundance patterns of the seed-specific Perl's pathway

1073

1074 **Supplemental Figure S12.** Transcript abundance patterns of hypoxia-regulated genes

1075 **Supplemental Figure S13.** RT-qPCR analysis of hypoxia and ABA effects

1076 **Supplemental Figure S14.** Transcript abundance patterns of ABA-related genes

1077 **Supplemental Figure S15.** Transcript abundance patterns of transcription/translation genes

1078 **Supplemental Figure S16.** Transcript abundance patterns of cell wall remodeling genes

1079 **Supplemental Table S1.** *Aethionema arabicum* seed and fruit harvest results

1080 **Supplemental Table S2.** *Aethionema arabicum* gene IDs, symbols and modules

1081 **Supplemental Table S3.** RT-qPCR primer used

1082 **Supplemental Data Set 1.** Gene annotations, DEGs, RPKM values, raw counts, overall sequencing and mapping statistics for each library, and SRA accessions

1083

1084 **Supplemental Data Set 2.** WGCNA modules and GO term enrichment analysis

1085 **Supplemental Data Set 3.** Promoter enrichment analysis (AME) and chord diagram data

1086 **Supplemental Data Set 4.** Promoter motif scanning (FIMO)

1087

1088

1089 **Conflict of interest**

1090 All authors declare that they have no conflict of interest.

1091

1092 **Acknowledgements:** We acknowledge the support of Katja Sperber, Teresa Lenser, Samik
1093 Bhattacharya, Sara Mayland-Quellhorst, Setareh Mohammadin, Safina Khan, Christopher
1094 Grosche, Giles Grainge, Thomas Holloway, Kazumi Nakabayashi and Michael Ignatz in
1095 discussions, harvesting of diaspores and other tasks. The authors are grateful for the
1096 excellent support by the Next Generation Sequencing Unit of the Vienna BioCenter Core
1097 Facilities (VBCF). We acknowledge the support of DataPLANT (NFDI 7/1 – 42077441) as part
1098 of the German National Research Data Infrastructure.

1099

1100 **Funding:**

1101 This work is part of the ERA-CAPS “SeedAdapt” consortium project led by G.L.-M. and was
1102 funded by grants from the Biotechnology and Biological Sciences Research Council (BBSRC)
1103 to G.L.M. (BB/M00192X/1); from the Natural Environment Research Council (NERC) through
1104 a Doctoral Training Grant to W.A. (NE/L002485/1); from the Deutsche
1105 Forschungsgemeinschaft (DFG) to G.T. (TH 417/10-1), K.M. (MU 1137/12-1), and S.A.R. (RE
1106 1697/8-1); from the Austrian Science Fund (FWF) to O.M.S. (FWF I1477); from the Austrian
1107 Science Fund (FWF) to Z.M. (FWF I3979-B25); from the Netherlands Organisation for
1108 Scientific Research (NWO) to M.E.S. (849.13.004); from Ministerio de Ciencia e Innovación
1109 (MCIN) to N.F.-P. (RYC2020-030219-I and PID2021-125805OA-I00); from the European
1110 Regional Development Fund-Project "Centre for Experimental Plant Biology" to D.T. (No.
1111 CZ.02.1.01/0.0/0.0/16_019/0000738); and by an Internal Grant Agency of Palacký University
1112 to O.N. (IGA_PrF_2023_031).

1113

1114 **Author Contribution Statement:**

1115 K.G., K.M., G.T., M.S., O.M.S., M.E.S., O.N., S.A.R. and G.L.-M. conceived the project and
1116 conceptualized the work. J.O.C., P.K.I.W. and K.G. performed the majority of experiments;
1117 K.G., Z.M. and J.O.C. prepared and handled samples; J.O.C., P.K.I.W., K.K.U., W.A., S.A.R.
1118 and G.L.-M. performed the transcriptomics data analysis. J.O.C., T.S. and M.P. performed
1119 RT-qPCR and hypoxia analyses. J.O.C., T.S. and M.P. performed germination,
1120 biomechanical experiments, and multispectral imaging analyses. N.F.-P., J.O.C. and S.A.R.
1121 developed and implemented the gene expression atlas. T.-P.N., K.G., W.A., K.M. and M.E.S.
1122 conducted the environmental simulation experiment and generated the plant material. I.P.,

1123 D.T., O.N. and M.S. performed the hormone analysis. J.O.C. and G.L.-M. wrote the
1124 manuscript. All authors read and commented on the manuscript.

1125

1126 **References**

1127

1128 Alexa, A., and Rahnenfuhrer, J. (2023). topGO: enrichment analysis for Gene Ontology. R
1129 package version 2.52.0.

1130 Andrade, A., Riera, N., Lindstrom, L., Alemano, S., Alvarez, D., Abdala, G., and Vigliocco, A.
1131 (2015). Pericarp anatomy and hormone profiles of cypselas in dormant and non-dormant
1132 inbred sunflower lines. *Plant Biol* 17, 351-360.

1133 Arshad, W., Marone, F., Collinson, M.E., Leubner-Metzger, G., and Steinbrecher, T. (2020).
1134 Fracture of the dimorphic fruits of *Aethionema arabicum* (Brassicaceae). *Botany* 98, 65-75.

1135 Arshad, W., Sperber, K., Steinbrecher, T., Nichols, B., Jansen, V.A.A., Leubner-Metzger, G.,
1136 and Mummenhoff, K. (2019). Dispersal biophysics and adaptive significance of dimorphic
1137 diaspores in the annual *Aethionema arabicum* (Brassicaceae). *New Phytol* 221, 1434-
1138 1446.

1139 Arshad, W., Lenser, T., Wilhelmsson, P.K.I., Chandler, J.O., Steinbrecher, T., Marone, F.,
1140 Pérez, M., Collinson, M.E., Stuppy, W., Rensing, S.A., Theissen, G., and Leubner-Metzger,
1141 G. (2021). A tale of two morphs: developmental patterns and mechanisms of seed coat
1142 differentiation in the dimorphic diaspore model *Aethionema arabicum* (Brassicaceae). *Plant*
1143 *J* 107, 166-181.

1144 Bailey, T.L., Johnson, J., Grant, C.E., and Noble, W.S. (2015). The MEME Suite. *Nucl Acids*
1145 *Res* 43, W39-W49.

1146 Barrero, J.M., Millar, A.A., Griffiths, J., Czechowski, T., Scheible, W.R., Udvardi, M., Reid,
1147 J.B., Ross, J.J., Jacobsen, J.V., and Gubler, F. (2010). Gene expression profiling identifies
1148 two regulatory genes controlling dormancy and ABA sensitivity in *Arabidopsis* seeds. *Plant*
1149 *J* 61, 611-622.

1150 Baskin, J.M., Lu, J.J., Baskin, C.C., Tan, D.Y., and Wang, L. (2014). Diaspore dispersal ability
1151 and degree of dormancy in heteromorphic species of cold deserts of northwest China: A
1152 review. *Perspect Plant Ecol Evol Sys* 16, 93-99.

1153 Batlla, D., Malavert, C., Farnocchia, R.B.F., Footitt, S., Benech-Arnold, R.L., and Finch-
1154 Savage, W.E. (2022). A quantitative analysis of temperature-dependent seasonal
1155 dormancy cycling in buried *Arabidopsis thaliana* seeds can predict seedling emergence in
1156 a global warming scenario. *J Expt Bot* 73, 2454-2468.

1157 Benech-Arnold, R.L., Gualano, N., Leymarie, J., Come, D., and Corbineau, F. (2006).
1158 Hypoxia interferes with ABA metabolism and increases ABA sensitivity in embryos of
1159 dormant barley grains. *J Exptl Bot* 57, 1423-1430.

1160 Bhattacharya, S., Sperber, K., Ozudogru, B., Leubner-Metzger, G., and Mummenhoff, K.
1161 (2019). Naturally-primed life strategy plasticity of dimorphic *Aethionema arabicum*
1162 facilitates optimal habitat colonization. *Sci Rep* 9, ARTN 16108.

1163 Bueso, E., Munoz-Bertomeu, J., Campos, F., Brunaud, V., Martinez, L., Sayas, E., Ballester,
1164 P., Yenush, L., and Serrano, R. (2014). *Arabidopsis thaliana* HOMEOBOX25 uncovers a
1165 role for gibberellins in seed longevity. *Plant Physiology* 164, 999-1010.

1166 Cadman, C.S.C., Toorop, P.E., Hilhorst, H.W.M., and Finch-Savage, W.E. (2006). Gene
1167 expression profiles of *Arabidopsis* Cvi seed during cycling through dormant and non-
1168 dormant states indicate a common underlying dormancy control mechanism. *Plant J* 46,
1169 805-822.

1170 Christianson, J.A., Wilson, I.W., Llewellyn, D.J., and Dennis, E.S. (2009). The low-oxygen
1171 induced NAC domain transcription factor ANAC102 affects viability of *Arabidopsis thaliana*
1172 seeds following low-oxygen treatment. *Plant Physiol* 149, 1724–1738.

1173 Dave, A., Vaistij, F.E., Gilday, A.D., Penfield, S.D., and Graham, I.A. (2016). Regulation of
1174 *Arabidopsis thaliana* seed dormancy and germination by 12-oxo-phytodienoic acid. *J Exptl
1175 Bot* 67, 2277-2284.

1176 Dominguez, C.P., Rodriguez, M.V., Batlla, D., de Salamone, I.E.G., Mantese, A.I., Andreani,
1177 A.L., and Benech-Arnold, R.L. (2019). Sensitivity to hypoxia and microbial activity are
1178 instrumental in pericarp-imposed dormancy expression in sunflower (*Helianthus annuus*
1179 L.). *Seed Sci Res* 29, 85-96.

1180 Donohue, K., Rubio de Casas, R., Burghardt, L., Kovach, K., and Willis, C.G. (2010).
1181 Germination, postgermination adaptation, and species ecological ranges. *Annual Review of
1182 Ecology, Evolution, and Systematics* 41, 293-319.

1183 Fernandez-Pascual, E., Mattana, E., and Pritchard, H.W. (2019). Seeds of future past: climate
1184 change and the thermal memory of plant reproductive traits. *Biol Rev* 94, 439-456.

1185 Fernandez-Pozo, N., and Bombarely, A. (2022). EasyGDB: a low-maintenance and highly
1186 customizable system to develop genomics portals. *Bioinformatics (Oxford, England)* 38,
1187 4048-4050.

1188 Fernandez-Pozo, N., Metz, T., Chandler, J.O., Gramzow, L., Merai, Z., Maumus, F., Scheid,
1189 O.M., Theissen, G., Schranz, M.E., Leubner-Metzger, G., and Rensing, S.A. (2021).
1190 *Aethionema arabicum* genome annotation using PacBio full-length transcripts provides a
1191 valuable resource for seed dormancy and Brassicaceae evolution research. Plant J 106,
1192 275-293.

1193 Finch-Savage, W.E., and Leubner-Metzger, G. (2006). Seed dormancy and the control of
1194 germination. New Phytol 171, 501-523.

1195 Finch-Savage, W.E., and Footitt, S. (2017). Seed dormancy cycling and the regulation of
1196 dormancy mechanisms to time germination in variable field environments. J Exptl Bot 68,
1197 843-856.

1198 Flokova, K., Tarkowska, D., Miersch, O., Strnad, M., Wasternack, C., and Novak, O. (2014).
1199 UHPLC-MS/MS based target profiling of stress-induced phytohormones. Phytochem 105,
1200 147-157.

1201 Footitt, S., Walley, P.G., Lynn, J.R., Hambidge, A.J., Penfield, S., and Finch-Savage, W.E.
1202 (2020). Trait analysis reveals DOG1 determines initial depth of seed dormancy, but not
1203 changes during dormancy cycling that result in seedling emergence timing. New Phytol
1204 225, 2035-2047.

1205 Gasch, P., Fundinger, M., Muller, J.T., Lee, T., Bailey-Serres, J., and Mustroph, A. (2016).
1206 Redundant ERF-VII transcription factors bind to an evolutionarily conserved *cis*-motif to
1207 regulate hypoxia-responsive gene expression in *Arabidopsis*. Plant Cell 28, 160-180.

1208 Gianella, M., Bradford, K.J., and Guzzon, F. (2021). Ecological, (epi)genetic and physiological
1209 aspects of bet-hedging in angiosperms. Plant Reprod 34, 21-36.

1210 Gomez-Porras, J.L., Riano-Pachon, D.M., Dreyer, I., Mayer, J.E., and Mueller-Roeber, B.
1211 (2007). Genome-wide analysis of ABA-responsive elements ABRE and CE3 reveals
1212 divergent patterns in *Arabidopsis* and rice. BMC Genomics 8, ARTN 260.

1213 Graeber, K., Linkies, A., Wood, A.T., and Leubner-Metzger, G. (2011). A guideline to family-
1214 wide comparative state-of-the-art quantitative RT-PCR analysis exemplified with a
1215 Brassicaceae cross-species seed germination case study. Plant Cell 23, 2045-2063.

1216 Graeber, K., Linkies, A., Steinbrecher, T., Mummenhoff, K., Tarkowská, D., Turečková, V.,
1217 Ignatz, M., Sperber, K., Voegele, A., de Jong, H., Urbanová, T., Strnad, M., and Leubner-
1218 Metzger, G. (2014). *DELAY OF GERMINATION 1* mediates a conserved coat dormancy
1219 mechanism for the temperature- and gibberellin-dependent control of seed germination.

1220 Proceedings of the National Academy of Sciences of the United States of America 111,
1221 E3571-E3580.

1222 Grafi, G. (2020). Dead but not dead end: Multifunctional role of dead organs enclosing
1223 embryos in seed biology. *Int J Mol Sci* 21, ARTN 8024.

1224 Grant, C.E., Bailey, T.L., and Noble, W.S. (2011). FIMO: scanning for occurrences of a given
1225 motif. *Bioinformatics* (Oxford, England) 27, 1017-1018.

1226 Gu, Z.G., Gu, L., Eils, R., Schlesner, M., and Brors, B. (2014). Circlize implements and
1227 enhances circular visualization in R. *Bioinformatics* (Oxford, England) 30, 2811-2812.

1228 Hall, J.C., Tisdale, T.E., Donohue, K., and Kramer, E.M. (2006). Developmental basis of an
1229 anatomical novelty: Heteroarthrocarpy in *Cakile lanceolata* and *Erucaria erucarioides*
1230 (Brassicaceae). *International Journal of Plant Sciences* 167, 771-789.

1231 Haudry, A., Platts, A.E., Vello, E., Hoen, D.R., Leclercq, M., Williamson, R.J., Forczek, E.,
1232 Joly-Lopez, Z., Steffen, J.G., Hazzouri, K.M., Dewar, K., Stinchcombe, J.R., Schoen, D.J.,
1233 Wang, X.W., Schmutz, J., Town, C.D., Edger, P.P., Pires, J.C., Schumaker, K.S., Jarvis,
1234 D.E., Mandakova, T., Lysak, M.A., van den Bergh, E., Schranz, M.E., Harrison, P.M.,
1235 Moses, A.M., Bureau, T.E., Wright, S.I., and Blanchette, M. (2013). An atlas of over 90,000
1236 conserved noncoding sequences provides insight into crucifer regulatory regions. *Nat
1237 Genet* 45, 891-898.

1238 Hoang, H.H., Bailly, C., Corbineau, F., and Leymarie, J. (2013). Induction of secondary
1239 dormancy by hypoxia in barley grains and its hormonal regulation. *J Exptl Bot* 64, 2017-
1240 2025.

1241 Holloway, T., Steinbrecher, T., Pérez, M., Seville, A., Stock, D., Nakabayashi, K., and
1242 Leubner-Metzger, G. (2021). Coleorrhiza-enforced seed dormancy: a novel mechanism to
1243 control germination in grasses. *New Phytol* 229, 2179-2191.

1244 Ignatz, M., Hourston, J.E., Tureckova, V., Strnad, M., Meinhard, J., Fischer, U., Steinbrecher,
1245 T., and Leubner-Metzger, G. (2019). The biochemistry underpinning industrial seed
1246 technology and mechanical processing of sugar beet. *Planta* 250, 1717-1729.

1247 Imbert, E. (2002). Ecological consequences and ontogeny of seed heteromorphism. *Perspect
1248 Plant Ecol Evol Sys* 5, 13-36.

1249 Iwasaki, M., Penfield, S., and Lopez-Molina, L. (2022). Parental and environmental control of
1250 seed dormancy in *Arabidopsis thaliana*. *Annual Review of Plant Biology* 73, 355-378.

1251 Joosen, R.V., Kodde, J., Willems, L.A., Ligterink, W., van der Plas, L.H., and Hilhorst, H.W.
1252 (2010). GERMINATOR: a software package for high-throughput scoring and curve fitting of
1253 *Arabidopsis* seed germination. *Plant J* 62, 148-159.

1254 Ju, L., Jing, Y.X., Shi, P.T., Liu, J., Chen, J.S., Yan, J.J., Chu, J.F., Chen, K.M., and Sun, J.Q.
1255 (2019). JAZ proteins modulate seed germination through interaction with ABI5 in bread
1256 wheat and *Arabidopsis*. *New Phytol* 223, 246-260.

1257 Khadka, J., Raviv, B., Swetha, B., Grandhi, R., Singiri, J.R., Novoplansky, N., Guterman, Y.,
1258 Galis, I., Huang, Z.Y., and Grafi, G. (2020). Maternal environment alters dead pericarp
1259 biochemical properties of the desert annual plant *Anastatica hierochuntica* L. *PLoS ONE*
1260 15, ARTN e0237045.

1261 Kürsteiner, O., Dupuis, I., and Kuhlemeier, C. (2003). The pyruvate decarboxylase1 gene of
1262 *Arabidopsis* is required during anoxia but not other environmental stresses. *Plant Physiol*
1263 132, 968-978.

1264 Langfelder, P., and Horvath, S. (2008). WGCNA: an R package for weighted correlation
1265 network analysis. *BMC Bioinformatics* 9, ARTN 559.

1266 Lenser, T., Tarkowska, D., Novak, O., Wilhelmsson, P.K.I., Bennett, T., Rensing, S.A.,
1267 Strnad, M., and Theissen, G. (2018). When the BRANCHED network bears fruit: How
1268 carpic dominance causes fruit dimorphism in *Aethionema*. *Plant J* 94, 352-371.

1269 Lenser, T., Graeber, K., Cevik, O.S., Adiguzel, N., Donmez, A.A., Grosche, C., Kettermann,
1270 M., Mayland-Quellhorst, S., Merai, Z., Mohammadin, S., Nguyen, T.P., Rumpler, F.,
1271 Schulze, C., Sperber, K., Steinbrecher, T., Wiegand, N., Strnad, M., Scheid, O.M.,
1272 Rensing, S.A., Schranz, M.E., Theissen, G., Mummenhoff, K., and Leubner-Metzger, G.
1273 (2016). Developmental control and plasticity of fruit and seed dimorphism in *Aethionema*
1274 *arabicum*. *Plant Physiology* 172, 1691-1707.

1275 Linkies, A., and Leubner-Metzger, G. (2012). Beyond gibberellins and abscisic acid: how
1276 ethylene and jasmonates control seed germination. *Plant Cell Rep* 31, 253-270.

1277 Liu, R.R., Wang, L., Tanveer, M., and Song, J. (2018). Seed heteromorphism: an important
1278 adaptation of halophytes for habitat heterogeneity. *Front Plant Sci* 9, ARTN 1515.

1279 Loades, E., Perez, M., Tureckova, V., Tarkowska, D., Strnad, M., Seville, A., Nakabayashi,
1280 K., and Leubner-Metzger, G. (2023). Distinct hormonal and morphological control of
1281 dormancy and germination in *Chenopodium album* dimorphic seeds. *Front Plant Sci* 14,
1282 ARTN 1156794.

1283 Lu, G.H., Paul, A.L., McCarty, D.R., and Ferl, R.J. (1996). Transcription factor veracity: Is
1284 GBF3 responsible for ABA-regulated expression of *Arabidopsis Adh*? *Plant Cell* 8, 847-
1285 857.

1286 Lu, J.J., Tan, D.Y., Baskin, J.M., and Baskin, C.C. (2015a). Post-release fates of seeds in
1287 dehiscent and indehiscent siliques of the diaspore heteromorphic species *Diptychocarpus*
1288 *strictus* (Brassicaceae). *Perspect Plant Ecol Evol Sys* 17, 255-262.

1289 Lu, J.J., Tan, D.Y., Baskin, C.C., and Baskin, J.M. (2017a). Role of indehiscent pericarp in
1290 formation of soil seed bank in five cold desert Brassicaceae species. *Plant Ecology* 218,
1291 1187-1200.

1292 Lu, J.J., Tan, D.Y., Baskin, C.C., and Baskin, J.M. (2017b). Delayed dehiscence of the
1293 pericarp: role in germination and retention of viability of seeds of two cold desert annual
1294 Brassicaceae species. *Plant Biol (Stuttg)* 19, 14-22.

1295 Lu, J.J., Zhou, Y.M., Tan, D.Y., Baskin, C.C., and Baskin, J.M. (2015b). Seed dormancy in six
1296 cold desert Brassicaceae species with indehiscent fruits. *Seed Sci Res* 25, 276-285.

1297 Mamut, J., Tan, D.-Y., Baskin, C.C., and Baskin, J.M. (2014). Role of trichomes and pericarp
1298 in the seed biology of the desert annual *Lachnoloma lehmannii* (Brassicaceae). *Ecol Res*
1299 29, 33-44.

1300 McLeay, R.C., and Bailey, T.L. (2010). Motif Enrichment Analysis: a unified framework and an
1301 evaluation on ChIP data. *BMC Bioinformatics* 11, ARTN 165.

1302 Mendiondo, G.M., Leymarie, J., Farrant, J.M., Corbineau, F., and Benech-Arnold, R.L. (2010).
1303 Differential expression of abscisic acid metabolism and signalling genes induced by seed-
1304 covering structures or hypoxia in barley (*Hordeum vulgare* L.) grains. *Seed Sci Res* 20, 69-
1305 77.

1306 Merai, Z., Graeber, K., Wilhelmsson, P., Ullrich, K.K., Arshad, W., Grosche, C., Tarkowska,
1307 D., Tureckova, V., Strnad, M., Rensing, S.A., Leubner-Metzger, G., and Mittelsten Scheid,
1308 O. (2019). *Aethionema arabicum*: a novel model plant to study the light control of seed
1309 germination. *J Expt Bot* 70, 3313-3328.

1310 Merai, Z., Xu, F., Musilek, A., Ackerl, F., Khalil, S., Soto-Jimenez, L.M., Lalatovic, K., Klose,
1311 C., Tarkowska, D., Tureckova, V., Strnad, M., and Scheid, O.M. (2023). Phytochromes
1312 mediate germination inhibition under red, far-red, and white light in *Aethionema arabicum*.
1313 *Plant Physiology* 192, 1584–1602.

1314 Mohammadin, S., Peterse, K., van de Kerke, S.J., Chatrou, L.W., Donmez, A.A.,
1315 Mummenhoff, K., Pires, J.C., Edger, P.P., Al-Shehbaz, I.A., and Schranz, M.E. (2017).
1316 Anatolian origins and diversification of *Aethionema*, the sister lineage of the core
1317 Brassicaceae. *Am J Bot* 104, 1042-1054.

1318 Mohammadin, S., Wang, W., Liu, T., Moazzeni, H., Ertugrul, K., Uysal, T., Christodoulou,
1319 C.S., Edger, P.P., Pires, J.C., Wright, S.I., and Schranz, M.E. (2018). Genome-wide
1320 nucleotide diversity and associations with geography, ploidy level and glucosinolate profiles
1321 in *Aethionema arabicum* (Brassicaceae). *Plant Sys Evol* 304, 619-630.

1322 Mohammed, S., Turckova, V., Tarkowska, D., Strnad, M., Mummenhoff, K., and Leubner-
1323 Metzger, G. (2019). Pericarp-mediated chemical dormancy controls the fruit germination of
1324 the invasive hoary cress (*Lepidium draba*), but not of hairy whitetop (*Lepidium*
1325 *appelianum*). *Weed Science* 67, 560-571.

1326 Mühlhausen, A., Lenser, T., Mummenhoff, K., and Theissen, G. (2013). Evidence that an
1327 evolutionary transition from dehiscent to indehiscent fruits in *Lepidium* (Brassicaceae) was
1328 caused by a change in the control of valve margin identity genes. *Plant J* 73, 824-835.

1329 Nambara, E., Okamoto, M., Tatematsu, K., Yano, R., Seo, M., and Kamiya, Y. (2010).
1330 Abscisic acid and the control of seed dormancy and germination. *Seed Sci Res* 20, 55-67.

1331 Nguyen, T.P., Muhlich, C., Mohammadin, S., van den Bergh, E., Platts, A.E., Haas, F.B.,
1332 Rensing, S.A., and Schranz, M.E. (2019). Genome improvement and genetic map
1333 construction for *Aethionema arabicum*, the first divergent branch in the Brassicaceae
1334 family. *G3-Genes Genom Genet* 9, 3521-3530.

1335 Nichols, B.S., Leubner-Metzger, G., and Jansen, V.A.A. (2020). Between a rock and a hard
1336 place: adaptive sensing and site-specific dispersal. *Ecol Lett* 23, 1370-1379.

1337 O'Malley, R.C., Huang, S.S.C., Song, L., Lewsey, M.G., Bartlett, A., Nery, J.R., Galli, M.,
1338 Gallavotti, A., and Ecker, J.R. (2016). Cistrome and epicistrome features shape the
1339 regulatory DNA landscape. *Cell* 165, 1280-1292.

1340 Papdi, C., Perez-Salamo, I., Joseph, M.P., Giuntoli, B., Bogre, L., Koncz, C., and Szabados,
1341 L. (2015). The low oxygen, oxidative and osmotic stress responses synergistically act
1342 through the ethylene response factor VII genes RAP2.12, RAP2.2 and RAP2.3. *Plant J* 82,
1343 772-784.

1344 Penfield, S., and MacGregor, D.R. (2017). Effects of environmental variation during seed
1345 production on seed dormancy and germination. *J Exptl Bot* 68, 819-825.

1346 Renard, J., Martinez-Almonacid, I., Castillo, I.Q., Sonntag, A., Hashim, A., Bissoli, G.,
1347 Campos, L., Munoz-Bertomeu, J., Ninoles, R., Roach, T., Sanchez-Leon, S., Ozuna, C.V.,
1348 Gadea, J., Lison, P., Kranner, I., Barro, F., Serrano, R., Molina, I., and Bueso, E. (2021).
1349 Apoplastic lipid barriers regulated by conserved homeobox transcription factors extend
1350 seed longevity in multiple plant species. *New Phytol* 231, 679-694.

1351 Rittenberg, D., and Foster, G.L. (1940). A new procedure for quantitative analysis by isotope
1352 dilution, with application to the determination of amino acids and fatty acids. *Journal of*
1353 *Biological Chemistry* 133, 737-744.

1354 Scheler, C., Weitbrecht, K., Pearce, S.P., Hampstead, A., Buettner-Mainik, A., Lee, K.,
1355 Voegele, A., Oracz, K., Dekkers, B., Wang, X., Wood, A., Bentsink, L., King, J., Knox, P.,
1356 Holdsworth, M., Müller, K., and Leubner-Metzger, G. (2015). Promotion of testa rupture
1357 during garden cress germination involves seed compartment-specific expression and
1358 activity of pectin methylesterases. *Plant Physiology* 167, 200-215.

1359 Seok, H.Y., Tran, H.T., Lee, S.Y., and Moon, Y.H. (2022). *AtERF71/HRE2*, an *Arabidopsis*
1360 AP2/ERF transcription factor gene, contains both positive and negative *cis*-regulatory
1361 elements in its promoter region involved in hypoxia and salt stress responses. *Int J Mol Sci*
1362 23, ARTN 5310.

1363 Shigeyama, T., Watanabe, A., Tokuchi, K., Toh, S., Sakurai, N., Shibuya, N., and Kawakami,
1364 N. (2016). alpha-Xylosidase plays essential roles in xyloglucan remodelling, maintenance
1365 of cell wall integrity, and seed germination in *Arabidopsis thaliana*. *J Exptl Bot* 67, 5615-
1366 5629.

1367 Silva, A.T., Ribone, P.A., Chan, R.L., Ligterink, W., and Hilhorst, H.W.M. (2016). A predictive
1368 coexpression network identifies novel genes controlling the seed-to-seedling phase
1369 transition in *Arabidopsis thaliana*. *Plant Physiology* 170, 2218-2231.

1370 Simura, J., Antoniadi, I., Siroka, J., Tarkowská, D., Strnad, M., Ljung, K., and Novak, O.
1371 (2018). Plant hormonomics: multiple phytohormone profiling by targeted metabolomics.
1372 *Plant Physiology* 177, 476-489.

1373 Sperber, K., Steinbrecher, T., Graeber, K., Scherer, G., Clausing, S., Wiegand, N., Hourston,
1374 J.E., Kurre, R., Leubner-Metzger, G., and Mummenhoff, K. (2017). Fruit fracture
1375 biomechanics and the release of *Lepidium didymum* pericarp-imposed mechanical
1376 dormancy by fungi. *Nature Communications* 8, 1868.

1377 Stamm, P., Topham, A.T., Mukhtar, N.K., Jackson, M.D.B., Tome, D.F.A., Beynon, J.L., and
1378 Bassel, G.W. (2017). The transcription factor ATHB5 affects GA-mediated plasticity in
1379 hypocotyl cell growth during seed germination. *Plant Physiology* 173, 907-917.

1380 Steinbrecher, T., and Leubner-Metzger, G. (2017). The biomechanics of seed germination. *J
1381 Expt Bot* 68, 765-783.

1382 Steinbrecher, T., and Leubner-Metzger, G. (2022). Xyloglucan remodelling enzymes and the
1383 mechanics of plant seed and fruit biology. *J Exptl Bot* 73, 1253-1257.

1384 Takeno, K., and Yamaguchi, H. (1991). Diversity in seed-germination behavior in relation to
1385 heterocarpy in *Salsola komarovii* Iljin. *Botanical Magazine-Tokyo* 104, 207-215.

1386 Untergasser, A., Cutcutache, I., Koressaar, T., Ye, J., Faircloth, B.C., Remm, M., and Rozen,
1387 S.G. (2012). Primer3 - new capabilities and interfaces. *Nucl Acids Res* 40, ARTN e115.

1388 Walck, J.L., Hidayati, S.N., Dixon, K.W., Thompson, K., and Poschlod, P. (2011). Climate
1389 change and plant regeneration from seed. *Global Change Biol* 17, 2145-2161.

1390 Wang, L., Hua, D.P., He, J.N., Duan, Y., Chen, Z.Z., Hong, X.H., and Gong, Z.Z. (2011).
1391 Auxin response factor2 (ARF2) and its regulated homeodomain gene HB33 mediate
1392 abscisic acid response in *Arabidopsis*. *Plos Genetics* 7, ARTN e1002172.

1393 Weitbrecht, K., Müller, K., and Leubner-Metzger, G. (2011). First off the mark: early seed
1394 germination. *J Exptl Bot* 62, 3289-3309.

1395 Wickham, H. (2016). *ggplot2: Elegant Graphics for Data Analysis*. (New York: Springer-
1396 Verlag).

1397 Wilhelmsson, P.K.I., Chandler, J.O., Fernandez-Pozo, N., Graeber, K., Ullrich, K.K., Arshad,
1398 W., Khan, S., Hofberger, J., Buchta, K., Edger, P.P., Pires, C., Schranz, M.E., Leubner-
1399 Metzger, G., and Rensing, S.A. (2019). Usability of reference-free transcriptome
1400 assemblies for detection of differential expression: a case study on *Aethionema arabicum*
1401 dimorphic seeds. *BMC Genomics* 20, ARTN 95.

1402 Yang, C.Y., Hsu, F.C., Li, J.P., Wang, N.N., and Shih, M.C. (2011). The AP2/ERF
1403 transcription factor AtERF73/HRE1 modulates ethylene responses during hypoxia in
1404 *Arabidopsis*. *Plant Physiology* 156, 202-212.

1405 Yoshida, T., Fujita, Y., Sayama, H., Kidokoro, S., Maruyama, K., Mizoi, J., Shinozaki, K., and
1406 Yamaguchi-Shinozaki, K. (2010). AREB1, AREB2, and ABF3 are master transcription
1407 factors that cooperatively regulate ABRE-dependent ABA signaling involved in drought
1408 stress tolerance and require ABA for full activation. *Plant J* 61, 672-685.

1409 Zhang, B., and Horvath, S. (2005). A general framework for weighted gene co-expression
1410 network analysis. *Stat Appl Genet Mol Biol* 4, ARTN 17.

1411 Zhang, Y.Z., Liu, Y., Sun, L., Baskin, C.C., Baskin, J.M., Cao, M., and Yang, J. (2022). Seed
1412 dormancy in space and time: global distribution, paleoclimatic and present climatic drivers,
1413 and evolutionary adaptations. *New Phytol* 234, 1770-1781.

1414

1415

1416

1417 **Figure legends**

1418

1419 **Figure 1** Dimorphic diaspore responses of *Aethionema arabicum* to ambient temperatures. A,
1420 Infructescence showing two morphologically distinct fruit types. Large, dehiscent (DEH) fruits
1421 contain four to six seed diaspores that produce mucilage (M^+) upon imbibition. Small,
1422 indehiscent (IND) fruits contain a single non-mucilaginous (M^-) seed each. For experiments
1423 with the bare M^- seed the pericarp was manually removed. B, The effect of parental
1424 temperatures (PT; ambient temperatures during reproduction) on the numbers and ratios of
1425 the fruit morphs in the 2016 harvest (large-scale) experiment (Supplemental Figure S1) and
1426 the 2014 harvest experiment (mean \pm SD values of 3 replicates; total numbers of fruits were
1427 normalized to the large-scale experiment to aid comparison of the relative numbers for IND
1428 and DEH; the 20°C and 25°C 2014 harvest was used in the Lenser *et al.* (2016) publication).
1429 C, The effect of imbibition temperatures on the maximal germination percentages (G_{max}) and
1430 the speed of germination expressed as germination rate ($GR_{50\%}$) of the dimorphic diaspores
1431 (M^+ seeds, IND fruits), and for comparison of bare M^- seeds (extracted from IND fruits by
1432 pericarp removal). Sampling temperatures for molecular analyses are indicated. Mean \pm SEM
1433 values of 3 replicate plates each with 20 seeds.

1434

1435

1436 **Figure 2** Principle components analysis (PCA) comparing the seed mRNA transcriptome data
1437 (RNA-sequencing analysis) of *Aethionema arabicum*. Mature M^+ and M^- seeds, and IND fruits
1438 harvested from plants at two different parental temperatures during reproduction (20 and
1439 25°C) were sampled in the dry state, and in the imbibed state at four different imbibition
1440 temperatures (9, 14, 20 and 24°C) and times indicated (e.g. 24 h); physiological time points
1441 ($T_{1\%}$) are also indicated. Indicated by asterisk, no germination occurred at 24°C imbibition
1442 temperature (precluding $T_{1\%}$ sampling) and 20 M^+ imbibed at 20°C was sampled only at 24h.
1443 PC1 and PC2 explain 25% and 14% of the variance; for PC3 and individual samples see
1444 Supplemental Figure S3. Large points indicate average coordinates from three replicates,
1445 with the location of each replicate relative to the average shown with a line (some lines are
1446 hidden by large point), time point label drop line differentiated by dotted line.

1447

1448

1449 **Figure 3** Weighted gene expression correlation network analysis (WGCNA) modules
1450 identified from dry and imbibed seed transcriptomes. WGCNA of 11260 genes identified
1451 eleven co-expressed gene modules, identified by color, across mature M^+ and M^- seeds, and
1452 IND fruits harvested from plants at two different parental temperatures during reproduction
1453 (20 and 25°C) sampled in the dry state, and in the imbibed state at four different imbibition
1454 temperatures (9, 14, 20 and 24°C) at multiple time points. In the center, genes were
1455 separated by PCA of expression across all samples (first two principal components) and
1456 colored by module membership. Largest points indicate genes identified with the highest
1457 module membership for each module, labeled, and two additional large points representing
1458 high module membership candidates for the given module. Outer plots show mean Z-score
1459 expression of module genes during imbibition for M^+ seeds, M^- seeds and IND fruits
1460 harvested from plants grown at 20°C and imbibed at 9°C. Expression of genes in modules for
1461 all samples is shown in Supplemental Figure S4.

1462

1463

1464 **Figure 4** Correlation of WGCNA module expression with sample traits (hormone metabolites,
1465 PCA coordinates) and clustering. Hormone metabolites included are abscisic acid (ABA),
1466 ABA degradation products phaseic acid (PA) and dihydrophaseic acid (DPA), salicylic acid
1467 (SA), jasmonic acid (JA) and its isoleucine conjugate (JA-Ile), *cis*-(+)-12-oxophytodienoic acid

1465 (OPDA), indole-3-acetic acid (IAA) and its degradation product 2-ox-IAA (oxIAA). Sample
1466 PCA coordinates (PC1, PC2, PC3) were included as traits. Imbibition time, parental and
1467 imbibition temperature, GR_{50%} and G_{max} of samples were included. M⁺ and M⁻ seed, and
1468 indehiscent fruit (IND, pericarp presence) were included as binary variables (Plus, 0 or 1;
1469 Minus, 0 or 1; IND, 0 or 1). Asterisks indicate correlation significance: * - p < 0.05, ** - p <
1470 0.01, *** - p < 0.0001) Correlation similarity tree was created using hierarchical clustering (1 -
1471 Pearson, average linkage using Morpheus, <https://software.broadinstitute.org/morpheus>).
1472

1473 **Figure 5** Comparative analysis of germination responses at different temperatures,
1474 associated abscisic acid (ABA) content and transcript abundance patterns of *Aethionema*
1475 *arabicum* dimorphic diaspores. Dimorphic diaspores (M⁺ seeds, IND fruits) and bare M⁻ seeds
1476 (extracted from IND fruits by pericarp removal) from two parental temperature regimes during
1477 reproduction (20°C versus 25°C) were compared for their germination kinetics, seed ABA
1478 contents (M⁺ seeds, bare M⁻ seeds, and M⁻ seeds encased inside the imbibed IND fruit) and
1479 seed transcript abundance patterns at four different imbibition temperatures (9, 14, 20 and
1480 24°C). Comparative results were obtained for physical (in hours) and physiological time points
1481 (T_{1%}, representing the population's onset of germination completion). Normalized transcript
1482 abundances in reads per kilobase per million (RPKM) from the transcriptomes (RNA-seq) are
1483 presented for the ABA biosynthesis 9-cis-epoxycarotenoid dioxygenase gene *AearNCED6*,
1484 the ABA 8'-hydroxylase gene *AearCYP707A3*, the plasma membrane ABA uptake transporter
1485 gene *AearABCG40*, and the *Delay of germination 1* dormancy gene *AearDOG1*. WGCNA
1486 modules (Figure 3) for these genes are indicated by the vertical color lines next to the graphs.
1487 For *Ae. arabicum* gene names and IDs see Supplemental Table S2 or the Expression Atlas
1488 (https://plantcode.cup.uni-freiburg.de/aetar_db/index.php); for RNAseq single values see the
1489 Expression Atlas or Supplemental Data Set 1. Mean ± SEM values of 3 (germination, RNA-
1490 seq) or 5 (ABA) replicates each with 20 (germination), 30-40 (ABA) and 60-80 (RNA-seq)
1491 seeds are presented.
1492

1493 **Figure 6** The effect of parental temperature (PT) on the biochemical and biomechanical
1494 properties of the IND pericarp and the pericarp-imposed dormancy of *Aethionema arabicum*.
1495 A, Comparative analysis of hormone metabolite contents in IND pericarps, M⁺ and M⁻ seeds
1496 from two parental temperature regimes (20°C versus 25°C) in the dry state and for ABA
1497 during imbibition at 9°C (see Supplemental Figure S6 for other imbibition temperatures and
1498 other hormone metabolites). Hormone metabolites presented: abscisic acid (ABA) and ABA
1499 degradation products phaseic acid (PA) and dihydrophaseic acid (DPA), salicylic acid (SA),
1500 jasmonic acid (JA) and its isoleucine conjugate (JA-Ile), *cis*-(+)-12-oxophytodienoic acid
1501 (OPDA). Mean ± SEM values of 5 (hormone metabolites) biological replicate samples are
1502 presented. B, The effect of parental temperature during reproduction on the IND pericarp
1503 resistance quantified by biomechanical analysis. Results are presented as box plots, whiskers
1504 are drawn down to the 10th percentile and up to the 90th (mean is indicated by '+'), n = 42.
1505 The micropylar (where the radicle emerges during fruit germination) pericarp half grown at
1506 20°C shows a slightly higher tissue resistance versus 25°C (p = 0.047). The non-micropylar
1507 half has a higher tissue resistance whilst not showing any difference between 20IND and
1508 25IND; see Supplemental Figure S8 for extended biomechanical properties. C, The effect of
1509 parental temperature on the IND pericarp biochemical composition as analyzed by
1510 multispectral imaging (MSI).
1511

1512 **Figure 7** Transcription factor (TF) and target *cis*-regulatory motif analysis of *Aethionema*
1513 *arabicum* gene expression with focus on hypoxia and ABA related genes. A, Chord diagram
1514 of identified TFs and their target genes in the WGCNA modules. Examples for TFs (*red* or
1515 *blue*) and their target genes (*black*). B, Transcript abundance patterns (RNA-seq) of the *Ae.*
1516 *arabicum Hypoxia responsive ERF* (*AearERF71/73*) TF and the alcohol dehydrogenase
1517 genes *AearADH1a* and *AearADH1b* in seeds of imbibed dimorphic diaspores (M^+ seeds, IND
1518 fruits) and bare M^- seeds from two parental temperature regimes (20°C versus 25°C) at four
1519 different imbibition temperatures (9, 14, 20 and 24°C). WGCNA modules (Figure 3) for these
1520 genes are indicated by the vertical color lines next to the graphs. Mean \pm SEM values of 3
1521 replicates each with 60-80 seeds are presented. C, Hypothetical working model for the
1522 pericarp-mediated hypoxia up-regulation ($P\uparrow$) and ABA signaling, and *cis*-regulatory motifs for
1523 the *Ae. arabicum ERF71/73*, *ADH1a*, *ADH1b*, and *DOG1* genes. Promoter motifs indicated
1524 include the hypoxia-responsive promoter element HRPE, the G-box and ABA-responsive
1525 element (ABRE), the ERF73 *cis*-regulatory element and HB-motifs for the binding of
1526 homeobox TFs (for details see Supplemental Figure S10). These motifs are the targets for the
1527 *AearERF71/73* TF (ERF7X, *red ellipse*) and the ABA related *ABI5*, *ABF* (ABRE-binding
1528 factors), *GBF* (G-box-binding factors), and *AREB3* TFs (*blue boxes*). D, Comparative analysis
1529 of the corresponding *Arabidopsis thaliana AtERF73*, *AtADH1* and *AtDOG1* gene 5'-regulatory
1530 regions (for details see Supplemental Figure S10). Note that *A. thaliana* has only one while
1531 *Ae. arabicum* has two ADH genes; see Supplemental Figure S9 for other fermentation-related
1532 genes. For *Ae. arabicum* gene names and IDs see Supplemental Table S2 or the Expression
1533 Atlas (https://plantcode.cup.uni-freiburg.de/aetar_db/index.php); for RNAseq single values
1534 see the Expression Atlas or Supplemental Data Set 1.

1535 **Figure 8** The effect of hypoxia and ABA on germination and gene expression of bare M^-
1536 seeds. A, RT-pPCR expression analysis of selected genes during *Aethionema arabicum* bare
1537 M^- seed imbibition under hypoxia ($4.5\pm0.2\%$ oxygen) and normoxia (21% oxygen) conditions
1538 $\pm 5\ \mu M$ abscisic acid (ABA). Bare M^- seeds were obtained from dry IND fruits by pericarp
1539 removal and imbibed at 14°C in continuous light. The 38 h timepoint (arrow) corresponds to
1540 $T_{1\%}$ of the control (normoxia without ABA). For additional genes and expression in IND fruits
1541 see Supplemental Figure S12. B, RT-pPCR expression analysis of genes representing the
1542 WGCNA modules used in Supplemental Figure S7 to investigate the effects of pericarp
1543 extract. C, Correlation analysis between the effects of the pericarp (IND fruits), hypoxia (M^-
1544 seeds) and ABA (M^- seeds) on the expression of 32 genes as compared to M^- seeds in
1545 normoxia (control). 'Treatments / control' ratios (y-axis) of fold-change values (from the dry
1546 state to 24 h or 38 h) were calculated and plotted against the 'IND fruit / control' ratios (x-axis).
1547 Linear regression lines indicate strong linear relationships for hypoxia versus pericarp (R^2
1548 0.79 and 0.70 for 38 h and 24 h, respectively) and for hypoxia+ABA versus pericarp (R^2 0.80
1549 and 0.75), but not for ABA versus pericarp (R^2 0.16 and 0.30). Mean \pm SEM values of 3
1550 (germination, RT-qPCR) biological replicate samples are presented. For *Ae. arabicum* gene
1551 names and IDs see Supplemental Table S2 or the Expression Atlas
1552 (https://plantcode.cup.uni-freiburg.de/aetar_db/index.php).
1553

1554 **Figure 9** Transcript abundance patterns (RNA-seq) of *Aethionema arabicum* ABA-related and
1555 homeobox (HB) TF genes. Results for *AearAREB3a*, *AearABI5*, *AearABF1*, *AearGBF3*, and
1556 *AearHB13* transcript abundances in seeds of imbibed dimorphic diaspores (M^+ seeds, IND
1557 fruits) and bare M^- seeds (extracted from IND fruits) from two parental temperature regimes
1558 (20°C versus 25°C) at four different imbibition temperatures (9, 14, 20 and 24°C) are

1560 presented (see Supplemental Figure S14 for other ABF, GBF and HB TFs). WGCNA modules
1561 (Figure 3) are indicated by the vertical color lines next to the graphs. For *Ae. arabicum* gene
1562 names and IDs see Supplemental Table S2 or the Expression Atlas
1563 (https://plantcode.cup.uni-freiburg.de/aetar_db/index.php); for RNAseq single values see the
1564 Expression Atlas or Supplemental Data Set 1. Mean \pm SEM values of 3 replicates each with
1565 60-80 seeds are presented.
1566

1567 **Figure 10** Transcript abundance patterns (RNA-seq) of *Aethionema arabicum* cell-wall
1568 remodeling protein genes in seeds of imbibed dimorphic diaspores (M^+ seeds, IND fruits) and
1569 bare M^- seeds. A, Effect of the pericarp on the expression ratios of expansin A and
1570 xyloglucan-related cell-wall remodeling protein genes in the M^- seeds of 24 h imbibed IND
1571 fruits and isolated M^- seeds. B, Xyloglucan remodeling is achieved by a battery of enzymes
1572 specifically targeting different bonds of xyloglucan structure as indicated. Among them are
1573 xyloglucan *endo*-transglycylases/hydrolases (XTHs) with xyloglucan *endo*-transglycylase
1574 (XET) enzyme activity (Holloway et al., 2021). C, Transcript abundance patterns of *Ae.*
1575 *arabicum* expansins A, XTHs and the α -xylosidase *Aear- α XYL1* in M^+ seeds, IND fruits and
1576 isolated M^- seeds from two parental temperature regimes (20°C versus 25°C) at four different
1577 imbibition temperatures (9, 14, 20 and 24°C). For other expansin and xyloglucan-related
1578 genes and *Ae. arabicum* gene IDs see Supplemental Figure S16 or the Expression Atlas
1579 (https://plantcode.cup.uni-freiburg.de/aetar_db/index.php); for RNAseq single values see the
1580 Expression Atlas or Supplemental Data Set 1. WGCNA modules (Figure 3) are indicated by
1581 the vertical color lines next to the graphs. Mean \pm SEM values of 3 replicates each with 60-80
1582 seeds are presented.
1583
1584

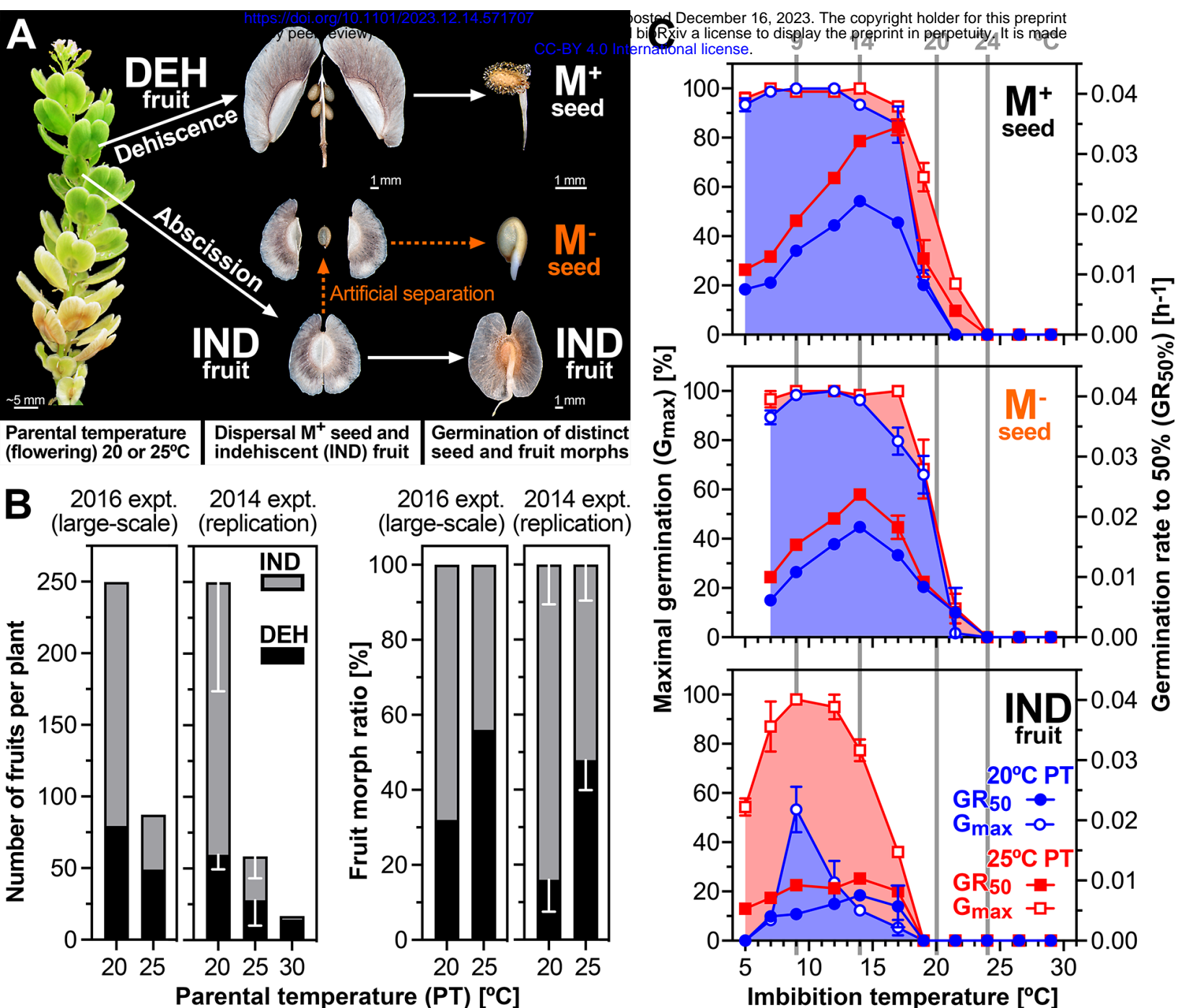


Figure 1 Dimorphic diaspore responses of *Aethionema arabicum* to ambient temperatures.

A, Infructescence showing two morphologically distinct fruit types. Large, dehiscent (DEH) fruits contain four to six seed diaspores that produce mucilage (M⁺) upon imbibition. Small, indehiscent (IND) fruits contain a single non-mucilaginous (M⁻) seed each. For experiments with the bare M⁻ seed the pericarp was manually removed.

B, The effect of parental temperatures (PT; ambient temperatures during reproduction) on the numbers and ratios of the fruit morphs in the 2016 harvest (large-scale) experiment (Supplemental Figure S1) and the 2014 harvest experiment (mean \pm SD values of 3 replicates; total numbers of fruits were normalized to the large-scale experiment to aid comparison of the relative numbers for IND and DEH; the 20°C and 25°C 2014 harvest was used in the Lenser et al. (2016) publication).

C, The effect of imbibition temperatures on the maximal germination percentages (G_{max}) and the speed of germination expressed as germination rate (GR₅₀) of the dimorphic diaspores (M⁺ seeds, IND fruits), and for comparison of bare M⁻ seeds (extracted from IND fruits by pericarp removal). Sampling temperatures for molecular analyses are indicated. Mean \pm SEM values of 3 replicate plates each with 20 seeds.

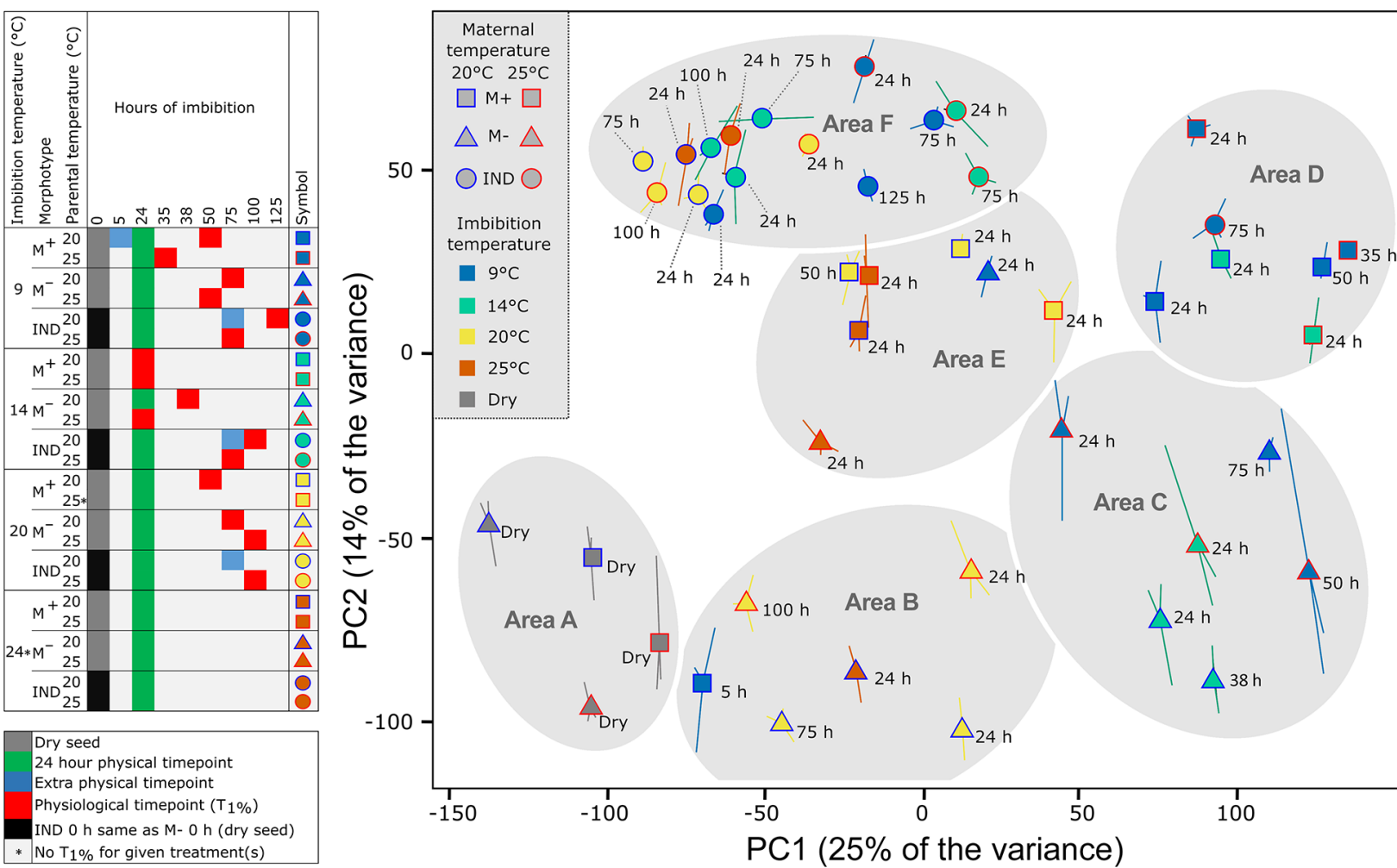


Figure 2 Principle components analysis (PCA) comparing the seed mRNA transcriptome data (RNA-sequencing analysis) of *Aethionema arabicum*. Mature M+ and M- seeds, and IND fruits harvested from plants at two different parental temperatures during reproduction (20 and 25°C) were sampled in the dry state, and in the imbibed state at four different imbibition temperatures (9, 14, 20 and 24°C) and times indicated (e.g. 24 h); physiological time points (T1%) are also indicated. Indicated by asterisk, no germination occurred at 24°C imbibition temperature (precluding T1% sampling) and 20M+ imbibed at 20°C was sampled only at 24h. PC1 and PC2 explain 25% and 14% of the variance; for PC3 and individual samples see Supplemental Figure S3. Large points indicate average coordinates from three replicates, with the location of each replicate relative to the average shown with a line (some lines are hidden by large point), time point label drop line differentiated by dotted line.

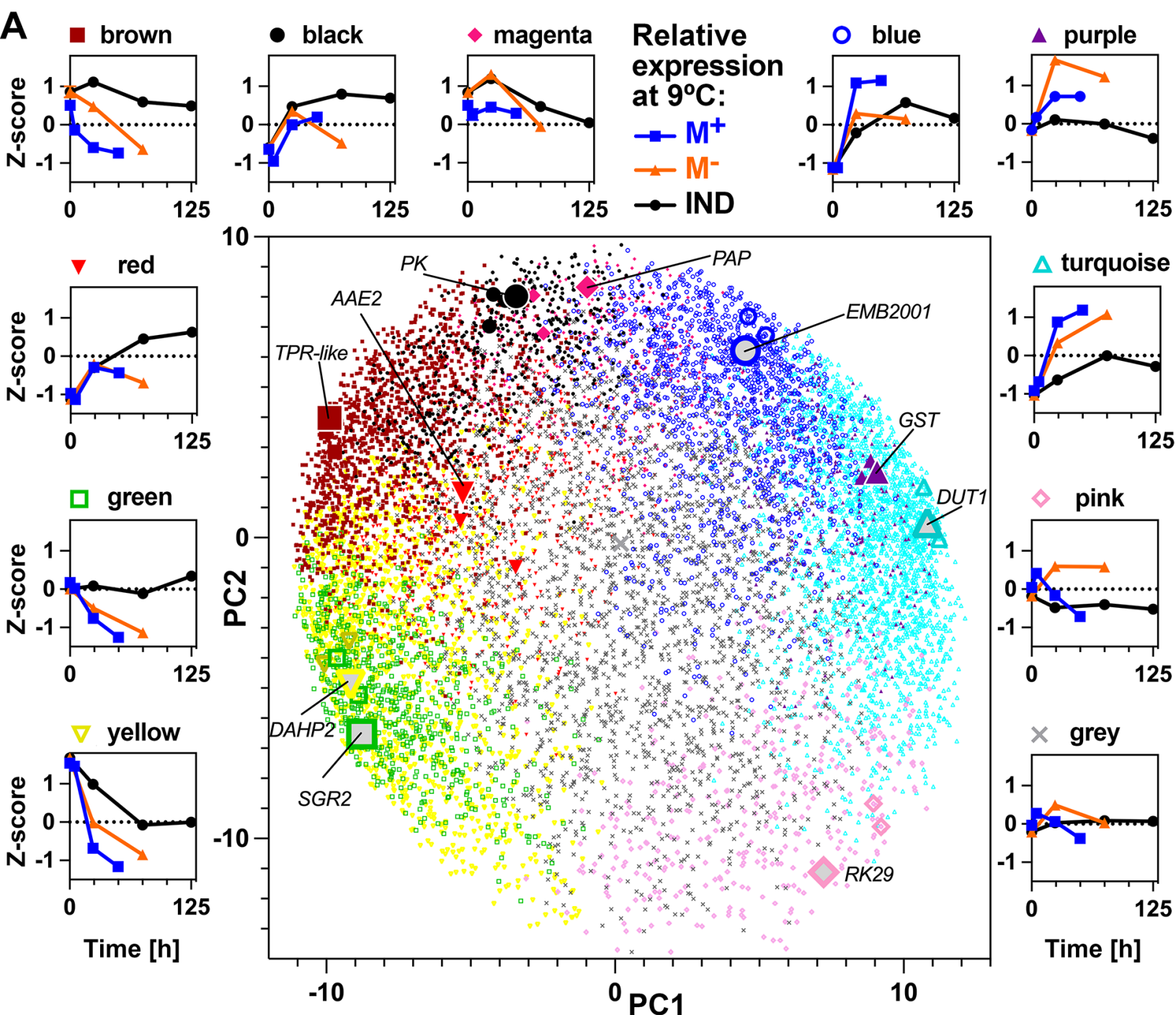


Figure 3 Weighted gene expression correlation network analysis (WGCNA) modules identified from dry and imbibed seed transcriptomes. WGCNA of 11260 genes identified eleven co-expressed gene modules, identified by color, across mature M^+ and M^- seeds, and IND fruits harvested from plants at two different parental temperatures during reproduction (20 and 25°C) sampled in the dry state, and in the imbibed state at four different imbibition temperatures (9, 14, 20 and 24°C) at multiple time points. In the center, genes were separated by PCA of expression across all samples (first two principal components) and colored by module membership. Largest points indicate genes identified with the highest module membership for each module, labeled, and two additional large points representing high module membership candidates for the given module. Outer plots show mean Z-score expression of module genes during imbibition for M^+ seeds, M^- seeds and IND fruits harvested from plants grown at 20°C and imbibed at 9°C. Expression of genes in modules for all samples is shown in Supplemental Figure S4.

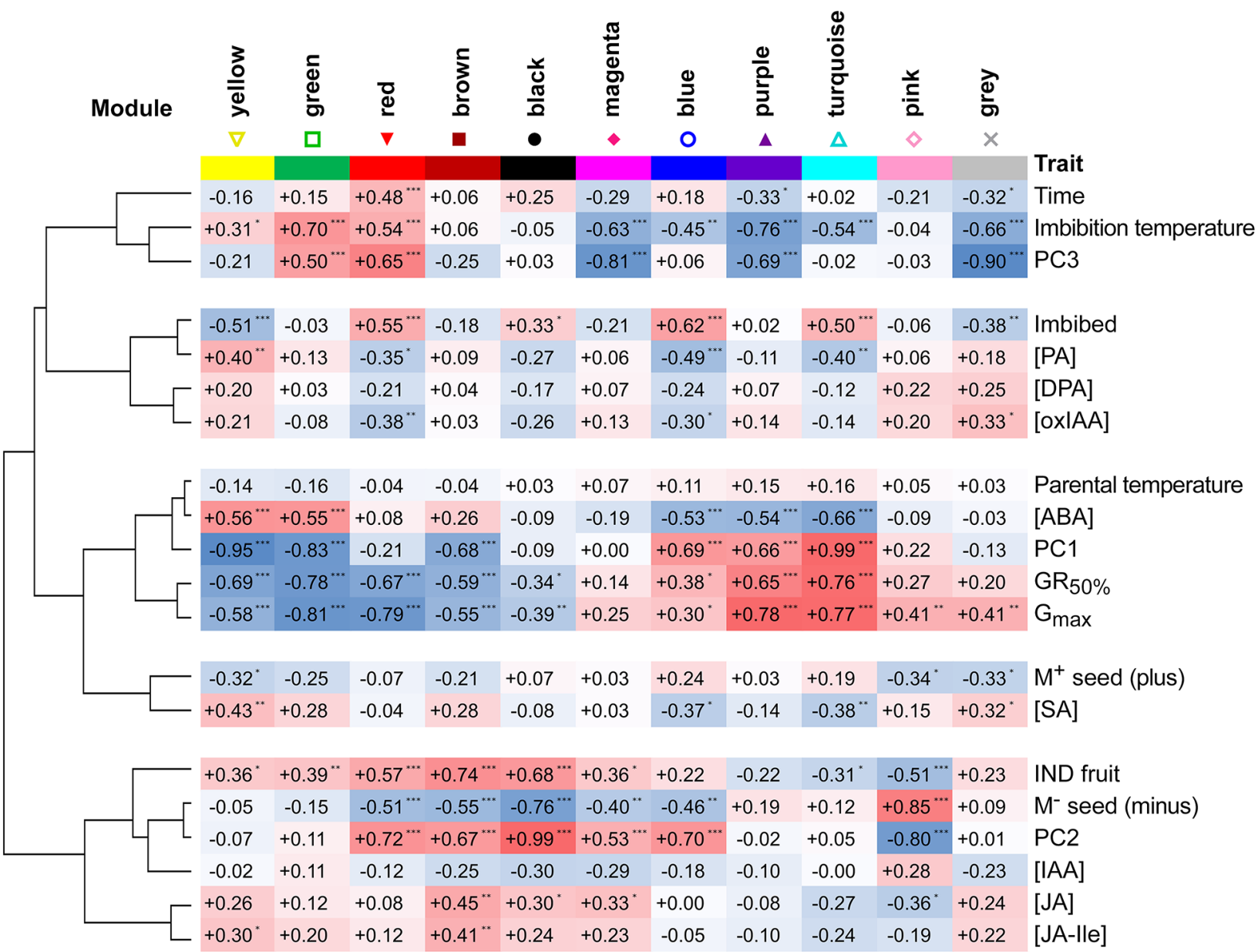


Figure 4 Correlation of WGCNA module expression with sample traits (hormone metabolites, PCA coordinates) and clustering. Hormone metabolites included are abscisic acid (ABA), ABA degradation products phaseic acid (PA) and dihydrophaseic acid (DPA), salicylic acid (SA), jasmonic acid (JA) and its isoleucine conjugate (JA-Ile), cis-(+)-12-oxophytodienoic acid (OPDA), indole-3-acetic acid (IAA) and its degradation product 2-ox-IAA (oxIAA). Sample PCA coordinates (PC1, PC2, PC3) were included as traits. Imbibition time, parental and imbibition temperature, GR50% and Gmax of samples were included. M+ and M- seed, and indehiscent fruit (IND, pericarp presence) were included as binary variables (Plus, 0 or 1; Minus, 0 or 1; IND, 0 or 1). Asterisks indicate correlation significance: * - $p < 0.05$, ** - $p < 0.01$, *** - $p < 0.0001$) Correlation similarity tree was created using hierarchical clustering (1 - Pearson, average linkage using Morpheus, <https://software.broadinstitute.org/morpheus>).

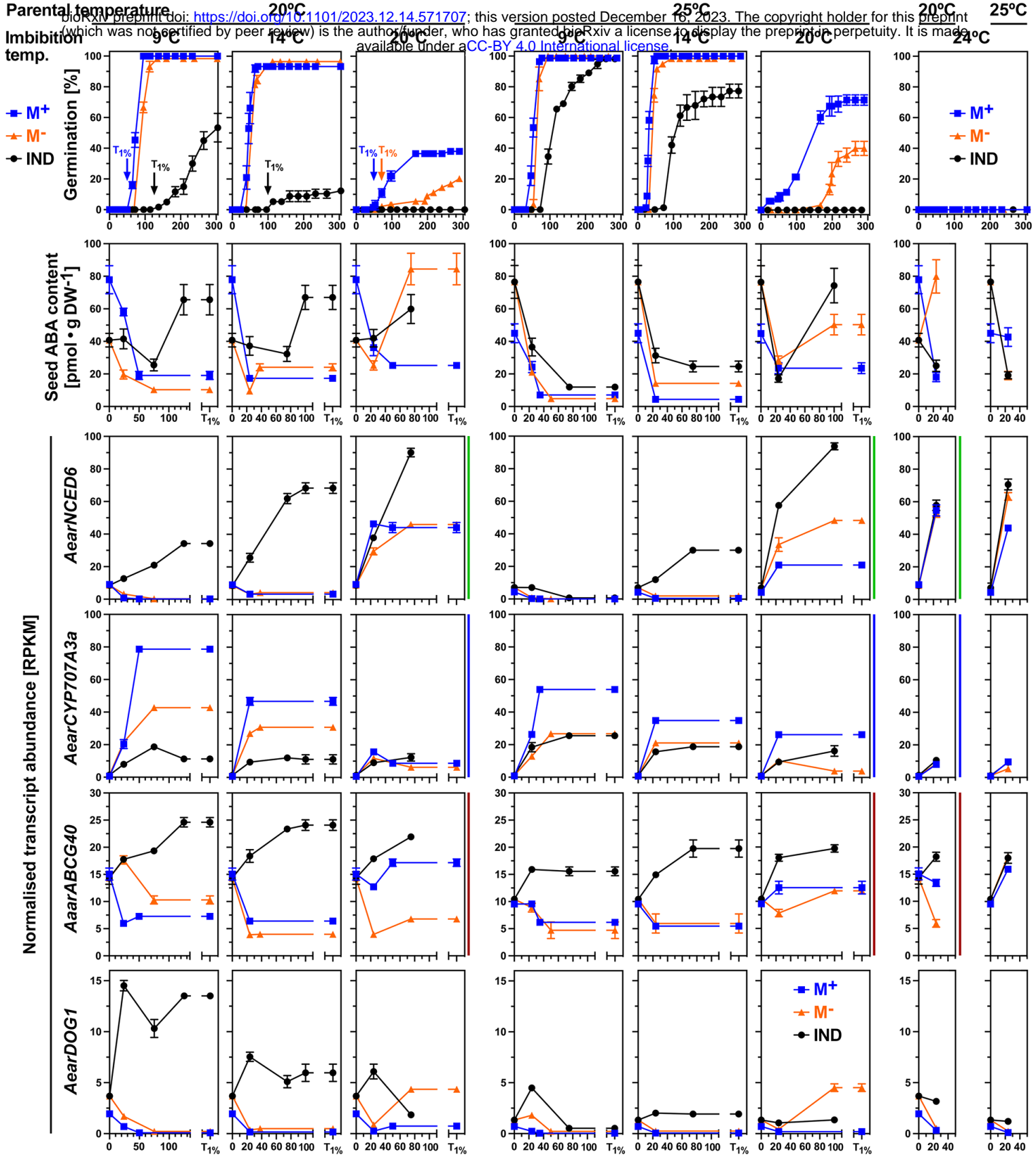


Figure 5 Comparative analysis of germination responses at different temperatures, associated abscisic acid (ABA) content and transcript abundance patterns of *Aethionema arabicum* dimorphic diaspores. Dimorphic diaspores (M+ seeds, IND fruits) and bare M- seeds (extracted from IND fruits by pericarp removal) from two parental temperature regimes during reproduction (20°C versus 25°C) were compared for their germination kinetics, seed ABA contents and seed transcript abundance patterns at four different imbibition temperatures (9, 14, 20 and 24°C). Comparative results were obtained for physical (in hours) and physiological time points (T1%, representing the population's onset of germination completion). Normalized transcript abundances in reads per kilobase per million (RPKM) from the transcriptomes (RNA-seq) are presented for the ABA biosynthesis 9-cis-epoxycarotenoid dioxygenase gene AearNCED6, the ABA 8'-hydroxylase gene AearCYP707A3, the plasma membrane ABA uptake transporter gene AearABCG40, and the Delay of germination 1 dormancy gene AearDOG1. WGCNA modules (Figure 3) for these genes are indicated by the vertical color lines next to the graphs. For *Ae. arabicum* gene names and IDs see Supplemental Table S2 or the Expression Atlas (https://plantcode.cup.uni-freiburg.de/aetar_db/index.php). Mean \pm SEM values of 3 (germination, RNA-seq) or 5 (ABA) replicates each with 20 (germination), 30-40 (ABA) and 60-80 (RNA-seq) seeds are presented.

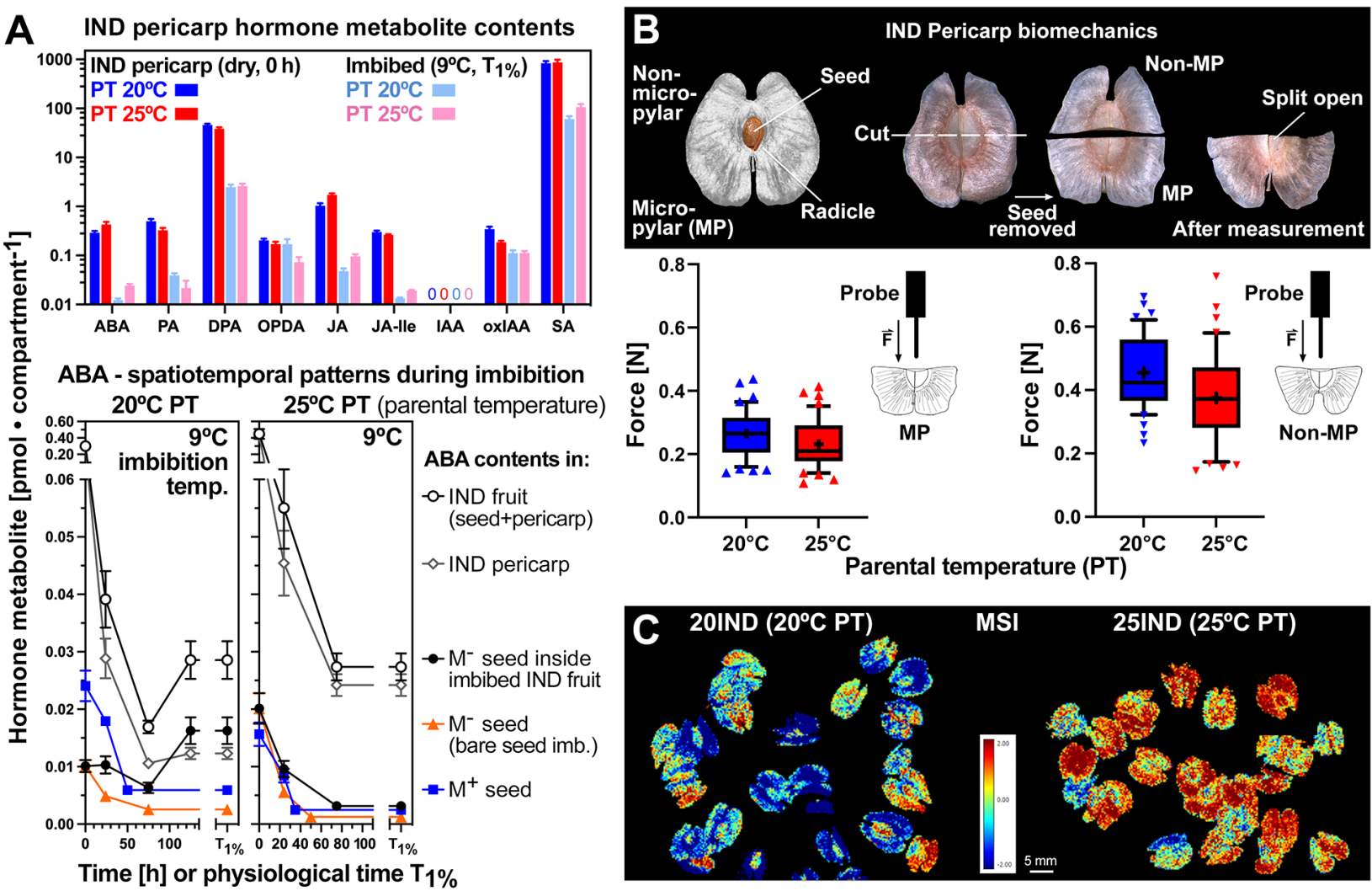
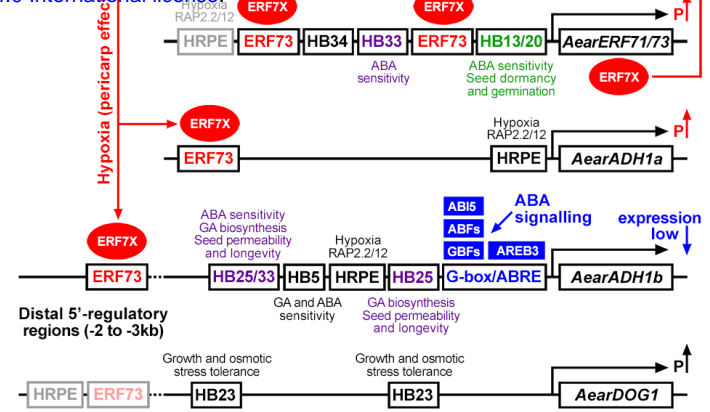
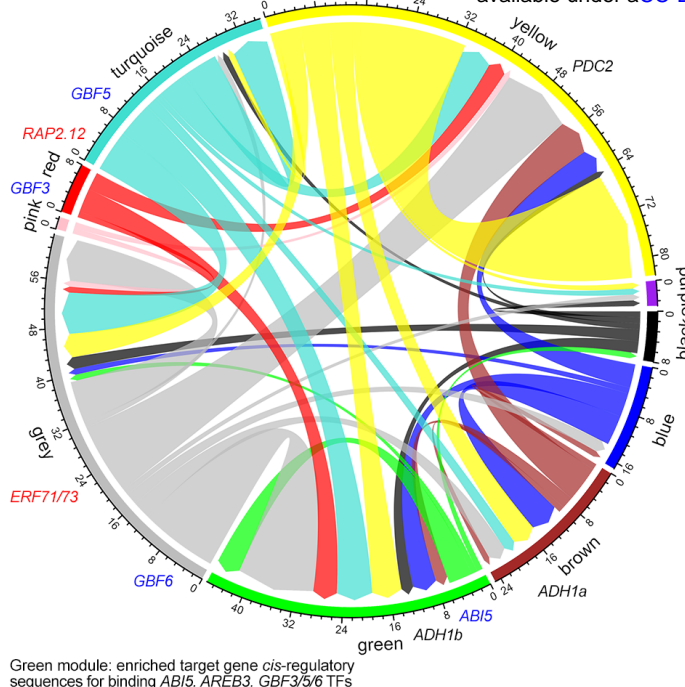


Figure 6 The effect of parental temperature (PT) on the biochemical and biomechanical properties of the IND pericarp and the pericarp-imposed dormancy of *Aethionema arabicum*.

A, Comparative analysis of hormone metabolite contents in IND pericarps, M+ and M- seeds from two parental temperature regimes (20°C versus 25°C) in the dry state and for ABA during imbibition at 9°C (see Supplemental Figure S6 for other imbibition temperatures and other hormone metabolites). Hormone metabolites presented: abscisic acid (ABA) and ABA degradation products phaseic acid (PA) and dihydrophaseic acid (DPA), salicylic acid (SA), jasmonic acid (JA) and its isoleucine conjugate (JA-Ile), cis-(+)-12-oxophytodienoic acid (OPDA). Mean \pm SEM values of 5 (hormone metabolites) biological replicate samples are presented.

B, The effect of parental temperature during reproduction on the IND pericarp resistance quantified by biomechanical analysis. Results are presented as box plots, whiskers are drawn down to the 10th percentile and up to the 90th (mean is indicated by '+'), n = 42. The micropylar (where the radicle emerges during fruit germination) pericarp half grown at 20°C shows a slightly higher tissue resistance versus 25°C (p = 0.047). The non-micropylar half has a higher tissue resistance whilst not showing any difference between 20IND and 25IND; see Supplemental Figure S8 for extended biomechanical properties. C, The effect of parental temperature on the IND pericarp biochemical composition as analyzed by multispectral imaging (MSI).



D *Arabidopsis thaliana* gene proximal 1-kb 5'-regulatory regions

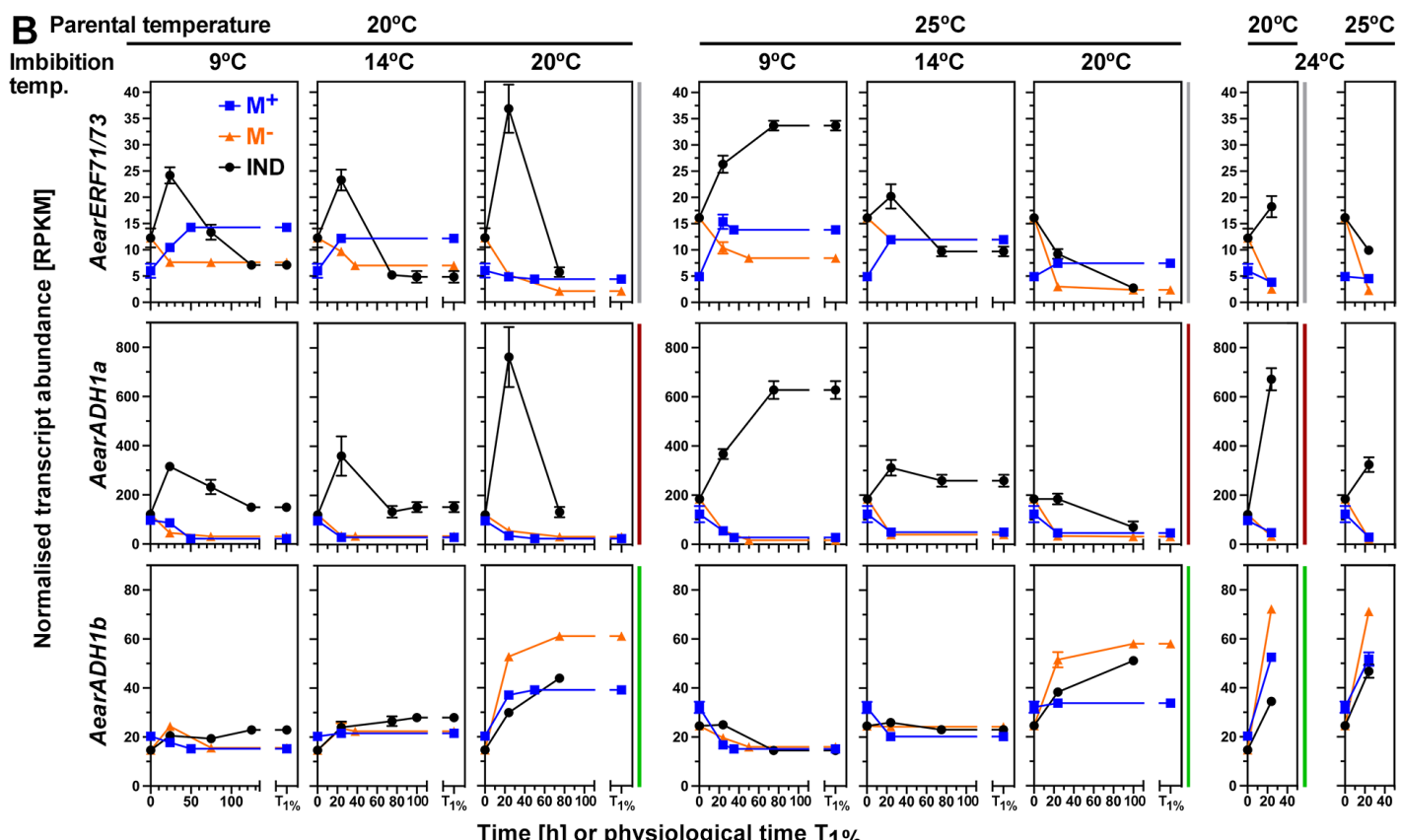
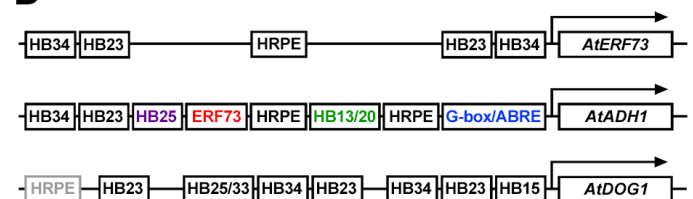


Figure 7 Transcription factor (TF) and target cis-regulatory motif analysis of *Aethionema arabicum* gene expression with focus on hypoxia and ABA related genes. **A**, Chord diagram of identified TFs and their target genes in the WGCNA modules. Examples for TFs (red or blue) and their target genes (black). **B**, Transcript abundance patterns (RNA-seq) of the *Ae. arabicum* Hypoxia responsive ERF (AearERF71/73) TF and the alcohol dehydrogenase genes AearADH1a and AearADH1b in seeds of imbibed dimorphic diaspores (M+ seeds, IND fruits) and bare M-seeds from two parental temperature regimes (20°C versus 25°C) at four different imbibition temperatures (9, 14, 20 and 24°C). WGCNA modules (Figure 3) for these genes are indicated by the vertical color lines next to the graphs. Mean \pm SEM values of 3 replicates each with 60-80 seeds are presented. **C**, Working model for the pericarp-mediated hypoxia up-regulation (P) and ABA signaling, and cis-regulatory motifs for the *Ae. arabicum* ERF71/73, ADH1a, ADH1b, and DOG1 genes. Promoter motifs indicated include the hypoxia-responsive promoter element HRPE, the G-box and ABA-responsive element (ABRE), the ERF73 cis-regulatory element and HB-motifs for the binding of homeobox TFs (for details see Supplemental Figure S9). These motifs are the targets for the AearERF71/73 TF (ERF7X, red ellipse) and the ABA related ABF5, ABF (ABRE-binding factors), GBF (G-box-binding factors), and AREB3 TFs (blue boxes). **D**, Comparative analysis of the corresponding *Arabidopsis thaliana* AtERF73, AtADH1 and AtDOG1 gene 5'-regulatory regions (for details see Supplemental Figure S9). Note that *A. thaliana* has only one while *Ae. arabicum* has two ADH genes; see Supplemental Figure S8 for other fermentation-related genes. For *Ae. arabicum* gene names and IDs see Supplemental Table S2 or the Expression Atlas (https://plantcode.cup.uni-freiburg.de/aetar_db/index.php).

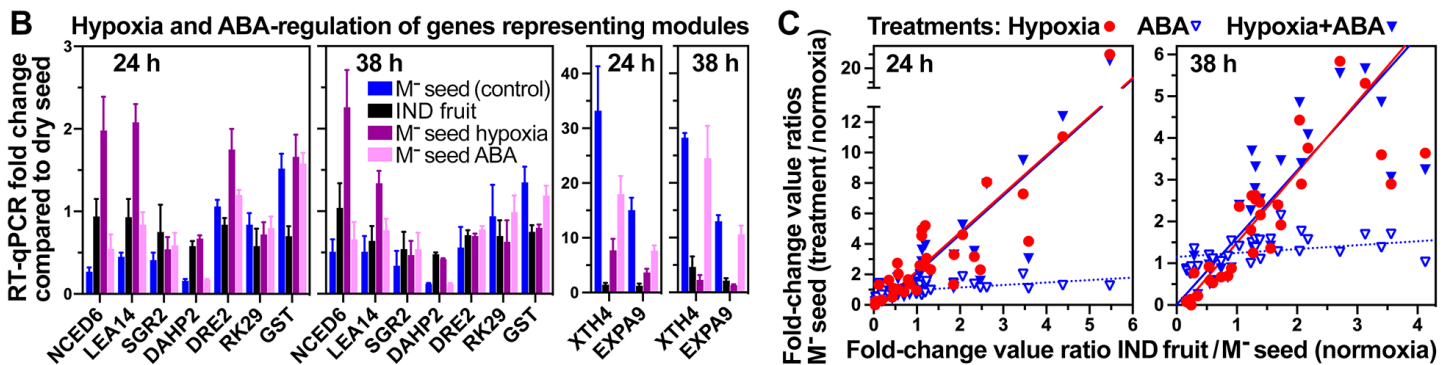
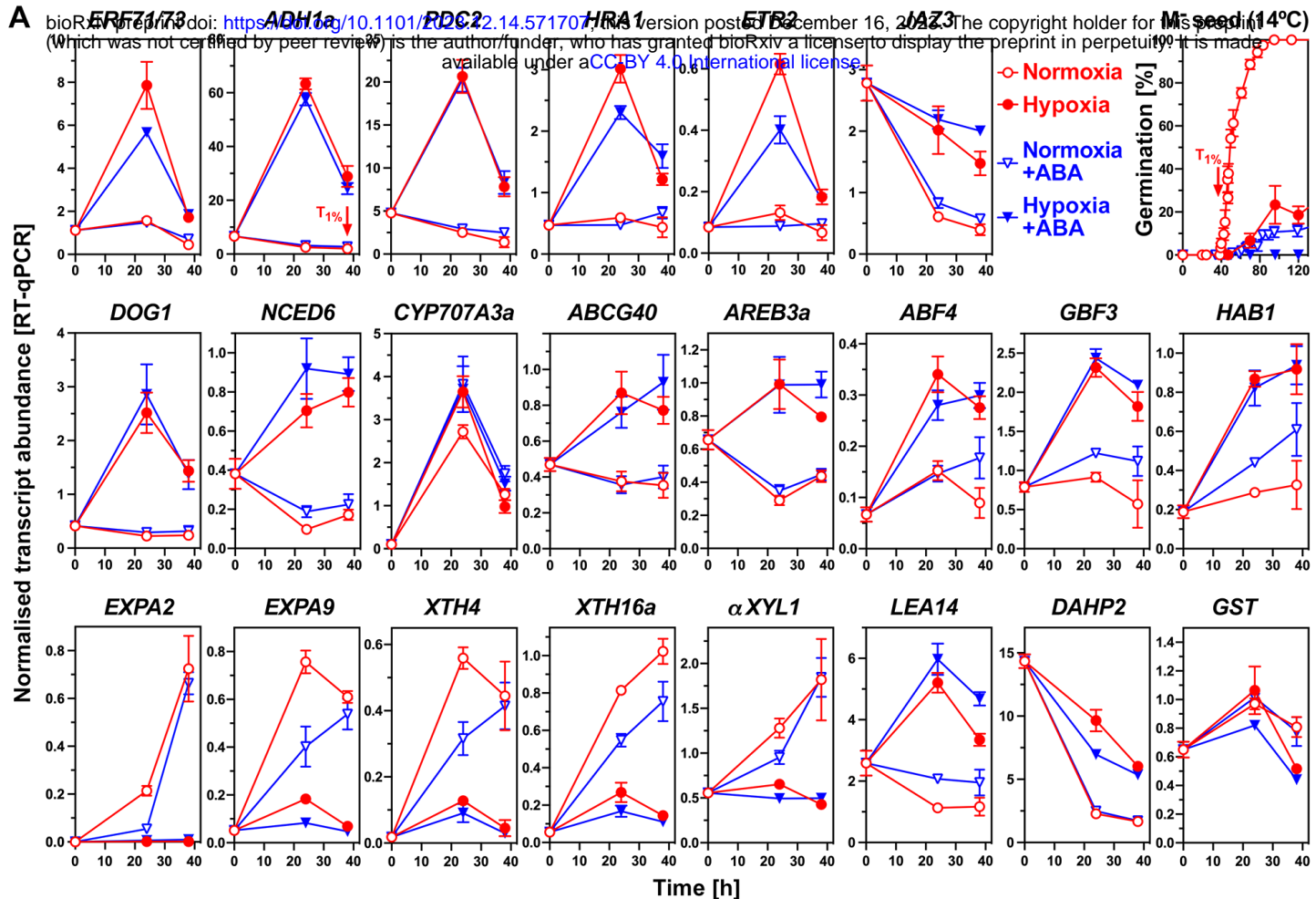


Figure 8 The effect of hypoxia and ABA on germination and gene expression of bare M- seeds.

A, RT-pPCR expression analysis of selected genes during *Aethionema arabicum* bare M- seed imbibition under hypoxia ($4.5 \pm 0.2\%$ oxygen) and normoxia (21% oxygen) conditions $\pm 5 \mu\text{M}$ abscisic acid (ABA). Bare M- seeds were obtained from dry IND fruits by pericarp removal and imbibed at 14°C in continuous light. The 38 h timepoint (arrow) corresponds to T1% of the control (normoxia without ABA). For additional genes and expression in IND fruits see Supplemental Figure S12.

B, RT-pPCR expression analysis of genes representing the WGCNA modules used in Supplemental Figure S7 to investigate the effects of pericarp extract.

C, Correlation analysis between the effects of the pericarp (IND fruits), hypoxia (M- seeds) and ABA (M- seeds) on the expression of 32 genes as compared to M- seeds in normoxia (control). 'Treatments / control' ratios (y-axis) of fold-change values (from the dry state to 24 h or 38 h) were calculated and plotted against the 'IND fruit / control' ratios (x-axis). Linear regression lines indicate strong linear relationships for hypoxia versus pericarp ($R^2 = 0.79$ and 0.70 for 38 h and 24 h, respectively) and for hypoxia+ABA versus pericarp ($R^2 = 0.80$ and 0.75), but not for ABA versus pericarp ($R^2 = 0.16$ and 0.30). Mean \pm SEM values of 3 (germination, RT-qPCR) biological replicate samples are presented. For *Ae. arabicum* gene names and IDs see Supplemental Table S2 or the Expression Atlas (https://plantcode.cup.uni-freiburg.de/aetar_db/index.php).

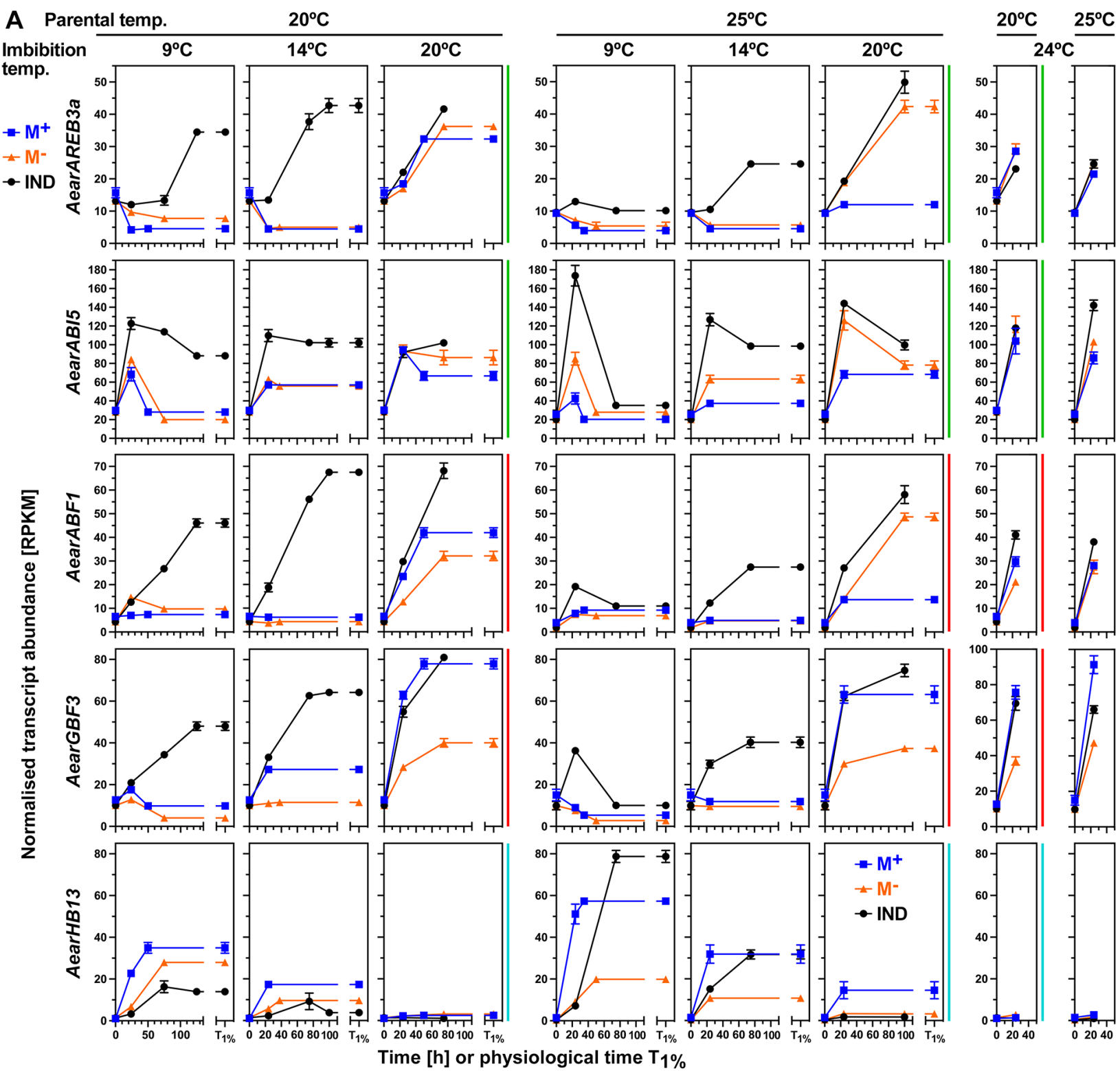


Figure 9 Transcript abundance patterns (RNA-seq) of *Aethionema arabicum* ABA-related and homeobox (HB) TF genes. Results for AearAREB3a, AearABI5, AearABF1, AearGBF3, and AearHB13 transcript abundances in seeds of imbibed dimorphic diaspores (M+ seeds, IND fruits) and bare M- seeds (extracted from IND fruits) from two parental temperature regimes (20°C versus 25°C) at four different imbibition temperatures (9, 14, 20 and 24°C) are presented (see Supplemental Figure S12 for other ABF, GBF and HB TFs). WGCNA modules (Figure 3) are indicated by the vertical color lines next to the graphs. For Ae. arabicum gene names and IDs see Supplemental Table S2 or the Expression Atlas (https://plantcode.cup.uni-freiburg.de/aetar_db/index.php). Mean \pm SEM values of 3 replicates each with 60-80 seeds are presented.

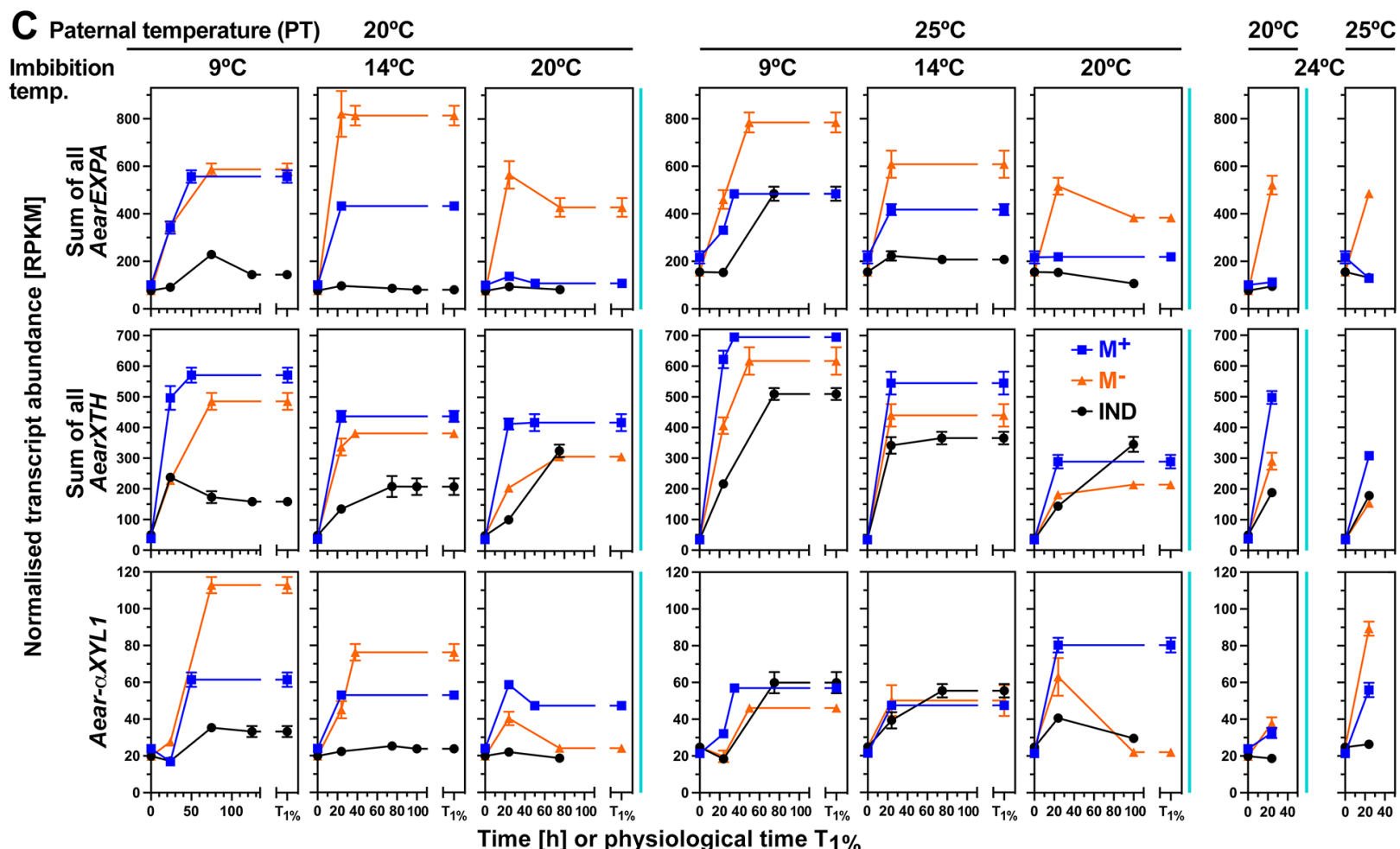
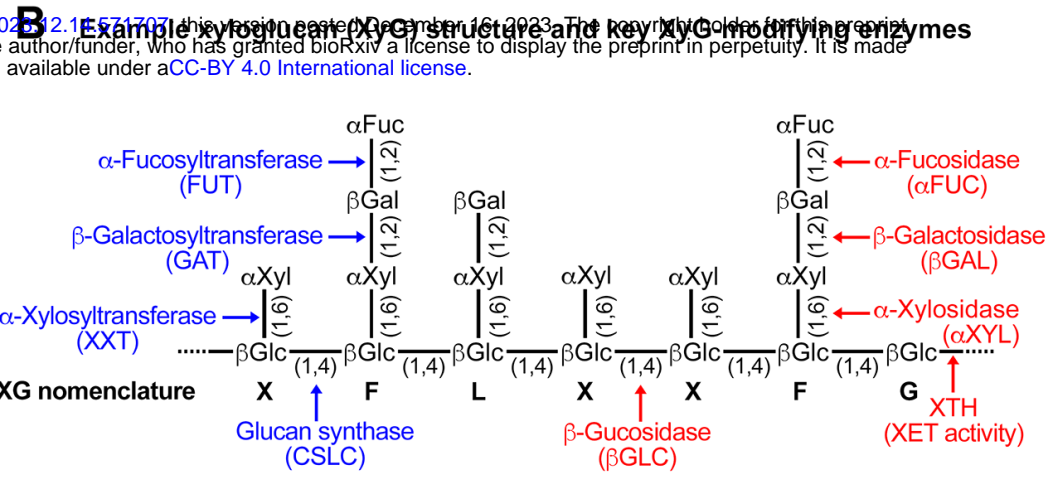
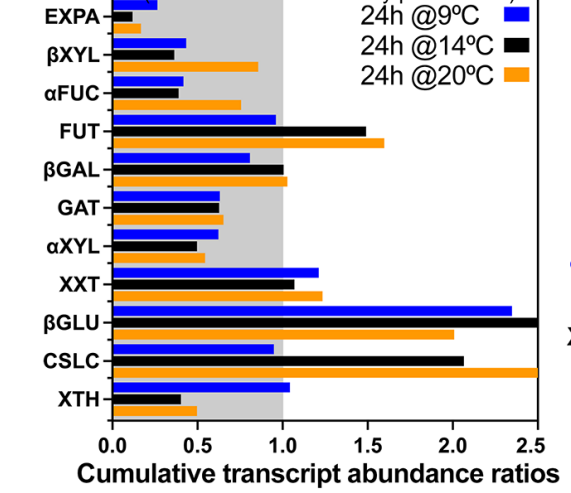


Figure 10 Transcript abundance patterns (RNA-seq) of *Aethionema arabicum* cell-wall remodeling protein genes in seeds of imbibed dimorphic diaspores (M+ seeds, IND fruits) and bare M- seeds.

A, Effect of the pericarp on the expression ratios of expansin A and xyloglucan-related cell-wall remodeling protein genes in the M- seeds of 24 h imbibed IND fruits and isolated M- seeds.

B, Xyloglucan remodeling is achieved by a battery of enzymes specifically targeting different bonds of xyloglucan structure as indicated. Among them are xyloglucan endo-transglycosylases/hydrolases (XTHs) with xyloglucan endo-transglycosylase (XET) enzyme activity (Holloway et al., 2021).

C, Transcript abundance patterns of *Ae. arabicum* expansins A, XTHs and the alpha-xylosidase Aear-aXYL1 in M+ seeds, IND fruits and isolated M- seeds from two parental temperature regimes (20°C versus 25°C) at four different imbibition temperatures (9, 14, 20 and 24°C). For other expansin and xyloglucan-related genes and *Ae. arabicum* gene IDs see Supplemental Figure S2 or the Expression Atlas (https://plantcode.cup.uni-freiburg.de/aetar_db/index.php). WGCNA modules (Figure 3) are indicated by the vertical color lines next to the graphs. Mean \pm SEM values of 3 replicates each with 60-80 seeds are presented.

Parsed Citations

Alexa, A, and Rahnenfuhrer, J. (2023). topGO: enrichment analysis for Gene Ontology. R package version 2.52.0.

Google Scholar: [Author Only](#) [Title Only](#) [Author and Title](#)

Andrade, A, Riera, N., Lindstrom, L., Alemano, S., Alvarez, D., Abdala, G., and Vigliocco, A (2015). Pericarp anatomy and hormone profiles of cypselas in dormant and non-dormant inbred sunflower lines. Plant Biol 17, 351-360.

Google Scholar: [Author Only](#) [Title Only](#) [Author and Title](#)

Arshad, W., Marone, F., Collinson, M.E., Leubner-Metzger, G., and Steinbrecher, T. (2020). Fracture of the dimorphic fruits of *Aethionema arabicum* (Brassicaceae). Botany 98, 65-75.

Google Scholar: [Author Only](#) [Title Only](#) [Author and Title](#)

Arshad, W., Sperber, K., Steinbrecher, T., Nichols, B., Jansen, V.A.A., Leubner-Metzger, G., and Mummenhoff, K. (2019). Dispersal biophysics and adaptive significance of dimorphic diaspores in the annual *Aethionema arabicum* (Brassicaceae). New Phytol 221, 1434-1446.

Google Scholar: [Author Only](#) [Title Only](#) [Author and Title](#)

Arshad, W., Lenser, T., Wilhelmsson, P.K.I., Chandler, J.O., Steinbrecher, T., Marone, F., Pérez, M., Collinson, M.E., Stuppy, W., Rensing, S.A., Theissen, G., and Leubner-Metzger, G. (2021). A tale of two morphs: developmental patterns and mechanisms of seed coat differentiation in the dimorphic diaspore model *Aethionema arabicum* (Brassicaceae). Plant J 107, 166-181.

Google Scholar: [Author Only](#) [Title Only](#) [Author and Title](#)

Bailey, T.L., Johnson, J., Grant, C.E., and Noble, W.S. (2015). The MEME Suite. Nucl Acids Res 43, W39-W49.

Google Scholar: [Author Only](#) [Title Only](#) [Author and Title](#)

Barrero, J.M., Millar, A.A., Griffiths, J., Czechowski, T., Scheible, W.R., Udvardi, M., Reid, J.B., Ross, J.J., Jacobsen, J.V., and Gubler, F. (2010). Gene expression profiling identifies two regulatory genes controlling dormancy and ABA sensitivity in *Arabidopsis* seeds. Plant J 61, 611-622.

Google Scholar: [Author Only](#) [Title Only](#) [Author and Title](#)

Baskin, J.M., Lu, J.J., Baskin, C.C., Tan, D.Y., and Wang, L. (2014). Diaspore dispersal ability and degree of dormancy in heteromorphic species of cold deserts of northwest China: A review. Perspect Plant Ecol Evol Sys 16, 93-99.

Google Scholar: [Author Only](#) [Title Only](#) [Author and Title](#)

Batlla, D., Malavert, C., Farnocchia, R.B.F., Footitt, S., Benech-Arnold, R.L., and Finch-Savage, W.E. (2022). A quantitative analysis of temperature-dependent seasonal dormancy cycling in buried *Arabidopsis thaliana* seeds can predict seedling emergence in a global warming scenario. J Expt Bot 73, 2454-2468.

Google Scholar: [Author Only](#) [Title Only](#) [Author and Title](#)

Benech-Arnold, R.L., Gualano, N., Leymarie, J., Come, D., and Corbineau, F. (2006). Hypoxia interferes with ABA metabolism and increases ABA sensitivity in embryos of dormant barley grains. J Exptl Bot 57, 1423-1430.

Google Scholar: [Author Only](#) [Title Only](#) [Author and Title](#)

Bhattacharya, S., Sperber, K., Ozudogru, B., Leubner-Metzger, G., and Mummenhoff, K. (2019). Naturally-primed life strategy plasticity of dimorphic *Aethionema arabicum* facilitates optimal habitat colonization. Sci Rep 9, ARTN 16108.

Google Scholar: [Author Only](#) [Title Only](#) [Author and Title](#)

Bueso, E., Munoz-Bertomeu, J., Campos, F., Brunaud, V., Martinez, L., Sayas, E., Ballester, P., Yenush, L., and Serrano, R. (2014). *Arabidopsis thaliana* HOMEOBOX25 uncovers a role for gibberellins in seed longevity. Plant Physiology 164, 999-1010.

Google Scholar: [Author Only](#) [Title Only](#) [Author and Title](#)

Cadman, C.S.C., Toorop, P.E., Hilhorst, H.W.M., and Finch-Savage, W.E. (2006). Gene expression profiles of *Arabidopsis Cvi* seed during cycling through dormant and non-dormant states indicate a common underlying dormancy control mechanism. Plant J 46, 805-822.

Google Scholar: [Author Only](#) [Title Only](#) [Author and Title](#)

Christianson, J.A., Wilson, I.W., Llewellyn, D.J., and Dennis, E.S. (2009). The low-oxygen induced NAC domain transcription factor ANAC102 affects viability of *Arabidopsis thaliana* seeds following low-oxygen treatment. Plant Physiol 149, 1724-1738.

Google Scholar: [Author Only](#) [Title Only](#) [Author and Title](#)

Dave, A., Vaistij, F.E., Gilday, A.D., Penfield, S.D., and Graham, I.A. (2016). Regulation of *Arabidopsis thaliana* seed dormancy and germination by 12-oxo-phytodienoic acid. J Exptl Bot 67, 2277-2284.

Google Scholar: [Author Only](#) [Title Only](#) [Author and Title](#)

Dominguez, C.P., Rodriguez, M.V., Batlla, D., de Salamone, I.E.G., Mantese, A.I., Andreani, A.L., and Benech-Arnold, R.L. (2019). Sensitivity to hypoxia and microbial activity are instrumental in pericarp-imposed dormancy expression in sunflower (*Helianthus annuus* L.). Seed Sci Res 29, 85-96.

Google Scholar: [Author Only](#) [Title Only](#) [Author and Title](#)

Donohue, K., Rubio de Casas, R., Burghardt, L., Kovach, K., and Willis, C.G. (2010). Germination, postgermination adaptation, and species ecological ranges. Annual Review of Ecology, Evolution, and Systematics 41, 293-319.

Google Scholar: [Author Only](#) [Title Only](#) [Author and Title](#)

Fernandez-Pascual, E., Mattana, E., and Pritchard, H.W. (2019). Seeds of future past: climate change and the thermal memory of plant reproductive traits. Biol Rev 94, 439-456.

Google Scholar: [Author Only](#) [Title Only](#) [Author and Title](#)

Fernandez-Pozo, N., and Bombarely, A. (2022). EasyGDB: a low-maintenance and highly customizable system to develop genomics portals. Bioinformatics (Oxford, England) 38, 4048-4050.

Google Scholar: [Author Only](#) [Title Only](#) [Author and Title](#)

Fernandez-Pozo, N., Metz, T., Chandler, J.O., Gramzow, L., Merai, Z., Maumus, F., Scheid, O.M., Theissen, G., Schranz, M.E., Leubner-Metzger, G., and Rensing, S.A. (2021). *Aethionema arabicum* genome annotation using PacBio full-length transcripts provides a valuable resource for seed dormancy and Brassicaceae evolution research. Plant J 106, 275-293.

Google Scholar: [Author Only](#) [Title Only](#) [Author and Title](#)

Finch-Savage, W.E., and Leubner-Metzger, G. (2006). Seed dormancy and the control of germination. New Phytol 171, 501-523.

Google Scholar: [Author Only](#) [Title Only](#) [Author and Title](#)

Finch-Savage, W.E., and Footitt, S. (2017). Seed dormancy cycling and the regulation of dormancy mechanisms to time germination in variable field environments. J Exptl Bot 68, 843-856.

Google Scholar: [Author Only](#) [Title Only](#) [Author and Title](#)

Flokova, K., Tarkowska, D., Miersch, O., Strnad, M., Wasternack, C., and Novak, O. (2014). UHPLC-MS/MS based target profiling of stress-induced phytohormones. Phytochem 105, 147-157.

Google Scholar: [Author Only](#) [Title Only](#) [Author and Title](#)

Footitt, S., Walley, P.G., Lynn, J.R., Hambridge, A.J., Penfield, S., and Finch-Savage, W.E. (2020). Trait analysis reveals DOG1 determines initial depth of seed dormancy, but not changes during dormancy cycling that result in seedling emergence timing. New Phytol 225, 2035-2047.

Google Scholar: [Author Only](#) [Title Only](#) [Author and Title](#)

Gasch, P., Fundinger, M., Muller, J.T., Lee, T., Bailey-Serres, J., and Mustroph, A. (2016). Redundant ERF-VII transcription factors bind to an evolutionarily conserved cis-motif to regulate hypoxia-responsive gene expression in *Arabidopsis*. Plant Cell 28, 160-180.

Google Scholar: [Author Only](#) [Title Only](#) [Author and Title](#)

Gianella, M., Bradford, K.J., and Guzzon, F. (2021). Ecological, (epi)genetic and physiological aspects of bet-hedging in angiosperms. Plant Reprod 34, 21-36.

Google Scholar: [Author Only](#) [Title Only](#) [Author and Title](#)

Gomez-Porras, J.L., Riano-Pachon, D.M., Dreyer, I., Mayer, J.E., and Mueller-Roeber, B. (2007). Genome-wide analysis of ABA-responsive elements ABRE and CE3 reveals divergent patterns in *Arabidopsis* and rice. BMC Genomics 8, ARTN 260.

Google Scholar: [Author Only](#) [Title Only](#) [Author and Title](#)

Graeber, K., Linkies, A., Wood, A.T., and Leubner-Metzger, G. (2011). A guideline to family-wide comparative state-of-the-art quantitative RT-PCR analysis exemplified with a Brassicaceae cross-species seed germination case study. Plant Cell 23, 2045-2063.

Google Scholar: [Author Only](#) [Title Only](#) [Author and Title](#)

Graeber, K., Linkies, A., Steinbrecher, T., Mummenhoff, K., Tarkowská, D., Turecková, V., Ignatz, M., Sperber, K., Voegele, A., de Jong, H., Urbanová, T., Strnad, M., and Leubner-Metzger, G. (2014). DELAY OF GERMINATION 1 mediates a conserved coat dormancy mechanism for the temperature- and gibberellin-dependent control of seed germination. Proceedings of the National Academy of Sciences of the United States of America 111, E3571-E3580.

Google Scholar: [Author Only](#) [Title Only](#) [Author and Title](#)

Grafi, G. (2020). Dead but not dead end: Multifunctional role of dead organs enclosing embryos in seed biology. Int J Mol Sci 21, ARTN 8024.

Google Scholar: [Author Only](#) [Title Only](#) [Author and Title](#)

Grant, C.E., Bailey, T.L., and Noble, W.S. (2011). FIMO: scanning for occurrences of a given motif. Bioinformatics (Oxford, England) 27, 1017-1018.

Google Scholar: [Author Only](#) [Title Only](#) [Author and Title](#)

Gu, Z.G., Gu, L., Eils, R., Schlesner, M., and Brors, B. (2014). Circlize implements and enhances circular visualization in R. Bioinformatics (Oxford, England) 30, 2811-2812.

Google Scholar: [Author Only](#) [Title Only](#) [Author and Title](#)

Hall, J.C., Tisdale, T.E., Donohue, K., and Kramer, E.M. (2006). Developmental basis of an anatomical novelty: Heteroarthrocarpy

in *Cakile lanceolata* and *Erucaria erucarioides* (Brassicaceae). *International Journal of Plant Sciences* 167, 771-789.

Google Scholar: [Author Only](#) [Title Only](#) [Author and Title](#)

Haudry, A., Platts, A.E., Vello, E., Hoen, D.R., Leclercq, M., Williamson, R.J., Forczek, E., Joly-Lopez, Z., Steffen, J.G., Hazzouri, K.M., Dewar, K., Stinchcombe, J.R., Schoen, D.J., Wang, X.W., Schmutz, J., Town, C.D., Edger, P.P., Pires, J.C., Schumaker, K.S., Jarvis, D.E., Mandakova, T., Lysak, M.A., van den Bergh, E., Schranz, M.E., Harrison, P.M., Moses, A.M., Bureau, T.E., Wright, S.I., and Blanchette, M. (2013). An atlas of over 90,000 conserved noncoding sequences provides insight into crucifer regulatory regions. *Nat Genet* 45, 891-898.

Google Scholar: [Author Only](#) [Title Only](#) [Author and Title](#)

Hoang, H.H., Bailly, C., Corbineau, F., and Leymarie, J. (2013). Induction of secondary dormancy by hypoxia in barley grains and its hormonal regulation. *J Expt Bot* 64, 2017-2025.

Google Scholar: [Author Only](#) [Title Only](#) [Author and Title](#)

Holloway, T., Steinbrecher, T., Pérez, M., Seville, A., Stock, D., Nakabayashi, K., and Leubner-Metzger, G. (2021). Coleorrhiza-enforced seed dormancy: a novel mechanism to control germination in grasses. *New Phytol* 229, 2179-2191.

Google Scholar: [Author Only](#) [Title Only](#) [Author and Title](#)

Ignatz, M., Hourston, J.E., Tureckova, V., Strnad, M., Meinhard, J., Fischer, U., Steinbrecher, T., and Leubner-Metzger, G. (2019). The biochemistry underpinning industrial seed technology and mechanical processing of sugar beet. *Planta* 250, 1717-1729.

Google Scholar: [Author Only](#) [Title Only](#) [Author and Title](#)

Imbert, E. (2002). Ecological consequences and ontogeny of seed heteromorphism. *Perspect Plant Ecol Evol Sys* 5, 13-36.

Google Scholar: [Author Only](#) [Title Only](#) [Author and Title](#)

Iwasaki, M., Penfield, S., and Lopez-Molina, L. (2022). Parental and environmental control of seed dormancy in *Arabidopsis thaliana*. *Annual Review of Plant Biology* 73, 355-378.

Google Scholar: [Author Only](#) [Title Only](#) [Author and Title](#)

Joosen, R.V., Kodde, J., Willems, L.A., Ligterink, W., van der Plas, L.H., and Hilhorst, H.W. (2010). GERMATOR: a software package for high-throughput scoring and curve fitting of *Arabidopsis* seed germination. *Plant J* 62, 148-159.

Google Scholar: [Author Only](#) [Title Only](#) [Author and Title](#)

Ju, L., Jing, Y.X., Shi, P.T., Liu, J., Chen, J.S., Yan, J.J., Chu, J.F., Chen, K.M., and Sun, J.Q. (2019). JAZ proteins modulate seed germination through interaction with ABI5 in bread wheat and *Arabidopsis*. *New Phytol* 223, 246-260.

Google Scholar: [Author Only](#) [Title Only](#) [Author and Title](#)

Khadka, J., Raviv, B., Swetha, B., Grandhi, R., Singiri, J.R., Novoplansky, N., Guterman, Y., Galis, I., Huang, Z.Y., and Grafi, G. (2020). Maternal environment alters dead pericarp biochemical properties of the desert annual plant *Anastatica hierochuntica* L. *PLoS ONE* 15, ARTN e0237045.

Google Scholar: [Author Only](#) [Title Only](#) [Author and Title](#)

Kürsteiner, O., Dupuis, I., and Kuhlemeier, C. (2003). The pyruvate decarboxylase1 gene of *Arabidopsis* is required during anoxia but not other environmental stresses. *Plant Physiol* 132, 968-978.

Google Scholar: [Author Only](#) [Title Only](#) [Author and Title](#)

Langfelder, P., and Horvath, S. (2008). WGCNA: an R package for weighted correlation network analysis. *BMC Bioinformatics* 9, ARTN 559.

Google Scholar: [Author Only](#) [Title Only](#) [Author and Title](#)

Lenser, T., Tarkowska, D., Novak, O., Wilhelmsson, P.K.I., Bennett, T., Rensing, S.A., Strnad, M., and Theissen, G. (2018). When the BRANCHED network bears fruit: How carpel dominance causes fruit dimorphism in *Aethionema*. *Plant J* 94, 352-371.

Google Scholar: [Author Only](#) [Title Only](#) [Author and Title](#)

Lenser, T., Graeber, K., Cevik, O.S., Adiguzel, N., Donmez, A.A., Grosche, C., Kettermann, M., Mayland-Quellhorst, S., Merai, Z., Mohammadin, S., Nguyen, T.P., Rumpler, F., Schulze, C., Sperber, K., Steinbrecher, T., Wiegand, N., Strnad, M., Scheid, O.M., Rensing, S.A., Schranz, M.E., Theissen, G., Mummenhoff, K., and Leubner-Metzger, G. (2016). Developmental control and plasticity of fruit and seed dimorphism in *Aethionema arabicum*. *Plant Physiology* 172, 1691-1707.

Google Scholar: [Author Only](#) [Title Only](#) [Author and Title](#)

Linkies, A., and Leubner-Metzger, G. (2012). Beyond gibberellins and abscisic acid: how ethylene and jasmonates control seed germination. *Plant Cell Rep* 31, 253-270.

Google Scholar: [Author Only](#) [Title Only](#) [Author and Title](#)

Liu, R.R., Wang, L., Tanveer, M., and Song, J. (2018). Seed heteromorphism: an important adaptation of halophytes for habitat heterogeneity. *Front Plant Sci* 9, ARTN 1515.

Google Scholar: [Author Only](#) [Title Only](#) [Author and Title](#)

Loades, E., Perez, M., Tureckova, V., Tarkowska, D., Strnad, M., Seville, A., Nakabayashi, K., and Leubner-Metzger, G. (2023). Distinct hormonal and morphological control of dormancy and germination in *Chenopodium album* dimorphic seeds. *Front Plant*

Sci 14, ARTN 1156794.

Google Scholar: [Author Only](#) [Title Only](#) [Author and Title](#)

Lu, G.H., Paul, A.L., McCarty, D.R., and Ferl, R.J. (1996). Transcription factor veracity: Is GBF3 responsible for ABA-regulated expression of *Arabidopsis Adh*? *Plant Cell* 8, 847-857.

Google Scholar: [Author Only](#) [Title Only](#) [Author and Title](#)

Lu, J.J., Tan, D.Y., Baskin, J.M., and Baskin, C.C. (2015a). Post-release fates of seeds in dehiscent and indehiscent siliques of the diaspore heteromorphic species *Diptychocarpus strictus* (Brassicaceae). *Perspect Plant Ecol Evol Sys* 17, 255-262.

Google Scholar: [Author Only](#) [Title Only](#) [Author and Title](#)

Lu, J.J., Tan, D.Y., Baskin, C.C., and Baskin, J.M. (2017a). Role of indehiscent pericarp in formation of soil seed bank in five cold desert Brassicaceae species. *Plant Ecology* 218, 1187-1200.

Google Scholar: [Author Only](#) [Title Only](#) [Author and Title](#)

Lu, J.J., Tan, D.Y., Baskin, C.C., and Baskin, J.M. (2017b). Delayed dehiscence of the pericarp: role in germination and retention of viability of seeds of two cold desert annual Brassicaceae species. *Plant Biol (Stuttg)* 19, 14-22.

Google Scholar: [Author Only](#) [Title Only](#) [Author and Title](#)

Lu, J.J., Zhou, Y.M., Tan, D.Y., Baskin, C.C., and Baskin, J.M. (2015b). Seed dormancy in six cold desert Brassicaceae species with indehiscent fruits. *Seed Sci Res* 25, 276-285.

Google Scholar: [Author Only](#) [Title Only](#) [Author and Title](#)

Mamut, J., Tan, D.-Y., Baskin, C.C., and Baskin, J.M. (2014). Role of trichomes and pericarp in the seed biology of the desert annual *Lachnoloma lehmannii* (Brassicaceae). *Ecol Res* 29, 33-44.

Google Scholar: [Author Only](#) [Title Only](#) [Author and Title](#)

McLeay, R.C., and Bailey, T.L. (2010). Motif Enrichment Analysis: a unified framework and an evaluation on ChIP data. *BMC Bioinformatics* 11, ARTN 165.

Google Scholar: [Author Only](#) [Title Only](#) [Author and Title](#)

Mendiondo, G.M., Leymarie, J., Farrant, J.M., Corbineau, F., and Benech-Arnold, R.L. (2010). Differential expression of abscisic acid metabolism and signalling genes induced by seed-covering structures or hypoxia in barley (*Hordeum vulgare* L.) grains. *Seed Sci Res* 20, 69-77.

Google Scholar: [Author Only](#) [Title Only](#) [Author and Title](#)

Merai, Z., Graeber, K., Wilhelmsson, P., Ullrich, K.K., Arshad, W., Grosche, C., Tarkowska, D., Tureckova, V., Strnad, M., Rensing, S.A., Leubner-Metzger, G., and Mittelsten Scheid, O. (2019). *Aethionema arabicum*: a novel model plant to study the light control of seed germination. *J Exptl Bot* 70, 3313-3328.

Google Scholar: [Author Only](#) [Title Only](#) [Author and Title](#)

Merai, Z., Xu, F., Musilek, A., Ackerl, F., Khalil, S., Soto-Jimenez, L.M., Lalatovic, K., Klose, C., Tarkowska, D., Tureckova, V., Strnad, M., and Scheid, O.M. (2023). Phytochromes mediate germination inhibition under red, far-red, and white light in *Aethionema arabicum*. *Plant Physiology* 192, 1584-1602.

Google Scholar: [Author Only](#) [Title Only](#) [Author and Title](#)

Mohammad, S., Peterse, K., van de Kerke, S.J., Chatrou, L.W., Donmez, A.A., Mummenhoff, K., Pires, J.C., Edger, P.P., Al-Shehbaz, I.A., and Schranz, M.E. (2017). Anatolian origins and diversification of *Aethionema*, the sister lineage of the core Brassicaceae. *Am J Bot* 104, 1042-1054.

Google Scholar: [Author Only](#) [Title Only](#) [Author and Title](#)

Mohammad, S., Wang, W., Liu, T., Moazzeni, H., Ertugrul, K., Uysal, T., Christodoulou, C.S., Edger, P.P., Pires, J.C., Wright, S.I., and Schranz, M.E. (2018). Genome-wide nucleotide diversity and associations with geography, ploidy level and glucosinolate profiles in *Aethionema arabicum* (Brassicaceae). *Plant Sys Evol* 304, 619-630.

Google Scholar: [Author Only](#) [Title Only](#) [Author and Title](#)

Mohammed, S., Turckova, V., Tarkowska, D., Strnad, M., Mummenhoff, K., and Leubner-Metzger, G. (2019). Pericarp-mediated chemical dormancy controls the fruit germination of the invasive hoary cress (*Lepidium draba*), but not of hairy whitetop (*Lepidium appelianum*). *Weed Science* 67, 560-571.

Google Scholar: [Author Only](#) [Title Only](#) [Author and Title](#)

Mühlhausen, A., Lenser, T., Mummenhoff, K., and Theissen, G. (2013). Evidence that an evolutionary transition from dehiscent to indehiscent fruits in *Lepidium* (Brassicaceae) was caused by a change in the control of valve margin identity genes. *Plant J* 73, 824-835.

Google Scholar: [Author Only](#) [Title Only](#) [Author and Title](#)

Nambara, E., Okamoto, M., Tatematsu, K., Yano, R., Seo, M., and Kamiya, Y. (2010). Abscisic acid and the control of seed dormancy and germination. *Seed Sci Res* 20, 55-67.

Google Scholar: [Author Only](#) [Title Only](#) [Author and Title](#)

Nguyen, T.P., Muhlich, C., Mohammadin, S., van den Bergh, E., Platts, A.E., Haas, F.B., Rensing, S.A., and Schranz, M.E. (2019). Genome improvement and genetic map construction for *Aethionema arabicum*, the first divergent branch in the Brassicaceae family. *G3-Genes Genom Genet* 9, 3521-3530.

Google Scholar: [Author Only](#) [Title Only](#) [Author and Title](#)

Nichols, B.S., Leubner-Metzger, G., and Jansen, V.A.A. (2020). Between a rock and a hard place: adaptive sensing and site-specific dispersal. *Ecol Lett* 23, 1370-1379.

Google Scholar: [Author Only](#) [Title Only](#) [Author and Title](#)

O'Malley, R.C., Huang, S.S.C., Song, L., Lewsey, M.G., Bartlett, A., Nery, J.R., Galli, M., Gallavotti, A., and Ecker, J.R. (2016). Cistrome and epicistrome features shape the regulatory DNA landscape. *Cell* 165, 1280-1292.

Google Scholar: [Author Only](#) [Title Only](#) [Author and Title](#)

Papdi, C., Perez-Salamo, I., Joseph, M.P., Giuntoli, B., Bogre, L., Koncz, C., and Szabados, L. (2015). The low oxygen, oxidative and osmotic stress responses synergistically act through the ethylene response factor VII genes RAP2.12, RAP2.2 and RAP2.3. *Plant J* 82, 772-784.

Google Scholar: [Author Only](#) [Title Only](#) [Author and Title](#)

Penfield, S., and MacGregor, D.R. (2017). Effects of environmental variation during seed production on seed dormancy and germination. *J Expt Bot* 68, 819-825.

Google Scholar: [Author Only](#) [Title Only](#) [Author and Title](#)

Renard, J., Martinez-Almonacid, I., Castillo, I.Q., Sonntag, A., Hashim, A., Bissoli, G., Campos, L., Munoz-Bertomeu, J., Ninoles, R., Roach, T., Sanchez-Leon, S., Ozuna, C.V., Gadea, J., Lison, P., Kranner, I., Barro, F., Serrano, R., Molina, I., and Bueso, E. (2021). Apoplastic lipid barriers regulated by conserved homeobox transcription factors extend seed longevity in multiple plant species. *New Phytol* 231, 679-694.

Google Scholar: [Author Only](#) [Title Only](#) [Author and Title](#)

Rittenberg, D., and Foster, G.L. (1940). A new procedure for quantitative analysis by isotope dilution, with application to the determination of amino acids and fatty acids. *Journal of Biological Chemistry* 133, 737-744.

Google Scholar: [Author Only](#) [Title Only](#) [Author and Title](#)

Scheler, C., Weitbrecht, K., Pearce, S.P., Hampstead, A., Buettner-Mainik, A., Lee, K., Voegele, A., Oracz, K., Dekkers, B., Wang, X., Wood, A., Bentsink, L., King, J., Knox, P., Holdsworth, M., Müller, K., and Leubner-Metzger, G. (2015). Promotion of testa rupture during garden cress germination involves seed compartment-specific expression and activity of pectin methylesterases. *Plant Physiology* 167, 200-215.

Google Scholar: [Author Only](#) [Title Only](#) [Author and Title](#)

Seok, H.Y., Tran, H.T., Lee, S.Y., and Moon, Y.H. (2022). AtERF71/HRE2, an *Arabidopsis* AP2/ERF transcription factor gene, contains both positive and negative cis-regulatory elements in its promoter region involved in hypoxia and salt stress responses. *Int J Mol Sci* 23, ARTN 5310.

Google Scholar: [Author Only](#) [Title Only](#) [Author and Title](#)

Shigeyama, T., Watanabe, A., Tokuchi, K., Toh, S., Sakurai, N., Shibuya, N., and Kawakami, N. (2016). alpha-Xylosidase plays essential roles in xyloglucan remodelling, maintenance of cell wall integrity, and seed germination in *Arabidopsis thaliana*. *J Expt Bot* 67, 5615-5629.

Google Scholar: [Author Only](#) [Title Only](#) [Author and Title](#)

Silva, A.T., Ribone, P.A., Chan, R.L., Ligterink, W., and Hilhorst, H.W.M. (2016). A predictive coexpression network identifies novel genes controlling the seed-to-seedling phase transition in *Arabidopsis thaliana*. *Plant Physiology* 170, 2218-2231.

Google Scholar: [Author Only](#) [Title Only](#) [Author and Title](#)

Simura, J., Antoniadi, I., Siroka, J., Tarkowská, D., Strnad, M., Ljung, K., and Novak, O. (2018). Plant hormonomics: multiple phytohormone profiling by targeted metabolomics. *Plant Physiology* 177, 476-489.

Google Scholar: [Author Only](#) [Title Only](#) [Author and Title](#)

Sperber, K., Steinbrecher, T., Graeber, K., Scherer, G., Clausing, S., Wiegand, N., Hourston, J.E., Kurre, R., Leubner-Metzger, G., and Mummenhoff, K. (2017). Fruit fracture biomechanics and the release of *Lepidium didymum* pericarp-imposed mechanical dormancy by fungi. *Nature Communications* 8, 1868.

Google Scholar: [Author Only](#) [Title Only](#) [Author and Title](#)

Stamm, P., Topham, A.T., Mukhtar, N.K., Jackson, M.D.B., Tome, D.F.A., Beynon, J.L., and Bassel, G.W. (2017). The transcription factor ATHB5 affects GA-mediated plasticity in hypocotyl cell growth during seed germination. *Plant Physiology* 173, 907-917.

Google Scholar: [Author Only](#) [Title Only](#) [Author and Title](#)

Steinbrecher, T., and Leubner-Metzger, G. (2017). The biomechanics of seed germination. *J Expt Bot* 68, 765-783.

Google Scholar: [Author Only](#) [Title Only](#) [Author and Title](#)

Steinbrecher, T., and Leubner-Metzger, G. (2022). Xyloglucan remodelling enzymes and the mechanics of plant seed and fruit biology. *J Expt Bot* 73, 1253-1257.

Google Scholar: [Author Only](#) [Title Only](#) [Author and Title](#)

Takeno, K., and Yamaguchi, H. (1991). Diversity in seed-germination behavior in relation to heterocarpy in *Salsola komarovii* Iljin. Botanical Magazine-Tokyo 104, 207-215.

Google Scholar: [Author Only](#) [Title Only](#) [Author and Title](#)

Untergasser, A., Cutcutache, I., Koressaar, T., Ye, J., Faircloth, B.C., Remm, M., and Rozen, S.G. (2012). Primer3 - new capabilities and interfaces. Nucl Acids Res 40, ARTN e115.

Google Scholar: [Author Only](#) [Title Only](#) [Author and Title](#)

Walck, J.L., Hidayati, S.N., Dixon, K.W., Thompson, K., and Poschlod, P. (2011). Climate change and plant regeneration from seed. Global Change Biol 17, 2145-2161.

Google Scholar: [Author Only](#) [Title Only](#) [Author and Title](#)

Wang, L., Hua, D.P., He, J.N., Duan, Y., Chen, ZZ, Hong, X.H., and Gong, ZZ (2011). Auxin response factor2 (ARF2) and its regulated homeodomain gene HB33 mediate abscisic acid response in *Arabidopsis*. Plos Genetics 7, ARTN e1002172.

Google Scholar: [Author Only](#) [Title Only](#) [Author and Title](#)

Weitbrecht, K., Müller, K., and Leubner-Metzger, G. (2011). First off the mark: early seed germination. J Exptl Bot 62, 3289-3309.

Google Scholar: [Author Only](#) [Title Only](#) [Author and Title](#)

Wickham, H. (2016). *ggplot2: Elegant Graphics for Data Analysis*. (New York: Springer-Verlag).

Google Scholar: [Author Only](#) [Title Only](#) [Author and Title](#)

Wilhelmsson, P.K.I., Chandler, J.O., Fernandez-Pozo, N., Graeber, K., Ullrich, K.K., Arshad, W., Khan, S., Hofberger, J., Buchta, K., Edger, P.P., Pires, C., Schranz, M.E., Leubner-Metzger, G., and Rensing, S.A (2019). Usability of reference-free transcriptome assemblies for detection of differential expression: a case study on *Aethionema arabicum* dimorphic seeds. BMC Genomics 20, ARTN 95.

Google Scholar: [Author Only](#) [Title Only](#) [Author and Title](#)

Yang, C.Y., Hsu, F.C., Li, J.P., Wang, N.N., and Shih, M.C. (2011). The AP2/ERF transcription factor AtERF73/HRE1 modulates ethylene responses during hypoxia in *Arabidopsis*. Plant Physiology 156, 202-212.

Google Scholar: [Author Only](#) [Title Only](#) [Author and Title](#)

Yoshida, T., Fujita, Y., Sayama, H., Kidokoro, S., Maruyama, K., Mizoi, J., Shinozaki, K., and Yamaguchi-Shinozaki, K. (2010). AREB1, AREB2, and ABF3 are master transcription factors that cooperatively regulate ABRE-dependent ABA signaling involved in drought stress tolerance and require ABA for full activation. Plant J 61, 672-685.

Google Scholar: [Author Only](#) [Title Only](#) [Author and Title](#)

Zhang, B., and Horvath, S. (2005). A general framework for weighted gene co-expression network analysis. Stat Appl Genet Mol Biol 4, ARTN 17.

Google Scholar: [Author Only](#) [Title Only](#) [Author and Title](#)

Zhang, Y.Z., Liu, Y., Sun, L., Baskin, C.C., Baskin, J.M., Cao, M., and Yang, J. (2022). Seed dormancy in space and time: global distribution, paleoclimatic and present climatic drivers, and evolutionary adaptations. New Phytol 234, 1770-1781.

Google Scholar: [Author Only](#) [Title Only](#) [Author and Title](#)